UNIVERSITY OF RWANDA

COLLEGE OF SCIENCE AND TECHNOLOGY

AFRICAN CENTRE OF EXCELLENCE IN THE INTERNET OF THINGS

IoT-ENABLED FAULT PREDICTION AND LOCATION DISCOVERY PLATFORM FOR THE ELECTRICAL POWER DISTRIBUTION SYSTEM: A CASE OF KENYA

GEORGE YOGO ODONGO

A thesis submitted in fulfillment of the requirements
for the degree of Doctor of Philosophy
in
The Internet of Things – Embedded Computing Systems

JULY 2023

UNIVERSITY OF RWANDA

COLLEGE OF SCIENCE AND TECHNOLOGY

AFRICAN CENTRE OF EXCELLENCE IN THE INTERNET OF THINGS

DOCTORAL THESIS

IoT-ENABLED FAULT PREDICTION AND LOCATION DISCOVERY PLATFORM FOR THE ELECTRICAL POWER DISTRIBUTION SYSTEM: A CASE OF KENYA

GEORGE YOGO ODONGO

A thesis submitted in fulfillment of the requirements
for the degree of Doctor of Philosophy
in
The Internet of Things – Embedded Computing Systems

Main Supervisor:	**Prof. Richard Musabe, PhD.**
Co-supervisor:	**Dr. Abubakar Diwani, PhD**
Resident Co-Supervisor:	**Prof. Damien Hanyurwimfura, PhD.**

JULY 2023

Statement of Original Authorship

I, Odongo George Yogo, do hereby declare that this thesis entitled "***IoT-Enabled Fault Prediction and Location Discovery Platform for the Electrical Power Distribution System: A Case of Kenya Power,***" submitted in partial fulfilment for the degree of *Doctor of Philosophy in the Internet of Things—Embedded Computing Systems* at the University of Rwanda/College of Science and Technology, is my original work and has not been submitted to any other university or higher learning institution for any other awards. I further declare that all sources of information used were acknowledged by a complete list of references and were well cited.

Odongo George Yogo.

George Yogo Odongo, a Ph.D. candidate of UR-ACEIoT registration number 219008380, successfully defended the thesis entitled "IoT-ENABLED FAULT PREDICTION AND LOCATION DISCOVERY PLATFORM FOR THE ELECTRICAL POWER DISTRIBUTION SYSTEM: A CASE OF KENYA", which he prepared after fulfilling the requirements specified in the associated legislations, before the jury whose signatures are appended below.

Thesis Supervisor: Prof. Richard Musabe, PhD
Rwanda Polytechnic, Rwanda

Co-supervisor: Dr. Abubakar Diwani, PhD
The State University of Zanzibar, Tanzania

Resident Co-Supervisor: Prof. Damien Hanyurwimfura,
University of Rwanda, Rwanda

Viva Voce Members:

1. Prof. Umaru Garba Wali (Chair)
University of Rwanda, Kigali, Rwanda

2. Dr. Enan Nyesheja
University of Lay Adventists of Kigali (UNILAK), Kigali, Rwanda

3. Prof. Michael George Masangala Zimba
Mzuzu University, Malawi

4. Prof. Dr. Hacı İLHAN
Yıldız Technical University,
Istanbul, Türkiye

Date of Defense: 10 July 2023

Dedication

I dedicate this work to my wife, Lilian Auma, who has encouraged me all the way and whose encouragement has made sure that I give it all it takes to finish what I have started. To my children, Adam and Gillian, who have been affected in every way possible by this quest. This work is also dedicated to my parents, Hillary and Dursila Atieno, who have always loved me unconditionally and whose good examples have taught me to work hard for the things that I aspire to achieve.

Acknowledgement

I am very grateful to the University of Rwanda and the African Center of Excellence in the Internet of Things (ACE-IoT) for the scholarship I received to pursue this doctoral study. I sincerely thank the director of the center, Prof. Damien Hanyurwimfura, the head of PhD research, Dr. Omar Gatera, and all the staff of the center. Specifically, I recognise Benjamin Hakizimana, Mugiraneza Jean, and Hakizimana Jacques, who have been very helpful to me.

My deepest and most sincere gratitude also goes out to my supervisors, Prof. Richard Musabe, Prof. Damien Hanyurwimfura, and Dr. Abubakar Diwani, for all of the assistance, advice, and counsel they provided throughout the PhD process.

Lastly, but certainly not least, I reserve my utmost appreciation and gratitude for my spouse, Lilian, and our two children, Adam and Gillian, who have endured my absence from home while I pursued studies abroad.

July 2023 George Yogo Odongo

Abstract

The power distribution network plays a crucial role in delivering electrical power to consumers. However, the lack of feedback mechanisms in legacy power grids prevalent in the Eastern and Southern Africa (ESA) region limits the ability of utility service firms to monitor and respond to abnormal conditions known as electrical faults. This often leads to prolonged blackouts for consumers.

This thesis explores the use of the Internet of Things (IoT) and machine learning to enhance remote fault monitoring on the electrical power distribution grid. The research adopts a design-science approach and investigates both incipient and sudden faults. For incipient faults, the focus is on oil-immersed transformers, with Dissolved Gas Analysis (DGA) data obtained from Kenya Power, a power utility firm in Kenya. The collected data, comprising 2912 records, is subjected to exploratory analysis, confirming its suitability for machine learning training. A machine learning model named KosaNET is developed, trained, and tested, demonstrating superior performance in detecting incipient faults compared to other algorithms, particularly for multinomial data.

To address sudden faults, a LoRa-based platform is developed and deployed. Current sensors are integrated into the distribution grid, and a LoRa-enabled microcontroller transmits data regularly via a gateway. Experimental results reveal that the LoRa-enabled platform successfully triggers an alert at the network monitoring centre within approximately 100 msec of a fault occurrence.

A machine-learning multinomial classification model was also offloaded to the edge of the network for condition monitoring of power transformer units. The model was built using the edge impulse service. From the results, an accuracy of 99.9% was attained, which shows that the edge-deployed machine learning model DGA can perform well even when deployed on the periphery of the network.

The original contributions of this study are manifold. Firstly, a machine learning model is developed to accurately interpret DGA data and detect incipient faults. Secondly, a

LoRa-enabled platform is designed, analysed, and tested for fault monitoring. Thirdly, an intuitive duty cycle is implemented to maximise battery lifespan. Fourthly, data processing and storage functions are offloaded to the edge of the network rather than relying solely on cloud-based solutions. Lastly, future research directions are proposed for further advancements in fault monitoring on the power distribution grid.

Overall, this research demonstrates the potential of IoT and machine learning to enhance fault monitoring and detection, paving the way for more efficient and proactive maintenance of the power distribution grid.

Keywords: AI, Condition monitoring, Edge computing, Gas Analysis, Incipient faults, Internet of Things, LoRa, Power Distribution

Table of Contents

Table of Figures

List of Tables

Nomenclature

ADR	Adaptive Data Rate
ANFIS	Adaptive Neurofuzzy Inference System
ANN	Artificial Neural Network
CD	Cellulose Decomposition
CDR	Coding Rate
CIGRÉ	Conseil International des Grands Réseaux Électriques
CPR	Chirp Rate
CSS	Chirp Spread Spectrum
CT	Current Transformer
dB	Decibel
DGA	Dissolved gas analysis
DHE	High Energy Discharge (Arcing)
DLE	Low Energy Discharge (Sparking)
DPM	Duval Pentagon Method
DR	Data Transmission Rate
DSO	Distributed System Operator
EDA	Exploratory Data Analysis
EEMD	Embedded Electronic Monitoring Device
emf	electromotive force
FLC	Fuzzy Logic Controller
FN	False Negatives
FP	False Positives
GPRS	General Packet Radio Service
GPS	Global Positioning System
H_2	Hydrogen
IDE	Integrated Development Environment
IEC	International Electrotechnical Commission
IEEE	The Institute of Electrical and Electronics Engineers

IoT	Internet of Things
IP	Internet Protocol
k-NN	k-Nearest Neighbour
KP	Kenya Power Company Limited
L-G	Line-to-Ground fault
L-L	Line-to-Line fault
LL-G	Double Line-to-ground fault
L-L-L	Line-to-Line-to-Line fault
L-L-L-G	Line-to-Line-to-ground fault
LoRa®	Long Range
LoRaWAN®	LoRa Wide Area Network
LTE-M	Long Term Evolution for Machines
LV	Low Voltage
MAC	Media Access Control
MCU	Microcontroller Unit
MLP	Multilayer perceptron
MQTT	Message Queuing Telemetry Transport
MV	Medium Voltage
N_2	Nitrogen
NB-IoT	Narrowband-IoT
NiMH	Nickel Metal Hydride
O_2	Oxygen
OpenWRT	Open wireless router
PD	Partial Discharge
PDC	Phasor Data Concentrators
PDS	Power Distribution System
PDT	Packet Delivery Time
PLC	Programmable Logic Controller
PMU	Phasor Measurement Units

PoE	Power-over-Ethernet
ppm	Parts Per Million
PPT	Power Point Tracking
PRR	Packet Reception Rate
PSO	Particle Swarm Optimisation
PSO	Power System Operator
PT	Potential Transformer
PTD	Partial Discharge
PV	Photovoltaic
PWM	Pulse Width Modulation
RF	Random Forests
RF	Radio Frequency
ROC	Region of Certainty
RPMA	Random Phase Multiple Access
RSSI	Received Signal Strength Indicator
RTC	Real-time Clock
SCADA	Supervisory Control and Data Acquisition
SDN	Software-Defined Networking
SF	Spreading Factor
SG	Smart Grid
SNR	Signal-to-Noise Ratio
SSA	Sub-Saharan Africa
SVM	Support Vector Machine
ToA	Time over the Air
TTN	The Things Network
WAN	Wide Area Network
WSN	Wireless Sensor Network

Chapter 1

Introduction

1.1 Background to the Research Project

Nowadays, the supply of electric power is so pervasive that it is now a commodity that is often taken for granted. However, the complexities of managing the power distribution grid and the efforts that go into maintaining a steady and stable supply are far from trivial but are becoming increasingly challenging [1]. Power distribution systems typically consist of network branches spread across hundreds of thousands of kilometres, as shown in Figure 1-1. As a result, they are highly susceptible to flaws caused by several factors, such as unfavourable weather and ageing infrastructure. Faults in the distribution network are to blame for more than 80% of customer outages [2]. Faults should be swiftly located, isolated, and fixed in order to lessen the social and economic burden of power outages. Outage management is the process of figuring out what went wrong and fixing it. A key part of this process is locating the precise location where a problem has occurred [2].

Fault detection techniques employed by utility service provision companies in the Eastern and Southern Africa (ESA) region have primarily relied on manual reporting by customers about power outages in their vicinity. This is especially true for the distribution line, where affected customers are expected to either make a telephone call or physically visit the offices of the affected utility company to report an incidence [1]. Whenever a fault occurs on a section of the power distribution grid, which consequently results in a shutdown of power, consumers are subjected to long and protracted episodes of blackouts. This is due to the slowness and unhurried manner in which it takes for the report about the fault to reach the nearest regional office, as well as the time it takes the regional office to respond, mobilise, and conduct repairs. The

technical team needs time to find the problem, figure out what needs to be fixed, and fix it, which can take days or even weeks, making the problem worse [3], [4]. This is especially true when expensive, uncertain parts need to be installed. This method of fault resolution is highly customer-laden and fails to aid in the speedy resolution of power blackouts, culminating in financial losses not only for the consumers but also for the service provider.

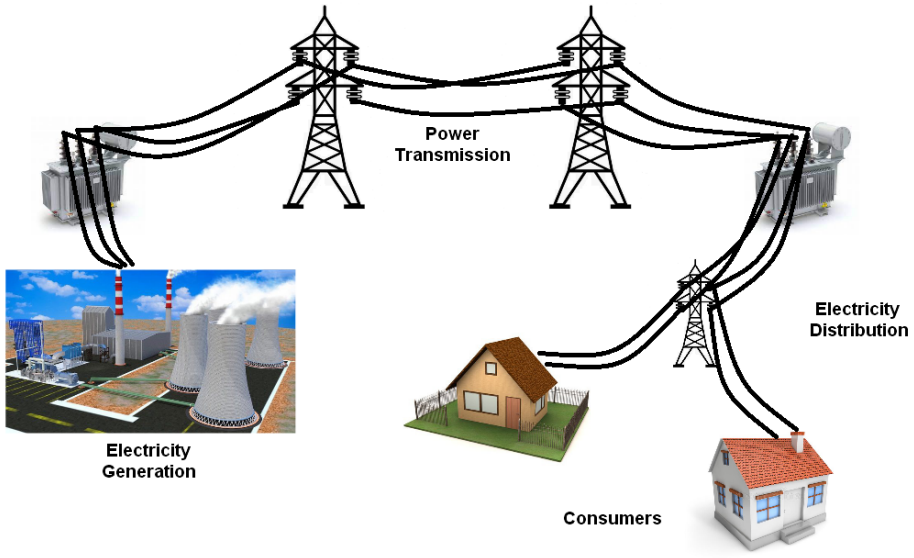

Figure 1-1: The electricity generation, transmission, and distribution (Source: Author)

The Internet of Things (IoT) combined with embedded machine learning (ML) algorithms has unlocked new potential avenues for real-time monitoring of problems within electricity distribution systems. The availability of high-precision sensors and telematics opens up new techniques for power distribution equipment condition monitoring. IoT is a field that is growing quickly. Embedded sensors can be used to monitor equipment, conduct data analytics, and make preventative maintenance plans.

The power distribution grid in Sub-Saharan Africa faces significant challenges in fault detection, localization, and response time, resulting in prolonged power outages and inefficient maintenance procedures. The lack of real-time monitoring capability and timely fault identification hampers the overall stability of the grid, exacerbating the region's energy deficit and hindering socio-economic development. The existing

system that utility service providers rely on for monitoring and fault location on the electric grid is inadequate because it does not monitor the distribution section of the network, and yet more than 80% of outages experienced by customers are attributed to faults on the distribution network [5], [6]. Not only is the distribution grid bigger in terms of coverage, but more than 80% of the faults observed on the grid manifest on the distribution network [7]. Grid operators have no means of monitoring their distribution grids in real-time. Instead, when a fault manifests itself on the distribution grid, affected customers are expected to either make a telephone call or visit the offices of the utility provider [1], [8]. Equipment will certainly fail, distribution lines will certainly break, and short circuits will surely occur, resulting in power outages, but without the user relaying this information to the utility provider, the company will remain completely unaware. This paucity of information not only lengthens the duration of the power outage but also results in revenue losses for both the utility provider and clients in terms of lost productivity. This has created a situation where consumers have levelled severe criticism against Kenya Power for operational inefficiencies [9]. Developing countries, and particularly those in the ESA region, cannot achieve full industrialization status if the current condition persists [10].

1.2 Statement of the Problem

There is a lack of research and empirical evidence regarding the effective utilisation of the Internet of Things (IoT) for fault monitoring in the electrical power system, particularly within the context of sub-Saharan Africa. The existing literature does not adequately address the specific challenges and opportunities associated with using IoT technologies to monitor faults and identify their precise location in the power distribution system. This knowledge gap hinders the development of efficient and reliable fault detection systems, leading to prolonged power blackouts and suboptimal maintenance strategies [1]. Therefore, there is a need for comprehensive research to explore the potential of IoT and machine learning algorithms in addressing these challenges and improving fault prediction and detection in the power distribution system, with a focus on a case study of Kenya Power (KP).

1.3 The General and Specific Research Objectives

This thesis investigated and explored how the Internet of Things (IoT) and machine learning techniques can be used to enhance remote fault monitoring on the electrical power distribution grid and to further identify the precise location where an incident has occurred. In particular, the following specific objectives have been achieved:

(i) A machine-learning model for fault prediction using dissolved gas data from the power distribution system has been designed and developed.

(ii) A reliable IoT-based platform incorporating sensors, data analytics, and communication infrastructure has been designed and developed for remote fault detection and monitoring of the power distribution network.

(iii) An edge-based machine-learning model for condition monitoring of electrical transformer units has been developed and evaluated.

1.4 Significance of the Study

The ancient electrical power system, which is commonly in use today, was not designed to allow for bi-directional communication. This lack of two-way communication has resulted in a total deficiency of feedback for the operator, who is unable to tell when issues such as power outages occur on their grids or when equipment that is deployed is in need of maintenance. Kenya experiences over 700 hours of blackouts annually that result in a loss to Kenya Power of 5.5% of the total annual sale of power [11]. Kenya Power had sales revenue of Sh144.1 billion last year (2021), implying that power disruptions cost the retailer close to Sh3 billion. A recent investigation by the Centre for Global Development implies that inconsistent electricity and interruptions cost some enterprises up to 31% of their sales in sub-Saharan Africa [12], [13]. Energy consumption in an economy is a key indicator of economic activity and is often a determinant of the growth rate of the gross domestic product (GDP). This means that higher energy absorption implies a bigger GDP, and vice versa. Even though some industrialised countries are pursuing smart grids as a potential solution, they have not comprehensively explored the use of the Internet of Things to solve this challenge. Additionally, many developing nations in sub-Saharan

Africa that give priority to other sectors like health and education view smart grids as expensive and requiring large initial investments.

In this study, we explore the use of IoT technology as a potential solution for creating robust feedback fault monitoring on the power distribution grid. IoT is a new technology that promulgates the idea that devices anywhere, at any time, using any means, can autonomously connect to the internet and share data and information, thus enhancing our (the user's) perception of the world around us. The discovery of novel fault monitoring techniques on the power grid may lead to the following results:

- Reliability and Resilience: Faults in the power distribution grid can lead to power outages, causing disruptions in daily life, businesses, and critical infrastructure. By developing effective fault detection methods, we can improve the grid's reliability and resilience, minimising downtime and ensuring uninterrupted electricity supply.
- Cost Efficiency: Traditional fault detection methods often rely on manual inspections or periodic maintenance, which can be time-consuming and costly. Implementing enhanced, automated fault detection techniques, such as IoT-based systems, can significantly reduce operational costs by identifying faults in real-time and enabling targeted repairs or maintenance activities.
- Faster Response and Restoration: Rapid detection of faults allows for quicker response times and faster restoration of power. With real-time monitoring and automated fault detection systems, utility companies can promptly identify the location and nature of the fault, enabling them to dispatch repair crews efficiently and minimise downtime for consumers.
- Preventive Maintenance: Early detection of faults can facilitate preventative maintenance practises. By identifying potential issues before they escalate into major faults or failures, proactive maintenance can be performed to prevent outages and extend the lifespan of the grid infrastructure. This helps optimise resource allocation and reduce infrastructure maintenance costs.

- ❖ Safety and Security: Faults in the power distribution grid can pose safety hazards, such as electrical fires or equipment malfunctions. By promptly detecting faults, safety risks can be mitigated, ensuring consumers' well-being and that of utility personnel. Additionally, effective fault detection systems can also contribute to grid security by detecting and alerting operators to anomalies or potential cyber threats.
- ❖ Grid Optimisation and Planning: Accurate fault detection data provides valuable insights into the power distribution grid's health and performance. Analysing fault patterns and trends can help utilities optimise grid operations, identify areas for infrastructure improvement, and plan future expansions or upgrades strategically.

On the whole, this research will benefit society by reducing downtime on the power grid. With reduced downtimes and shorter durations of power blackouts, it is expected that this will result in greater volumes of production that, in turn, will result in improved economic performance. This will in turn result in higher per capita income and, hence, lower levels of poverty in society. This study's findings are expected to find relevance with power system operators, especially those who spend hundreds of hours troubleshooting the power distribution system and lose thousands of dollars in downtime. It has been reported in the literature that upwards of 85% of faults that manifest on the power grid occur on the power distribution system. By simply solving the issue of fault detection, we anticipate that the duration of power outages on the grid can be kept to a minimum. This will not only result in high levels of customer satisfaction but also in higher productivity, which will have a positive effect on the GDP.

1.5 Statement of Contribution

In this dissertation, we have introduced several smart grid features into the legacy power grid by developing an IoT-based platform that can be used for efficient monitoring of the power grid for faults, particularly those that are incipient. The

platform consists of sensors that monitor various parameters that were analysed using an ML-trained model. The following is a recap of some of the research contributions of the study:

1. A machine-trained model christened KosaNET has been developed that was able to take in six inputs and produce a single output that represented a predicted fault. The six independent inputs were numerical in nature, with the dependent variable being categorical. The full discussion of the KosaNET model is discussed in the first journal paper found in [14].
2. A LoRa-enabled cloud-based platform to host the KosaNET model has been created. We developed, analysed, and evaluated the platform and presented our results in the second journal paper presented in [15].
3. This thesis has exposed performance issues related to long-range data communication, particularly when using LoRa. Lessons learned and best practises when deploying LoRa have been documented.
4. This study has implemented a duty cycle of about 1%. Since idle components were put to “sleep” when not performing any tasks, we were able to maximise the lifespan of the battery. This significantly reduced the power consumption of the model and greatly extended the lifespan of the electronic monitoring device.
5. We have designed and built an AI prediction model to relegate data processing and storage functions to the networks’ edge rather than in the cloud, as presented in [16]. The main advantage of this is that the model worked in areas where there is no Internet connectivity, yet it still maintained a high degree of accuracy.
6. Finally, this study has suggested future research directions that researchers in the field can focus on.

1.6 Thesis Outline

The linkage between the problem statement, objectives, and articles is illustrated in Figure 1-2. The problem statement was decomposed into three objectives. Each objective generated a publication, as shown in the figure. A concluding chapter is then

written, summarising the thesis. The research was carried out in several stages and was preceded by an exhaustive literature review on the existing tools and methods for fault monitoring of the electricity distribution network. In the first and preliminary stages, different approaches to fault monitoring of the electricity distribution network were examined and compared in terms of their efficiency and cost implications. During this process, fault monitoring parameters and potential predictors were identified and selected. The second phase involved the conceptualization, design, and development of the predictive model KosaNet. The model was tested using actual DGA data that was obtained from Kenya Power Ltd., the country's sole provider of electricity. The data was divided into 2912 records and arranged into seven columns, with the seventh column labelling the observed fault. Six of the columns contained input variables that represented the gas levels in ppm (parts per million). The third stage involved the modelling, development, and deployment of an Internet of Things platform for efficiently monitoring the power distribution system. The monitoring system included a web-based interface for data sharing and visualisation. The prototype was deployed and tested on an actual distribution network in the South Rift region of Kenya. In the fourth stage, the model was deployed to the edge of the network. A miniature library was created so that it was possible to deploy the library on devices low on resources, such as Arduino.

The six chapters that make up this thesis's substance are described as follows:

Chapter 1: Provides a backdrop for the research, a statement of the problem, the research aims and objectives, the research contributions, and the thesis outline.

Chapter 2: This chapter comprises a summarised narration of the literature review. It talks about the power system in Kenya, fault finding and prediction techniques on the power distribution network, fault types and their causes in the electrical power system, the use of IoT and machine learning in the power utility sector, long-range and wide-area data transmission methods, low-power IoT techniques, dissolved gas analysis (DGA) fault interpretation

methods, and explorative data analysis. Particular attention is paid to LoRa, which is subsequently used throughout the research experiment.

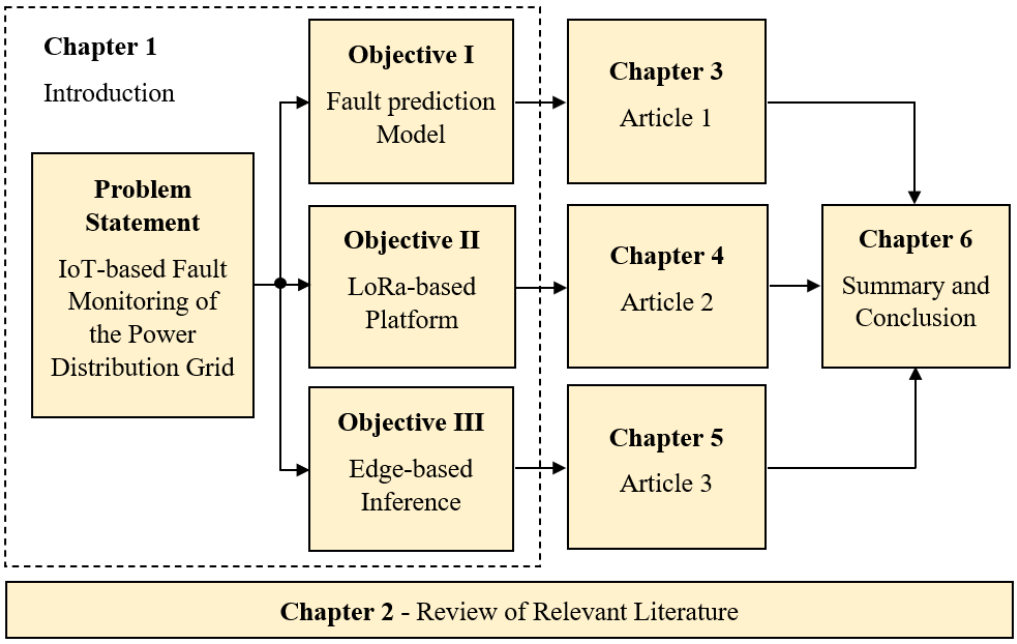

Figure 1-2: Problem Statement, Objectives, and Article Linkage (Source: Author)

Chapter 3: Describes the multinomial classification model that was developed for DGA data. This comprises the experimental arrangement and protocols, the distribution of generated gases, the main gases generated by each type of fault, as well as the results reported in the literature. Particular attention was paid to models with multiclassification capability. A comparison of their performances is also presented in this chapter.

Chapter 4: Describes in detail an IoT-based, self-powered fault detection and location reporting rostrum for the power distribution grid. The platform incorporated long-range (LoRa) technology for the wide-area transmission of data. It describes in detail how the platform is designed, developed, and tested.

Chapter 5: Describes a platform for online condition monitoring of oil-immersed transformers. In this chapter, we specifically discuss the development of a library that can be deployed on Arduino. The library was developed using Tiny Machine Learning (TinyML), which is a briskly growing and emerging

technological space at the cloverleaf of machine learning algorithms and lowly-priced embedded devices.

Chapter 6: Concludes this thesis by recapping the main findings made in the three phases of this research. It recapitulates the key findings of this study and makes recommendations for future research on relevant themes.

Chapter 2

Literature Review

2.1 Introduction

The electrical power grid of today has metamorphosed into a gigantic and sophisticated entity supplying millions of consumers with electrical power. In order to respond to the modern demands and expectations of the electrical power grid, such as self-healing, consumer involvement, enhanced power quality, and availability, many countries in the developed world have expressed interest in the smart grid (SG). The smart grid is an expanding network of automated computing, transmission systems, and new tools and technologies that work together to transform the grid into one that is greener, more reliable, responsive, secure, and effective. It is made up of an ever-expanding network of transmission cables, technologies, and equipment that work together to react quickly to the electrical demands of the twenty-first century [17], [18]. The smart grid enables a two-way interchange of data and information between the service provider and its users. The smart grid facilitates the incorporation of emerging technologies such as solar and wind-produced energy as well as the charging of plug-in electric vehicles.

The smart grid is expected to replace the old infrastructure of the contemporary power grid with consumer engagement, and utilities will be able to better connect with consumers to aid in the management of their electrical needs. The smart grid allows customers to take charge of their power consumption. Utilities may provide their customers with far better information for the management of their electricity bills by regularly measuring the home's electricity consumption using a smart metre. However, due to the high installation cost, many countries in sub-Saharan Africa have not considered the smart grid a viable solution to their ongoing predicament.

2.2 Power Distribution System in Kenya

The electricity power system can be split into three generic segments, specifically generation, transmission, and distribution. In broad terms, the distribution system is that section of the electric power system that is between the power substation and the customers' service switches [19]. The power distribution substation takes several design considerations into account. Two of these are the high-side voltage and the low-side voltage. The voltage of the high-side bus may range anywhere between 34.5 kV and 345 kV. The low-side voltage is typically between 240 V and 110 V, depending on the region. The distribution system comprises several components: distribution substations, sub-transmission systems, distribution transformers, secondary circuits, and distribution primary feeders [20].

Kenya's energy sector is unbundled into five sub-sectors: generation, transmission, distribution, regulation, and policy. The major industry players in the power sector in Kenya are Kenya Power (KP), Kenya Electricity Generation Company (KenGen), Geothermal Development Company (GDC), and Kenya Electricity Transmission Co. Ltd. (KETRACO). GDC and KenGen are in the generation sector, while KETRACO is tasked with stepping up the generated electricity to 132 kV, 220 kV, and 400 kV and transmitting it up to a stepdown substation, where the electricity is stepped down to 66/33 kV for Kenya Power to distribute to the final consumers. In Kenya, Kenya Power is the only power distribution company. The company purchases energy from power generation companies and sells it to end consumers. Kenya's transmission network spans over 14,724 km [12] and comprises lines of different voltages.

Kenya's energy mix currently comprises green energy sources, with solar, wind, hydro, and geothermal contributing about 81% of total power generated in 2021 [21]. The rest is made up of biomass, imports, and thermal sources. Geothermal is rapidly expanding as more investments are made to wean off expensive heavy fuel oil (HFO) plants and become less dependent on hydroelectricity, which is significantly reduced during the dry season and during rainwater scarcity. Figure 2-1 shows the energy mix of Kenya as

of June 2021 [22]. The diagram shows that Kenya is heavily reliant on renewable energy sources for its energy needs.

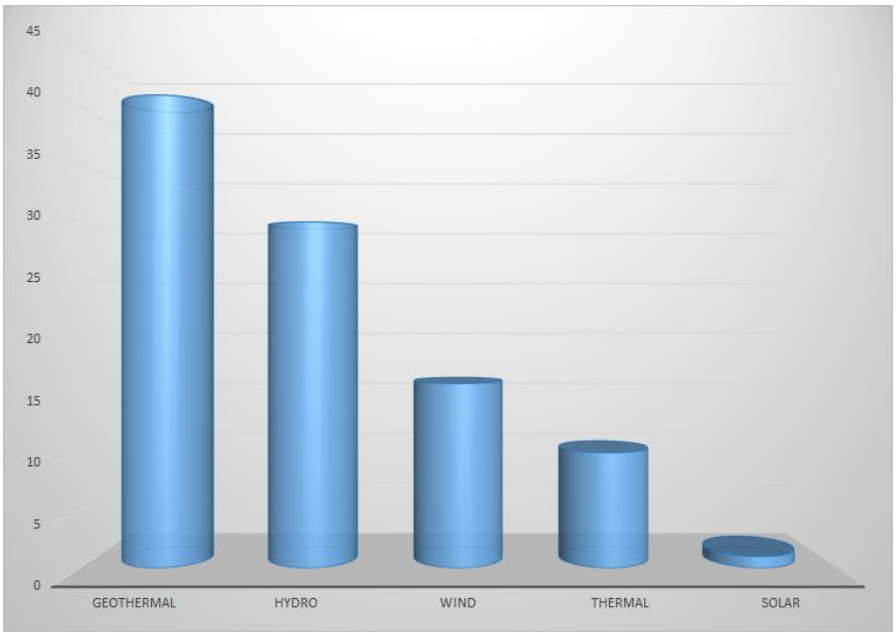

Figure 2-1: Kenya's Energy Mix (Source: Author using data from [21])

We now report on some of the fault detection techniques that have been reported in the literature.

2.3 Fault Detection and Prediction Techniques on the Distribution Network

The electric distribution network is vulnerable to many types of faults. These faults can be attributed to man-made or natural causes (such as lightning strikes). Regardless of the cause, fault conditions are undesirable not only because they affect system reliability and result in costly repairs but also because they result in power outages, thereby interrupting the customers' productivity [23].

Detecting faults and finding the site of their occurrence is an expansive field of study, and several detection schemes for electrical grids have been discussed in the literature. These can be classified into two main categories: conventional techniques and artificial intelligence techniques [24]. The latter includes techniques such as artificial neural networks, support vector machines, fuzzy logic, genetic algorithms (GA), and

matching approaches, while the former includes the traveling wave method and impedance-based methods. In [25], the authors combined the wavelet transform with the traveling wave distance measuring principle to detect and localise power system faults. The fault point was located by using the double terminal method of the travelling wave. In [26], the travelling wave approach to fault location is once again examined, but this time the authors use the wavelet domain to correct for the dispersion effect that the travelling wave causes. Because of this, it is now possible to mathematically pinpoint the position of the error. This approach is not without its drawbacks, chief among them being the requirement of high-speed data capture equipment.

In [27], a real-time online fuzzy logic-based fault detection and classification method is presented. It considered post-fault currents for the three phases and positive sequence current samples. The authors were, however, more interested in transmission line faults than distribution line faults, which have more frequent manifestations. In [28], fuzzy logic is used to detect and locate faults on overhead transmission lines with better membership functions. The fuzzy logic system, however, fails to consider faults beyond the transmission line. In [29], a fault detection scheme for renewable energy systems based on wavelet transformation is presented. Through a mathematical analysis of signals in time and frequency, the wavelet transformation can determine whether or not a circuit has a high impedance because of its sensitivity to rapid changes.

ZigBee is shown to be capable of detecting and localising defects on the transmission line [30]. This capability is proven. When a fault with high impedance is discovered, it will transmit a signal to the substation that is closest to the location. However, there has been no research conducted into how electromagnetic interference affects communication. For the purpose of monitoring the transmission line described in [31], a high-impedance fault detection approach is utilised. The GSM network serves as the vehicle for all internal communication within the system. The method, on the other hand, is not sufficiently scalable to accommodate the extensive nature of the

transmission network. In reference number [32], the concept of using sensor networks for monitoring and locating faults in subterranean distributed lines is discussed. The authors proposed installing a distributed sensor network above ground along with many probes that would be planted underground in order to monitor key distribution lines. The proposed method, however, overlooks overhead lines. A framework that is proposed in reference number [33] is one that is based on wireless sensor networks and that consists of a clustering method. The framework makes the promise that it will stabilise the energy consumption of the networks by utilising a hybrid media access protocol that can manage varying levels of traffic. A method for the location of faults is described in reference number [34]. This method makes use of fault indicators that are attached to the switch and combines them with the distribution power grid. The authors hypothesise that a fault indicator might be inserted in the feeder segment and that by analysing the signals that were produced, the precise location of the segment that was faulty could be established. However, the system has excessive reliance on SCADA, which is an expensive technology. The authors of [35] investigated different approaches to fault localization based on centric systems that can be used for medium distribution voltages. A DC voltage test is utilised by the system in order to locate faults that are underground. The subject of [36] is fault detection and localization in underground cables. To do this, the authors use a technique that is based on Ohm's law and involves connecting a collection of resistors to each other in such a way that each resistance represents a specified cable length in kilometres. Failures in the power grid can be anticipated via neural network learning, as shown in [37]. The research showed that neural networks can be utilised to construct predictive tools that can be employed for the examination of the components of an electric grid. An investigation on the use of machine learning as a methodology for facilitating predictive maintenance of electrical substation equipment is presented in [38]. Infrared thermography is the method used to obtain a heat signature. The use of an infrared camera allowed for the generation of thermal pictures, which were then analysed and divided into defect and non-defect categories. However, deep learning methods were

not investigated in this particular study. A model that can forecast the frequency of the power system after a disturbance is discussed in reference number [39]. A cross-entropy ensemble algorithm was used for this purpose. The research, on the other hand, did not consider the issue from the point of view of machine learning. In conclusion, it should be mentioned that a number of different methods have been taken in order to address the issue of detecting defects and discovering their location on the electric grid. The vast majority of these techniques, however, call for an excessive number of distinct pieces of apparatus, which renders them infeasible to implement, while others are both inefficient and prohibitively expensive. In contrast, the strategy that we have chosen to implement here is not just effective but also practical and efficient.

2.4 Types of Faults and Their Causes

A fault is any change that is not wanted and that throws off the natural equilibrium of the power system. The majority of power system problems result in a condition known as a short circuit, which takes place when an insulator fails to perform its function properly. Insulation has broken down, which is a problem because insulation is the substance that should be placed between high and low voltages to prevent an unexpected flow of current. If the magnitudes of the three-phase voltages as well as the phase discrepancies between them are the same in relation to one another, then it is said that the voltages are balanced [40]. Additionally, there is no difference in the mutual impedance that exists between the three phases.

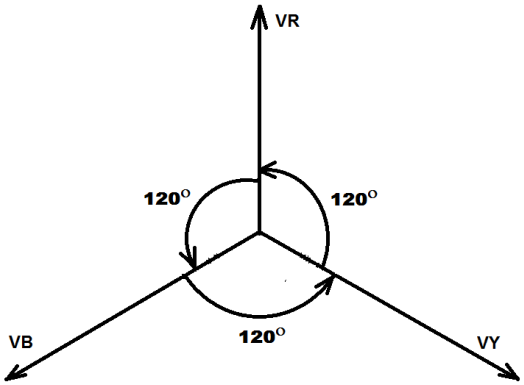

Figure 2-2: A three-phase balanced system (Adapted from [41])

The electrical power system typically runs in a balanced condition, where all the equipment carries normal load currents and the line voltages remain within predetermined levels. These conditions allow the system to function without interruptions or disruptions in service. A three-phase balanced system is shown in Figure 2-2. Inaccuracies within the system, on the other hand, may result in the disruption of this situation. If the electrical current that is flowing during a fault is greater than the interrupting rating of the protective device, the results can be catastrophic and pose a significant risk to human life [40], [42]. Furthermore, they have the potential to cause serious injuries as well as extensive damage to the apparatus. Because it is producing a low-resistance state between the two conductors that are delivering electric power, the current that is flowing through a short-circuit defect is often several times larger than the current that is flowing normally. This causes an excessive amount of current to flow through the power system via the channel of low resistance, which may even cause the power source to explode, resulting in intense heat and a fire. This is the outcome of an excessive amount of current flowing through the power system [43].

During normal operation, the electrical power network is frequently vulnerable to a wide variety of different types of defects. It is possible for the specific characteristic values of the equipment, such as impedance, to shift from their normal values to new ones once a failure occurs, and this will continue until the fault has been resolved.

Table 2-1: Types of Faults that manifest on the Power Network System

TYPE OF FAULT	SHORT FORM	SYMMETRICAL OR UNSYMMETRICAL	ODDS
Three phase line to ground fault	3LG	Symmetrical	2 – 3%
Three phase line to line fault	3LL	Symmetrical	Less than 1%
Single phase to ground	1LG	Unsymmetrical	70 – 80%
Line to line fault	1LL	Unsymmetrical	15 – 20%
Double line to ground fault	2LG	Unsymmetrical	Less than 10%

There are a variety of different factors that can contribute to the fault circumstances listed in Table 2-1, including the weather, smoke from nearby fires, broken equipment, or even human error [44]. Lightning strikes, accumulation of snow and ice on transmission lines, heavy rains, and strong winds are all examples of environmental conditions that have a high probability of disrupting the power supply and causing damage to electrical installations. Other environmental factors that have a high likelihood of causing either of these things include smoke particle-induced ionisation of the air around the overhead wires, which can result in the creation of sparks between the lines or between the conductors and insulators [45], [46]. As a result of the high voltages caused by the flashover, insulators will lose their capacity to provide insulation. Due to malfunction, insulation failure, or ageing of windings and cables, a wide variety of electrical equipment, such as motors, reactors, generators, transformers, and switching devices, can cause short circuits [47], [48]. This can result in high current flow in these equipment or devices, which causes greater damage to them. Errors caused by humans occur when the rating of devices or equipment is inaccurate or when a technician forgets to return metallic or conducting pieces after performing servicing or maintenance on the device.

2.4.1 Symmetrical Faults

If there is a short circuit affecting any of the phases, then it is said to be a symmetrical fault in the system. In the event that a symmetrical fault shunts to the ground, potentially damagingly high currents are grounded, which will prevent further damage to the equipment. The only possible sequences for symmetrical faults are positive ones, as they are balanced. Inconsistencies in symmetry can be seen in one of two ways:

1. Three-phase line-to-ground fault
2. Three-phase line-to-line fault

2.4.1.1 Three-phase line-to-ground fault

When a fault of this type occurs, each of the three phase wires will short out and become grounded. This defect results in a balance fault and has a chance of occurrence that ranges between 2 and 3 percent.

2.4.1.2 Three-phase line-to-line fault

The three-phase line-to-line flaw has similarities with a three-phase line-to-ground fault; however, with this defect, the phase wires are shorted but there is no simultaneous grounding. A balance fault is produced as a result of this. In addition, a balance fault is produced as a result of this defect, and the probability that this problem would arise is significantly lower than 1%. In addition, the likelihood of this defect occurring is significantly lower than 1%.

2.4.2 Unsymmetrical faults

Unsymmetrical faults are any defects in the power system that cause it to be off-kilter in some way. These flaws contain components with positive, negative, and zero sequences, respectively. There are several distinct varieties of asymmetrical defects, including the following:

1. Single-phase to ground fault
2. Two-phase to ground fault
3. Phase-to-phase fault
4. Open circuit fault

2.4.2.1 Single-phase to ground fault

When a problem of this nature arises, the phase wire or the ground wire may be the one that becomes disconnected due to a short. This kind of fault can occur when the insulation is damaged, the phase conductor is broken, and there is a short circuit between the phase conductor and the ground. According to some estimates, there is a 70–80% likelihood that this flaw will manifest itself [46]. Because there are three phases suspended on a pole, which runs for several miles, and because on both sides of the pole

there are vegetation and animals that are around it, this kind of defect occurs most frequently in power systems [47], [48]. As a result, there will be a line-to-ground fault created if a tree limb accidentally brushes up against that line. This type of fault is recreated when, for example, a monkey, a bird, or any other animal touches the ground and line wires simultaneously. It will result in a disruption in the normal functioning of the line that is grounded.

The load current is presumed to be zero because it is assumed that the system is not loaded at the time of the fault. Figure 2-3 illustrates a three-phase system with the neutral grounded. The line currents of the system are I_R, I_Y and I_B whereas the potential difference is E_R, E_Y and E_B and Z is the impedance.

$$\begin{bmatrix} I_{RO} \\ I_{R1} \\ I_{R2} \end{bmatrix} = \frac{1}{3}\begin{bmatrix} 1 & 1 & 1 \\ 1 & \alpha & \alpha^2 \\ 1 & \alpha^2 & \alpha \end{bmatrix}\begin{bmatrix} I_R = I_F \\ I_Y = 0 \\ I_B = 0 \end{bmatrix}$$

$$I_{RO} = \frac{I_R}{3}; \qquad I_{R1} = \frac{I_R}{3} \qquad I_{R2} = \frac{I_R}{3}$$

$$I_{RO} = I_{R1} = I_{R2} = \frac{I_R}{3} = \frac{I_f}{3}$$

$$I_{R1} = \frac{I_f}{3}$$

$$I_f = 3I_{R1} \tag{2-1}$$

Equation 2-1 demonstrates that the fault current will be extremely high and has the potential to significantly impair the surrounding machinery.

2.4.2.2 Two-phase to ground fault

Any two of the phases can become short-circuited with the ground wire when a two phase-to-ground fault occurs. The likelihood of encountering a defect of this kind is far lower than 10% [47]. Let us suppose for a moment that the load on the system had been removed prior to the occurrence of the current. This would imply that there was no flow of current across the circuit. A two-phase ground fault is the name given to the defect

that occurs when any two phases of the grid are accidentally connected to the ground and to each other as shown in Figure 2-4.

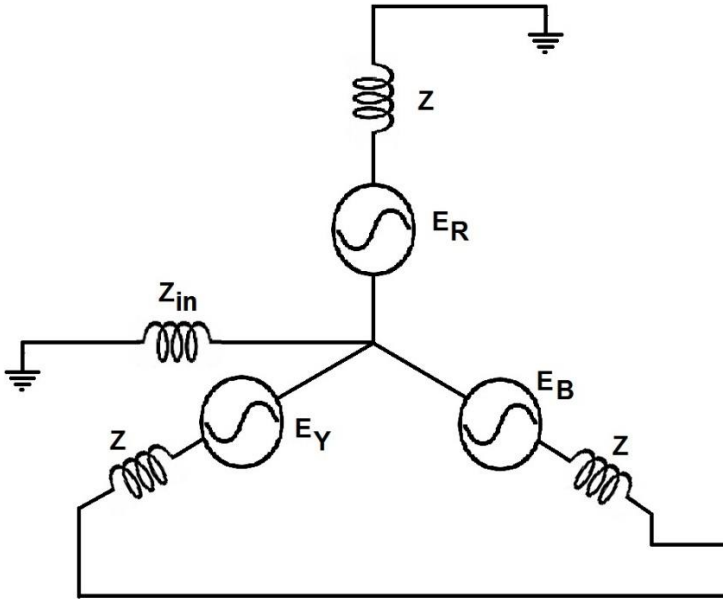

Figure 2-3: Three-phase diagrammatic illustration with a grounded neutral (Adapted from [41])

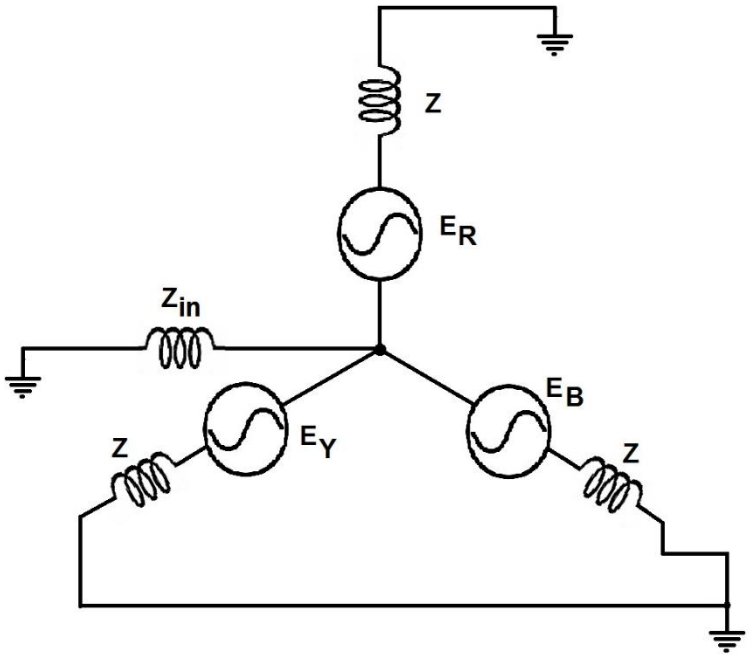

Figure 2-4: Double phase to ground fault (Adapted from [41])

Assuming that the Y and B phases have become disconnected from the system and are now flowing to the earth, in this scenario, the system will experience a significant current flow resulting from the fault. The value of the fault current I_F will be as follows:

$$I_F = I_{Y+} I_B$$

$$\text{So } V_B = V_Y = 0$$

Therefore, the current can be denoted as:

$$I_{RO} + I_{R1} + I_{R2} = 0$$

And the sequence of voltage drops can be obtained using Equation 2-2:

$$\begin{bmatrix} V_{RO} \\ V_{R1} \\ V_{R2} \end{bmatrix} = \frac{1}{3} \begin{bmatrix} 1 & 1 & 1 \\ 1 & \alpha & \alpha^2 \\ 1 & \alpha^2 & \alpha \end{bmatrix} \begin{bmatrix} V_R \\ V_Y = 0 \\ V_B = 0 \end{bmatrix}$$

$$V_{RO} = \frac{1}{3}[V_R + 0 + 0]$$

$$V_{RO} = \frac{V_R}{3}; \quad V_{R1} = \frac{V_R}{3}; \quad V_{R2} = \frac{V_R}{3}$$

$$V_{RO} = V_{R1} = V_{R2} = \frac{V_R}{3} \tag{2-2}$$

To get the currents when the circuits are connected in parallel, the magnitude of the current can be determined using Equation 2-3.

$$I_{RO} = \frac{1}{3}[I_R + I_Y + I_B]$$

$$I_{RO} = \frac{1}{3}[0 + I_F]$$

$$I_f = 3I_{R0} \tag{2-3}$$

2.4.2.3 Phase-to-Phase fault

The phase wires are shorted out in this kind of fault that involves any two phases and results in the power system's characteristics losing their balance, as shown in Figure 2-5. The likelihood of this kind of fault occurring is between 15 and 20%.

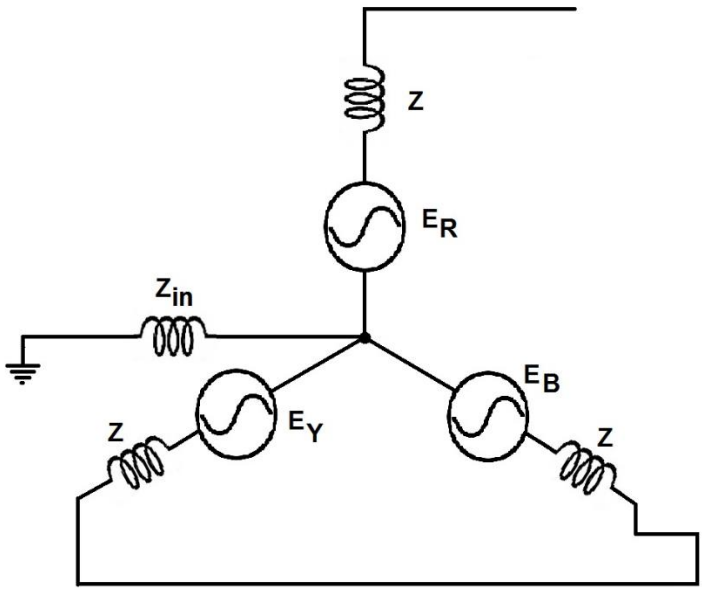

Figure 2-5: Phase-to-Phase Fault (Adapted from [41])

In order to analyse this fault, it is assumed that there is no load on the system when the defect occurs, which implies that the current is null. The current is zero in all phases because the fault is not present. It is further assumed that the B phase and Y phase are shorted when the fault occurs, in which case the currents I_B and I_Y cease to be zero as shown in Equation 2-4. As a result of the two terminals being shorted, their combined potential is zero.

$$V_B - V_Y = 0$$

$$V_B = V_Y$$

$$I_Y = I_f = -I_B \tag{2-4}$$

Supposing the R phase is taken as the reference phase after a fault has occurred, I_R will cease to be zero. Furthermore, I_B, I_Y and I_R will be imbalanced, and the current in the R phase will no longer be zero, as shown in Equation 2-5.

$$I_R = 0$$

$$\begin{bmatrix} I_{RO} \\ I_{R1} \\ I_{R2} \end{bmatrix} = \frac{1}{3}\begin{bmatrix} 1 & 1 & 1 \\ 1 & \alpha & \alpha^2 \\ 1 & \alpha^2 & \alpha \end{bmatrix}\begin{bmatrix} I_R = 0 \\ I_Y = 0 \\ I_B = -I_F \end{bmatrix}$$

$$I_{RO} = \frac{1}{3}[0 + I_F + (-I_F)] \tag{2-5}$$

Due to the fact that this channel is reserved only for zero sequence current, Z_{in} will not have any current flowing through it, neither negative nor positive. The magnitude of the fault current can be calculated as follows:

$$I_{R1} = \frac{1}{3}[0 + \alpha I_F + (-\alpha^2 I_F)]$$

$$I_{R1} = \frac{1}{3} I_F[\alpha - \alpha^2]$$

$$3I_{R1} = I_F[\alpha - \alpha^2]$$

$$I_F = \frac{3I_{R1}}{[\alpha - \alpha^2]} \tag{2-6}$$

$$I_{R2} = -\frac{1}{3} I_F[\alpha - \alpha^2] \tag{2-7}$$

Equation (2-8) can be derived from Equation (2-6) and Equation (2-7) as follows.

$$I_{R1} = -I_{R2} \tag{2-8}$$

2.4.2.4 Open circuit fault

The open circuit fault results in the interruption of the conducting route, leading to a cessation of current flow through the system. This occurs when one or more of the phase wires become broken, causing an imbalanced current to flow. Consequently, the equipment is at risk of overheating. Blown fuses or improper operation of the circuit breaker in one or both phases can cause this fault.

2.4.2.5 Winding fault:

A winding fault is a critical issue that occurs when the windings of a transformer or motor sustain damage and subsequently short out. This type of fault can have significant implications for the performance, reliability, and safety of the electrical apparatus. When the windings become damaged, such as due to insulation breakdown, mechanical stress, or thermal stress, it can lead to various types of faults, including short circuits. This opening line highlights the fundamental nature of a winding fault as a result of damage and subsequent shorting of the windings.

2.5 IoT and Machine Learning in the Power Utility Sector

The concept of an “Internet of Things” (IoT) interconnected world is increasingly inching closer and closer to becoming a reality as technology continues to infiltrate deeper and deeper into the fundamental aspects of our everyday lives. IoT is an evolving, innovative paradigm that proposes that commonplace devices can connect to the internet anywhere and everywhere and that these devices can independently send and receive information [49]. The apparatus may be outfitted with one or more sensors and actuators, which would enable them to probe their environment, send data for analysis to some cloud-based platform, and receive instructions on how to proceed based on the results of the processing [50]. The equipment may also be fitted with a processor, which would allow it to communicate with the sensors and actuators [51]. The Internet of Things has resulted in the proliferation of sensor-enabled devices in many different fields of human endeavour, including medicine, transportation, agriculture, the energy sector, and industry [51]. The investigation of the usage of

intelligent electronic devices is a trend that runs throughout all of these applications. This is a common feature. Specifically, there has been an application of machine-learning algorithms, which are programs that give otherwise mindless machines artificial intelligence. Computers are given the power to learn on their own through the study of machine learning, an area of computer science that makes computers appear to learn something without the need for explicit programming [52]. The swift proliferation of Internet-capable, Internet-ready devices has catapulted modern society into a new era, one in which machines and nodes have the independent capacity to gather data from their surroundings and respond to the data so gathered. Individuals and organisations have begun to wonder what kinds of insights may be derived from the amount of data gathering capabilities that are currently available. However, because more and more smart gadgets are being used in everyday life, the capacity to collect data in terms of volume, variety, and speed is only going to continue to grow. This, as a result, calls for new approaches to data analytics, particularly those that are able to process streaming data [53], [54]. The scaling up of machine learning algorithms to tackle the challenge of enormous data sets is an ongoing research focus. In the reference [55], the difficulties that arise for machine learning as a result of a disproportionate increase in the size of either the training set or the test set as well as the dimensionality are investigated. In the article referred to as [23], the process of fault location utilises a combination of the Monte Carlo, fault tree, and risk matrix methods. According to the findings presented in reference [56], the k-nearest neighbour (*k*NN) method can reliably categorise binary series signals with an extremely high degree of precision. In the article cited as [57], Jinzhong *et al*. examine a variety of methods that are implemented into computer technology in order to create artificial intelligence. In particular, the author contrasts several machine learning approaches, such as support vector machines (SVM), artificial neural networks (ANN), fuzzy logic interference systems (FLIS), and clustering-based algorithms. They come to the conclusion that in order to obtain excellent results with SVM, an algorithm whose basis is statistical theory, the training set must be kept relatively

small. They get their conclusion using ANN, which is that an issue with data overfitting is seen quite frequently. It was discovered that fuzzy logic interference systems reliance on anecdotal experiences resulted in accuracy losses, which were problematic. On the other hand, it was discovered that strategies based on clustering were unable to provide any information regarding the defect. A comparison of three different classification methods is shown in reference [58]. These algorithms are referred to as distance-weighted k-nearest neighbour (W*k*NN), decision trees (DT), and support vector machines (SVM). According to the findings of the research, the performance of the decision tree classifier is significantly lower when the smaller sample sizes that were employed for the training phase are taken into consideration. During the training and post-training testing, however, it was discovered that support vector machines were significantly slower than decision trees.

2.6 Long-Range and Wide-Area Data Transmission Technologies

Low-Power Wide Area Network, commonly abbreviated as LPWAN, is a non-wired wide area networking technique that links battery-driven devices that have low bandwidth to one another at low bit rates across long distances [59], [60]. LPWANs, or low-power wide-area networks, were designed specifically for machine-to-machine and IoT networks. Compared to standard mobile networks, LPWANs have lower operating costs and higher power efficiency. In addition to this, they have the capacity to serve a larger number of linked devices across a wider area. Uplink speeds of up to 200 kbps are possible with LPWANs, which can handle packet sizes ranging from 10 to 1,000 bytes. The extended range of LPWAN can be anywhere from two to one thousand kilometres, depending on the technology [61]. The vast majority of LPWANs are organised on a star topology, which is very similar to that of Wi-Fi in that every node is connected right away to the access point placed centrally in the network. The term "low-power wide area network" (LPWAN) really refers to a collection of distinct low-power wide area network technologies that can be implemented in a variety of ways. Low-power wide-area networks (LPWANs) have the flexibility to make use of unlicensed or licensed frequencies and may offer either

patented or free-to-use alternative standards. One of the most frequently deployed low-power wide-area networks (LPWANs) in use today is the proprietary and unlicensed Sigfox. With ultra-narrowband technology, only one operator is permitted within a certain nation. This technology can run on public networks in the 868 MHz or 902 MHz frequency bands. Although it is capable of delivering communications over distances of up to 1,000 kilometres in line-of-sight applications, 31–60 kilometres in rural regions, and 4–11 kilometres in urban settings, its transmission is restricted to no more than one hundred and fifty messages of 12 bytes daily [62], [63]. Downlink transmissions are capped at a maximum of four packets of eight bytes per day. It is also possible for interference to occur when sending data back to endpoints. Random-phase multiple access, sometimes known as RPMA, is an LPWAN created by Ingenu Inc. Even though RPMA's reach is less than that of Sigfox (up to 50 kilometres when there is an obstacle-free line of sight and about 5 to 10 kilometres when there is not), it provides superior communication in both directions. The fact that it operates at 2.4 GHz, however, makes it subject to interference from other wireless technologies such as Wi-Fi and Bluetooth, as well as from physical structures. In addition to this, its power consumption is often higher than that of alternative LPWAN solutions [64], [65]. The unlicensed LoRa network, which is standardised and supported by the LoRa Alliance, broadcasts on many sub-gigahertz frequencies. As a result, it is less susceptible to interference than licensed networks. LoRa is a form of modulation that is a descendant of chirp spread spectrum (CSS), and it gives customers the ability to define packet size. While the source code for LoRa is available to everyone, Semtech Corporation, the firm that developed the technology, is the only source for the transceiver chip that is required to use LoRa. LPWAN devices and gateways are able to communicate with one another thanks to LoRaWAN, which serves as the media access control (MAC) layer protocol. Weightless SIG has created three Low Power Wide Area Network (LPWAN) standards: Weightless-N, which is unidirectional; Weightless-P, which is bidirectional; and Weightless-W, which operates off of underutilised TV spectrum and is bidirectional [66], [67]. LTE-M and NB-IoT are

standards that were developed by the 3GPP, and both use licensed radio spectrum. They can be quickly integrated into the existing infrastructure for cellular communication, thus enabling a swift expansion of service portfolios. NB-IoT, which also goes by the name CAT-NB1, is able to function by utilising the LTE and GSM infrastructure that is already in place. It uses only 200 kHz of the available bandwidth while still providing uplink and downlink speeds of approximately 200 kbps. CAT-M1, which is also known as LTE-M, provides a bandwidth that is higher than that provided by NB-IoT. In fact, LTE-M provides the highest bandwidth of any LPWAN technology. LPWAN, in contrast to earlier wireless technologies, offers battery-efficient and pervasive wide-area connectivity. This makes it possible to implement additional M2M and IoT applications that were previously unfeasible due to exorbitant costs. The amount of data that may be communicated is, however, a significant limitation in this regard. However, according to research by James Brehm *et al.*, the majority of Internet of Things devices (86%) use less than 3 MB of data each month [68]. Furthermore, the 3GPP forecasts that more than ninety-nine percent of low-power WAN end nodes will transmit no more than 145 KB of data on a monthly basis [69], [70]. The battery life of cellular networks is notoriously short, and the coverage they provide can occasionally be spotty. In addition to this, cellular technologies are frequently abandoned. It is not possible to sunset cellular coverage due to the fact that many IoT devices are installed for a period of ten years or longer. Radio frequency (RF) technologies, which include near-field communications (NFC) and Bluetooth, do not have the reach that is necessary for numerous IoT deployments. Zigbee, which is a mesh-based technology, is preferable for intermediate-distance IoT applications like smart buildings and smart homes. Zigbee offers large data speeds but is significantly worse than LPWAN in terms of how efficiently it uses battery power. A variety of machine-to-machine and IoT deployments are now possible thanks to LPWANs, many of which were previously impossible due to power and budgetary limitations. With decreased power needs, extended range, and minimised costs compared to traditional cellular networks, LPWANs offer an advantage over traditional mobile networks. The

particular application at hand, specifically the required speed, data volumes, and area covered, determines the choice of a low-power wide-area network (LPWAN) to use. Applications that seldom require the uplink of minute messages are the ones that can benefit the most from the use of LPWANs. Downlink capabilities are included in the majority of LPWAN implementations. Applications such as industrial IoT deployments, precision agriculture, smart cities, smart lighting, energy management, asset monitoring and tracking, livestock monitoring, manufacturing, and smart metering are frequent places to see LPWANs in use. LPWAN is a new player that has recently appeared on the scene, and because it is relatively new, it is in a state of perpetual improvement and is by no means fully developed. Because many LPWAN variants are still in the early stages of their rollouts and extensive testing in the real world has not yet been carried out, it is difficult to predict how well each will operate throughout the course of its lifetime.

2.7 Low-Power Techniques for IoT Applications

When installing platforms for the Internet of Things, one of the primary considerations should be to maximise the efficiency of the sensors and actuators in terms of energy use [71]. Nevertheless, the Internet of Things systems themselves are enormous energy users due to the fact that they frequently need to send a great deal of data and require communication between a variety of devices within limited amounts of time [72]. Because of this, a lot of power is required to maintain the Internet of Things (IoT) system and move the enormous amount of data that IoT devices collect. In order to save energy, innovators in the Internet of Things should research strategies that aim to reduce the amount of power that IoT devices consume. A prototype of a low-priced, low-power Internet of Things-based wireless sensor network for groundwater monitoring (LWNGM) is provided in reference number [73]. The ATmega328P microcontroller platform served as the foundation for the system, which also had sensors for measuring pressure and humidity. According to the findings of the study, a significant improvement in energy efficiency may be made by putting Internet of Things devices to sleep at regular intervals of six hours. When this method of energy

efficiency was utilised in conjunction with other methods of energy harvesting, the system was able to achieve energy autonomy and function without the need for continuous attention since it was able to perform without interruptions. The research also demonstrated that it is feasible for Internet of Things nodes to obtain all of their power requirements from solar sources alone. The research described in reference [74] indicates how power optimized waveforms, otherwise known as POWs, can improve the energy-harvesting efficiency of sensors that sit passively, thereby expanding their range and ensuring their durability. The authors start out by reiterating the fundamental conditions that must be met in order to successfully develop an IoT system. First, the gadgets need to be non-wired and have extensive ranges. Second, they must not require batteries. Third, the prices of the devices must be competitive. The authors say that power-optimised waveforms are one of the many ways that circuits can collect energy efficiently at low power levels, which increases their reliability and range. This is done by designing an excitation signal with a high peak-to-average power ratio. Henkel *et al*. [75] argued that IoT devices need to be reliable and that a variety of factors affect how much power the various components of an IoT device use at any given time. These parameters include the power mode of the various elements and peripherals, the voltage and frequency settings, the instructions being executed, the architecture of the core, and the technology scaling mode. Henkel *et al*. also promoted the need for dependability in IoT devices. As a result, it was decided that effective energy management and ultra-low power consumption are important design considerations at both the hardware application level and the software application level and that ultra-low power and energy-efficient designs must be taken into account in each of the functional phases of an IoT device, which were found to be the gathering of data, the processing and management of data, the storage of data, and the transmission and communication of data. This was a conclusion that was reached after it was determined that effective energy management and ultra-low power consumption are crucial design considerations for both traditional methods of fault monitoring for the electrical power system, which are becoming increasingly linked to high financial costs and low returns

on investment (ROI). However, there are a number of issues that have prevented the deployment of remote monitoring systems for the electrical power system, the two most significant of which are the terminal equipment's limited capacity and the data storage and processing's low level of intelligence [76]. At the moment, the most significant issues are the high cost of receiving and transmitting the physical information from remote users' physical information in real-time, as well as the lack of high degrees of automation and reliance on artificial operations [76], [77]. These are the primary challenges. Emergent digital technologies, for example, remote monitoring systems, offer an incredible amount of opportunity for finding solutions to these problems. To compare and contrast the usefulness of on-site and off-site monitoring systems, a case study approach was chosen as the method of investigation. A comparison study between remote monitoring and traditional on-site monitoring systems found that monitoring construction projects remotely resulted in improved project performance in terms of their objectives and goals. This was true for both project efficiency and resource optimisation, and it was determined using comparable projects involving the same client and organisation. Because there is an immediate need for increased productivity in the construction industry, it is very necessary for remote monitoring systems to be implemented at both the organisational and national echelons. In addition, the necessity for additional research and studies into the scalability of its application is vital, and this need applies equally to large construction conglomerates as well as small and medium-sized construction businesses. As a result of the development of the Internet of Things (IoT) and machine-to-machine (M2M) connections, the number of devices that are capable of connecting to the internet on their own is skyrocketing at an incredible rate [69]. Experts predict that by 2025, the number of devices connected to the Internet will reach a staggering 75 billion [78], [79]. Remarkably, only one-third of these connected devices will consist of traditional computing devices such as computers, smartphones, smartwatches, and tablets. This projection highlights the expanding landscape of the Internet of Things (IoT) as an array of diverse devices, ranging from sensors and appliances to industrial equipment

and wearables, join the global network of interconnected devices. This represents an annual growth rate that is between 20 and 30 percent. The Internet of Things has a significant potential to have an impact on a wide variety of enterprises, and there are hundreds of use cases for it in contexts where having wireless connectivity is either necessary or advantageous.

2.8 Analysis of Gases Dissolved in Mineral Oil

Transformer oil, which maintains its stability even when heated to extremely high temperatures, is created through the refinery of crude oil. Transformer oil is a crucial element in the efficient operation of a transformer because it prevents arcs from forming, distributes heat throughout the device, and serves as an insulator. The oil starts to break down when it is put under various thermal and electrical stresses, which causes the production of a variety of oil-soluble gaseous compounds [80]. In addition to other oil properties like permittivity, viscosity, and turbidity, the presence of gases that have been dissolved in the oil has a significant impact on the health of the transformer. Since transformer oil quality degrades over time, particularly as a result of prolonged exposure to high temperatures and the absorption of moisture, it is crucial to keep an eye on the oil's condition [81]. Transformer oil is vulnerable to deterioration because of the intricate chemical changes that can happen over time from its prolonged use. Deterioration of the transformer oil is a leading cause of transformer failure [82]. The chemical reactions that are occurring result in the production of wax, fumes, sludge, and liquid byproducts. Oxidation will take place in the presence of oxygen, metal, and moisture when electrical stress and high temperatures are applied. This will cause the production of acids and free radicals. As a direct result of this process, sludge is created, which settles to the bottom and coats the container's walls, decreasing its ability to transfer heat. Power transformers are prone to a wide range of issues because they frequently operate at extremely high temperatures and are put under mechanical and electrical strain. So, problems like mechanical deformation of the windings and core, partial discharge, overheating, and arcing would cause the mechanical integrity and dielectric insulation system of the transformer to break down. The failure of a

transformer in the power grid has a significant effect on the economy and the finances of the company that owns the grid due to the inability to meet contractual obligations and the potential cost of replacing the transformer. In order to keep the transformer operating at the recommended level of efficiency and maintain the high availability and stability of the electrical network, it is therefore becoming more and more crucial to spot potential issues as soon as they arise. In this way, dissolved gas analysis, or DGA, of a transformer is thought to be one of the best ways to figure out what's wrong with an oil-filled power transformer. DGA can show where thermal and electrical stresses are putting pressure on the insulation of a power transformer. You can find an analysis of dissolved gases in a transformer here. The ability of DGA to identify flaws in their early stages allows for an estimation of the severity of a fault. It is possible to use either online or offline condition monitoring techniques to calculate the amount of gas present. The interpretation of DGA results can then be done in a variety of ways. How accurately these techniques can be applied depends on the operator's level of experience and knowledge of the pertinent materials and machinery. The gas inside the transformer has the capacity to serve as a marker for a number of problems. Whether or not a fault develops in the transformer will affect both the quantity of these gases as well as their ratios. The underlying condition and the extent of internal damage can be precisely determined by analysing the various gases that are currently present [83]. The most frequent causes of gas generation inside an already-running transformer are thermal or electrical in origin. As a result, DGA not only finds and identifies potential flaws but also improves safety and equipment dependability while at the same time cutting down on maintenance costs [84]. According to the International Electrotechnical Commission (IEC), the International Council on Large Electric Systems (CIGRE), and the IEEE, some examples of typical issues that can arise in transformers that are already in use include the following:

1. Partial Discharge (PD): A partial discharge occurs when a confined section of a solid or fluid insulation material under high voltage stress experiences a partial collapse but does not entirely seal the space in between two conducting materials.

Partial discharges indicate that the electric field strength has exceeded the natural resistance of the insulator. Partial discharges are due to contaminants or irregularities in the insulating materials [85], [86].

2. Energy Discharges: An energy discharge is the creation of a local conducting path or short circuit between capacitive stress grading foils, which causes sparking around loose connections [85], [87].

3. Thermal faults refer to the circulation of electric current in insulating paper that results from excessive dielectric losses. These losses are themselves associated with moisture or improperly selected insulating materials that result in excessive dielectric temperatures [86], [87].

2.9 Exploratory Data Analysis

Data exploration, or exploratory data analysis (EDA), refers to the critical approach of carrying out preliminary investigations on data so as to detect patterns, check assumptions, test hypotheses, and spot anomalies with the use of summary statistics and visual aids. EDA enables one to understand the characteristics and aspects of the data to be used for modelling. In order to carry out a successful data exploratory analysis, the data has to be clean and must not have any redundancies, null values, or missing values. EDA involves a series of techniques and procedures that are followed in order to enable the identification of the vital parameters in the data set and the removal of all the gratuitous noise that may affect the accuracy of the conclusions reached during model building. There are two basic objectives for conducting EDA: first, to identify the faulty points in the data, and second, to understand the relationship between the various variables, which would give a wider perspective on the data by exploiting the relationship between the data. As shown in Figure 2-6, EDA begins by having a good understanding of the variables in the data set. The properties of the dataset, such as the number of columns and rows as well as their data types, have to be understood. The next step is to remove redundancies from the data set.

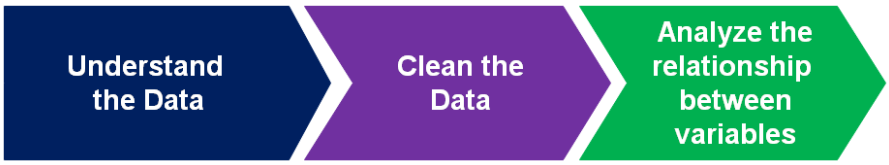

Figure 2-6: The steps involved in the EDA process (Source: Author)

There are generally two ways in which cross-classification is achieved during exploratory data analysis: firstly, there is either a graphical or non-graphical approach, and secondly, each technique is either multivariate or univariate, depending on its nature. Techniques that are not graphically represented often entail the computation of summary statistics, while methods that are graphically represented simply summarise the data in a manner that is diagrammatic or visual. Univariate methods focus on analysing only one variable (or data column) at a time, while multivariate techniques focus on analysing two or more variables simultaneously in order to discover the relationships that exist between them. In the vast majority of situations, multivariate EDA will be bivariate, which indicates that it will concentrate on only two factors; in very rare circumstances, it may incorporate three or more variables. Accordingly, there are four distinct categories of exploratory data analysis: multivariate graphical, univariate non-graphical, multivariate non-graphical, and univariate graphical. In terms of the tools used, the most commonly used tools in exploratory data analysis are Python and R. In summary, exploratory data analysis (EDA) is a scholarly, creative, methodological, and artistic approach that aims to thoroughly examine every nuance and facet of the data at an early stage.

2.10 Design Science Research

The goal of the field of study known as “design science research” is to provide information that may be used to guide the design of objects like models, methodologies, software, or ideas. These objects are more commonly referred to as artefacts. This design knowledge assists research and practise in future projects to design objects in a methodical and scientific manner. This design and its applications have the potential to produce design-oriented knowledge, which, in turn, may

contribute to a DSR knowledge corpus. Design science research is a method of conducting research whose objective is to build a new reality (that is, find solutions to issues) as opposed to either describing a current reality or assisting in the process of making sense of it. Figure 2-7 shows the conceptual framework for design science research.

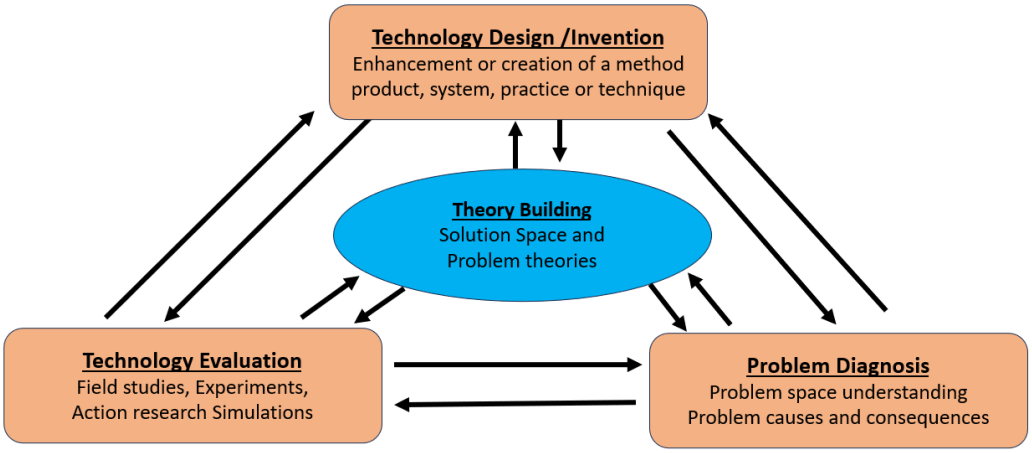

Figure 2-7: Conceptual framework for design science research

According to Baskerville *et al*. [88] and Horváth [94], there are two main goals that should be kept in mind when conducting design science research: first, to apply the knowledge gained to find solutions to problems, bring about differences, or enhance solutions that already exist; and second, to produce original information, new insight, and conceptual interpretations. Both authors emphasise the importance of this dual mandate. In addition, Horváth [89] provided an overview of a subtype of DSR that is referred to as "design inclusive research". A study of actual creative design actions is included in this research, and it is situated in the middle of exploratory and confirmative research activities. This is one of the distinguishing features of this investigation. In a nutshell, confirmative research action compartmentalises the DSR into three phases [89]: (1) the problem is explored, inducted, and deduced in its context, and the activities and hypotheses are also set; (2) the solutions are designed and tested; and (3) the hypothesis is verified, the research validated, and the generalisation is made to various types of applications.

According to Teixeira *et al*. [90], Lapo *et al*. [91], and Peffers *et al*. [92], the design science research process typically consists of the following stages or actions: (1) the problem is identified, defined, and justified; (2) the aims for the end result are defined; (3) the objects are designed and developed (paradigms, replicas, approaches, etc.); According to Peffers *et al*. [92], researchers do not always begin from the initial stride (i.e., identifying the problem), but they do work their way outwards, beginning from the place of entry into the study and completing the process. In other words, researchers are not compelled to begin with identification, which is the first step. A DSR endeavour will invariably produce a meaningful item as its final deliverable. According to the DSR project, this artefact "can be a process or a product; it can be a methodology, a procedure, a tool, a technique, a technology, any combination of the foregoing, or some other technique for attaining some objective [93]."

Attention must be focused on individuals by both product designers and market researchers if there is to be any possibility of connection between individuals or individuals and products [94]. This is because most initiatives are based on people (also known as users), and people will use or perform the finished product in some capacity. It is highly recommended to adopt ideas, actions, cues, and techniques. This is due to the fact that "the emphasis on people and their particular experiences, wants, and daily routines has become standard and forms the foundation of nearly every design process."

Both Mao *et al*. [95] and Chammas *et al*. [96] note that the International Organisation for Standardisation (ISO) is in charge of creating the technical standards that the user-centred design methodology has to conform to (ISO TR 18529, ISO 13407, and ISO 9241–210). According to the research carried out by Chammas *et al*. [96], a UCD project will exhibit all six of the following traits: The following are characteristics of user-centred design:

(1) It is predicated on an in-depth comprehension of the users as well as their respective jobs and settings.

(2) User participation is encouraged at every step of the process.

(3) It incorporates progressive evaluation, with the primary focus being on the wants and desires of the users as well as how and whether those needs and aspirations are realised;

(4) During the design process, that naturally iterates, assessing and improving the solution depending on the new information collected.

(5) It takes into account the entirety of the users' experience, and

(6) It involves the perspectives and views of several disciplines.

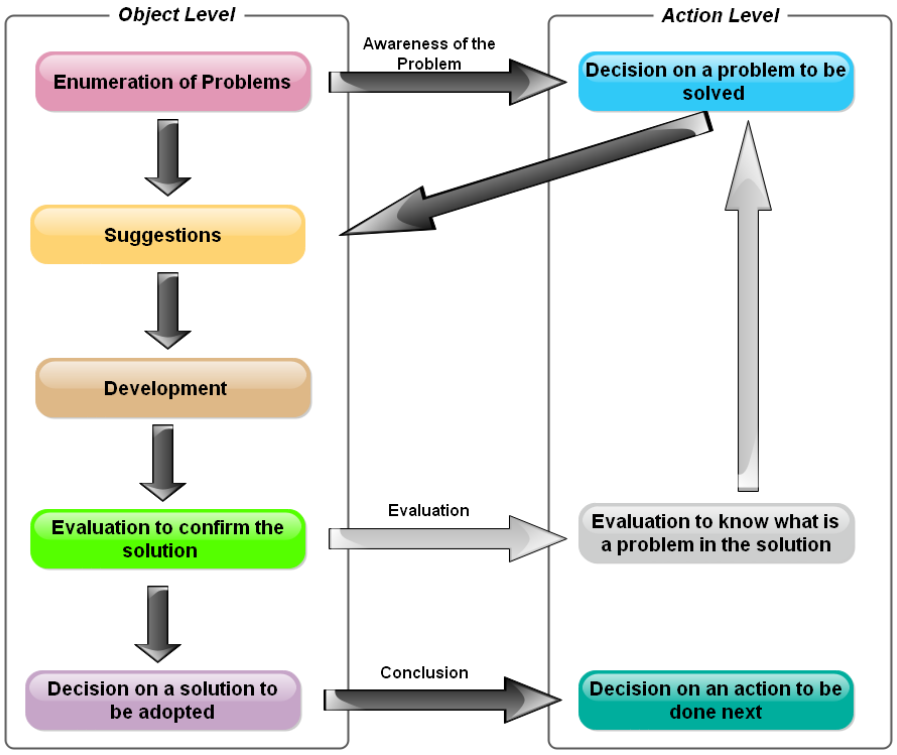

Figure 2-8: The design cycle

Simon [97], who emphasised the contrasts between natural science and design science, is credited with the development of the concept of "science of design," which dates back more than half a century. More specifically, Dresch *et al.* [98] suggested that the most evident objective of design science is to design: to produce something that does not yet exist or to improve existing solutions in order to get better results. This was stated as the purpose of design science. Research in the field of design science is

referred to as "research that conceives new deliberate relics to deal with a generalised category of problem and evaluates its utility for solving problems of that type," according to one definition of the term [98]. Modelling is an essential part of the design process in practical engineering, and it is also an activity that is helpful in the study of engineering education (EER). The Design Science Research (DSR) paradigm was used in this work, as described in [99], [100]. and is further described diagrammatically in Figure 2-8.

Chapter 3

Multinomial Classification of DGA Data for Incipient Fault Detection in Oil Impregnated Power Transformers

3.1 Introduction

The transformer is a critical piece of equipment in the generation, transmission, and distribution of electricity [101]. They are also expensive and account for massive capital expenditures on the contemporary electrical network. Not only do they necessitate large financial investments, but the overall reliability and dependability of the electricity grid are primarily dependent on their operational stability [102], [103]. It is therefore imperative that utility companies give priority to failure prevention and the maintenance of an optimal operational status of their electrical network. Maintaining these assets in an optimal and efficient state is a key priority for many electric utilities globally. In fact, these utility companies spend a significant portion of their annual budgets on condition monitoring and asset maintenance [104], [105]. Condition monitoring and asset management are therefore key concerns for all electric utility providers. With a typical electrical network deploying transformers by the thousands, condition monitoring easily becomes a labour-intensive and time-consuming exercise [106].

The basic principle upon which a transformer works is that of mutually induced magnetic flux that links the primary with the secondary windings. When an AC current flows through the primary windings, it induces a voltage that is greater than or less than that across the secondary windings, depending on whether the unit is a stepdown or step-up transformer [41], [101]. The frequency of the induced and inducing voltages, however, remains unchanged. Figure 3-1 depicts the basic construction of a transformer.

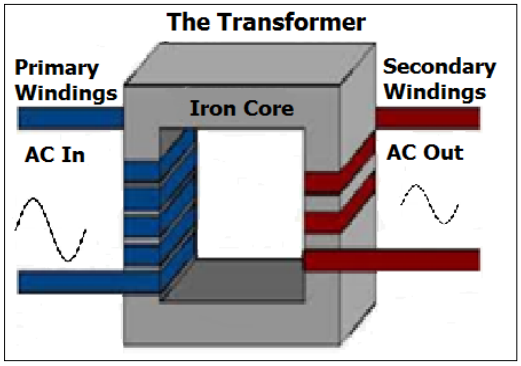

Figure 3-1: Arrangement of a Single-Phase Transformer's Windings and Core

The transformer comprises an intricate arrangement of a pair of coils wound on an iron core. To prevent the iron core from acting as a conductor, it is assembled using thin layers of varnish-coated steel [107]. During normal operation, an alternating current on the primary windings produces a changing flux within the core. The flux in turn induces an electromotive force (emf) within the core, which in turn sets up the circulating currents called eddy currents. Eddy currents produce losses, which manifest as heat. Equation (3-1) can be used to calculate the magnitude of this loss [108].

$$P_e = K_e B_m^2 t^2 f^2 V \text{ watts} \quad (3\text{-}1)$$

Where P_e is the hysteresis loss in Watts, K_e is the Stein-Metz hysteresis coefficient; t is the material thickness, B_m is the flux, f is the rate of magnetic oscillations, and V is the volume in m^3.

As is seen from Equation (3-1), the heating up of a transformer during operation is anticipated. The concern, therefore, is how to prevent and manage the excessive buildup of heat before it reaches destructive levels. Several techniques have been used to accomplish this. One of these is to immerse the transformer core and winding in mineral oil. Oil not only serves as a coolant but also as an insulating material [86].

Recent studies suggest that many transformers do not live up to their expected lifespan of between 25 and 35 years [102]. In Kenya, for instance, as many as 10–12% of the population of distribution transformers are prematurely retired each year, compared to

an international average of between 1 and 2% in the more industrialised countries [102]. The failure of a single transformer disrupts economic activity for both consumers and the utility company [109]. For continued reliability and availability, there must be continuous monitoring and maintenance of the transformer. However, with the huge number of transformers deployed in an electrical network, monitoring and maintenance are daunting tasks that require massive labour and time. Kenya Power has reported that it owns about 70,000 transformers countrywide, installed at various locations scattered all around the country [110].

Dissolved and free gas analysis is a widely used and highly regarded means of detecting incipient faults in oil-immersed transformers. DGA reliably gauges a transformer's operational status and is extensively used in routine maintenance [111], [112]. It is an investigative process in which oil samples collected from oil-immersed transformers are inspected for fault gases. The concentration, ratio, and type of the gases tell a tale about the internal condition of the transformer. Insulating oil not only performs functions like cooling the unit and dousing arcs, but more significantly, it dissolves any gases produced as a result of cellulose deterioration or ambient moisture from the environment. A common cause of early transformer failure is the deterioration of the insulating oil. It is estimated that about 70–80% of the faults in a transformer are incipient in nature, which implies that any effort to detect these faults can potentially reduce the manifestation of faults on the grid by a similar margin [42], [111].

Classical methods of DGA interpretation include key gases, Duval, and nomography [113], [114]. The interpretation of DGA data has for decades relied on these classical approaches. These classical approaches, however, tend to rely extensively on the experience, judgement, and intuition of a human expert rather than technical formulation. This reliance on a human benefactor has often led to an inconclusive assessment of the severity of the faults or, in the extreme case, a misidentification altogether [115]. Numerous studies have been conducted that propose methods by which the severity of incipient power transformer faults can be determined. In [116],

for instance, Prasojo *et al*. studied fuzzy logic to determine faults on power transformers created by using gas levels and gas rates as well as interpreting DGA data. The Duval Pentagon Method (DPM) was assimilated, with the Support Vector Machine (SVM) algorithm being the chosen interpretation method. The study resulted in an accuracy score of 97.5%. Malik *et al.* [117] conducted a study that designed a smart fuzzy reinforcement learning-based fault classifier for transformers. DGA data, collected from actual transformers and other credible secondary sources, was used. The results showed that the suggested fuzzy reinforcement learning technique is superior as compared to other contemporary approaches, attaining an accuracy score of 99.7%. Fuzzy logic models, however, tend to perform poorly when subjected to new data. Chatterjee *et al.* [118] discussed a multilayer perceptron (MLP) network with boundaries defined using a fuzzy class. The model is centred on Duval's Pentagon and gas ratio combination. A multilayer perceptron network was trained on actual DGA records with fault conditions specifically marked. The proposed method had a good ROC for some fault conditions, while for others, the uncertainty was high. Generally, the method yielded an overall accuracy of only 83%. In addition, the method has low performance when dealing with multinomial data. It is from this perspective that we propose to develop a model that elegantly handles multinomial DGA data while simultaneously maintaining high accuracy. The proposed model will be installed on a cloud-based server that will perform DGA data interpretation. This cloud-based machine will act as a data aggregator. According to Bustamante *et al*. [84] proposal, sensors mounted on the transformer must send real-time DGA data readings for analysis and display at the monitoring and control centre. This solution is designed to use low-cost devices and only requires the purchase of an inexpensive IoT monitoring device that costs about $100. The mounting of the monitoring device physically on the transformer will be done by using an inlet and outlet valve fashioned as a closed loop.

Recent advancements in field-deplorable computer technology have revived interest in the deployment of computing technology for mundane tasks, especially those that

are labour-intensive. In this regard, various research scholars have undertaken several studies to explore novel approaches to automated fault-finding on the electrical grid. For instance, in [119], Benmahamed *et al*. evaluated the k-NN algorithm and Naïve Bayes to diagnose transformer oil insulation through the analysis of DGA data. Five input vectors, namely the Duval triangle reports, Dornrenberg ratios, Roger's ratios, and DGA data (in percentages and ppm), were used in the study to map to five output classes. The rate of accuracy for both classifiers was determined using 155 samples. Results showed that the *k*-NN algorithm generally performed better than Naïve Bayes, with an accuracy score of 92% when Duval's triangle reports were considered. Tanfilyeva *et al*. [120] undertook a study that described the application of two fault determination techniques: k-Nearest Neighbour (*k*-NN) and Bayesian classifier algorithms. A data set with 1340 entries for seven gases was used to build the classifier. The researchers discovered that after setting k to 13 (k = 13), there was no further improvement in accuracy. Chatterjee *et al*. [118] proposed a new DGA procedure that works by combining the gas ratio method with Duval's Pentagon 1, two techniques that are known to have high prediction accuracy. In essence, the technique is a blend of the gains of the ratio and graphical methods. The faulty zones were identified based on the level of confidence in the prediction. The study resulted in an overall prediction accuracy of 83%. An interesting observation was made in [115], where it was noted that interpretation methods based on ratios may fail to make accurate inferences when multiple fault conditions exist in the data set. To correct this, an enhanced approach is introduced to overcome the limitations of conservative DGA analysis practises, in addition to automating and standardising the DGA interpretation techniques. An expert system was built using gene expression programming. The results showed that the proposed approach provided greater reliability than others that utilised individual conventional techniques that are currently embraced in industrial practise.

Parejo *et al*. [32] made a proposition that entailed installing a network of sensors to overlay the main power cables of the distribution network. The setup involved installing a network node in each manhole along the line. The node consists of a

current transformer that encircles every cable individually. This kind of setup permits the system operator to monitor the currents in each phase of the underground feeder system of the distribution network. The setup involved installing a network node in each manhole along the line. The node consists of a current transformer that encircles every cable individually. The current transformer permits simultaneous, continuous measurement and communication, non-intrusively. Illias *et al.* [121] used swarm optimisation techniques and artificial neural networks to predict incipient transformer faults. It was noted that ANN is a good approach for modelling relationships that are difficult to describe explicitly. Evolutionary PSO techniques mimic the natural behaviour of how birds flock or fish school together. Implementation of the ANN and PSO algorithms was done in the MATLAB programming language. The efficacy of several PSO techniques when combined with ANN was compared with the experimental outcome of the real fault diagnosed. The results showed that the evolutionary PSO yielded the highest accuracy score, at 98%. In yet another study, Illias and Liang [122] modified evolutionary particle swarm optimisation and combined it with support vector machines. This proposed hybrid algorithm was proposed to identify incipient faults. Dissimilar arrangements of PSO factors were tested and evaluated to identify values with the highest accuracy. Results showed that the SVM-MEPSO-TVAC method offered the best precision, averaging 99.5%. The SVM-MEPSO-TVAC technique was therefore proposed as a substitute technique for the incipient diagnosis of DGA results.

3.2 Methods and Modelling

Distribution and power transformers operate in diverse environments that make them susceptible to generic failures, whose consequence is prolonged episodes of power outages and disrupted economic activity [123]. Unlike overhead conductors that are easy to troubleshoot and repair, transformers are factory sealed, thus depriving engineers and technicians of the opportunity to inspect their internal components. Failures of in-service transformers cause significant losses to power utility companies, in addition to costly repair or replacement costs and the risk of explosion or fire.

Dissolved gas analysis is the only technique available that makes it possible to detect incipient transformer failures [124]. While DGA techniques have relatively high measurement accuracy, DGA interpretation techniques rely more on technical personnel expertise than on systematic formulation [117], [121]. This study therefore seeks to propose and implement a new machine-learning-based DGA interpretation technique that interprets DGA results accurately, particularly when dealing with multinomial data.

3.2.1 Materials and Methods

The data used in this work was obtained from Kenya Power Ltd., the sole power distribution company in the East African Republic of Kenya. It had 2912 records organised into seven columns, six of which are input variables representing gas levels in ppm (parts per million), and the seventh is the label indicating the fault that was observed. Six categories of faults were observed in the dataset, with an additional label indicating a normal working condition. A simulation approach in the Python programming language was used, using the following packages, dependencies, and libraries: Pandas, NumPy, Matplotlib, SciPy, and Scikit Learn. After the data was obtained, an exhaustive exploration of the data was carried out, as outlined in Section 4.2.3. The goal of the exploratory exercise was to profile the data so that anomalies and patterns could be discovered. With exploratory data analysis, one is able to handle missing values, deal appropriately with outlying data points, normalise and scale numeric values, and encode categorical features. EDA also makes it possible to obtain descriptive and visual representations of the data [125].

After data quality and confirmation issues were addressed, the interpretation of the DGA data commenced, and a model was developed using the steps illustrated in Figure 3-2.

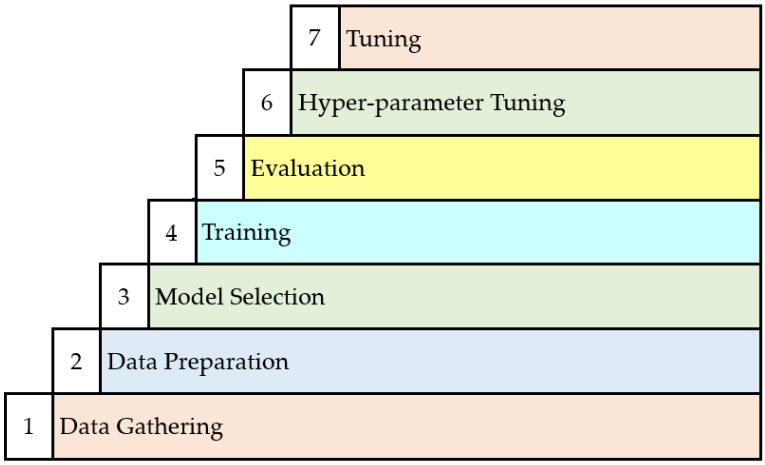

Figure 3-2: Seven-step machine learning process

3.2.2 Dissolved Gases Analysis

One of the most prevalent techniques for detecting progressing faults in transformers immersed in oil is gas analysis [126], [127]. DGA became an established art following the discovery in 1928 by Buchholz [128] that by extracting and studying dissolved gases generated during a progressively deteriorating condition in oil-filled transformers, one would be able to detect the problem with adequate precision. Since the gases formed in the course of the slow evolution of faults are dissolved in oil, extracting and analysing these dissolved gases can foretell the onset of incipient fault conditions [115], [126]. DGA includes faults that are identifiable through corona discharge, heating of the core, arcing, and partial discharge. This early detection of emergent faults not only results in appreciable cost savings but also in intangible benefits such as the timely decommissioning of faulty transformer units, whose continued use may be risky. Additionally, early detection of emergent faults allows personnel to create a maintenance outage schedule for units in a precautionary state and document anomalies for newly purchased units under warranty. Cost savings are attained by preventing or alleviating damage to the transformer [86].

Dissolved gas analysis, which discriminates between normal and abnormal conditions, is founded on the premise that an oil-immersed transformer in proper working conditions generates little or no gases. The DGA process begins with the collection of

oil samples from the transformer. The samples are then subjected to tests and procedures to determine the identity and quantity of liquefied gases [105]. Ethane (C_2H_6), ethylene (C_2H_4), oxygen (O_2), methane (CH_4), acetylene (C_2H_2), nitrogen (N_2), and hydrogen (H_2). (C2H6), ethylene (C2H4), oxygen (O2), methane (CH4), acetylene (C2H2), nitrogen (N2), and hydrogen (H2) are some of the gases that are often dissolved in oil that are of interest for DGA analysis. Fault gases are classified into three types [129], [130] namely:

1. Hydrogen gas and hydrocarbons: H_2, CH_4, C_2H_2, C_2H_4.
2. Carbon oxides: CO_2 and CO
3. Non-fault gases: N_2 and O_2

The quantity and ratio of these gases will vary depending on whether a fault is developing in the transformer or not [131], [132]. A critical evaluation of the variation of gases present can precisely determine the underlying condition and the extent to which internal damage has been occasioned [83], [133]. The leading causes of gas formation within an in-service transformer are either of thermal or electrical origin. DGA not only detects and identifies possible faults but also improves the safety and reliability of the equipment while minimising maintenance costs [84]. Typical faults that manifest in in-service transformers have been identified in [81], [85], [86] and are described in Table 3-1 [81].

When mineral oil heats up to between 150°C and 500°C, methane, ethane, ethylene, and hydrogen are formed in varying quantities. Acetylene is produced in large quantities as the temperature rises above 500°C [42], [112]. In the presence of high temperatures, paper insulation and other solid insulating materials are known to produce carbon monoxide. At temperatures lower than 300°C, carbon dioxide is produced. Gas chromatography isolates each dissolved gas from all others, making it possible to analyse and measure their individual concentrations. The American Society for Testing and Materials (ASTM) provides standard procedures for collecting

samples of oil from transformers [134] and further details the analytical laboratory processes that separate and measure gas concentrations [135].

Table 3-1. Fault Code for Classic Faults in Oil-Immersed Transformers

TYPE	FAULT
PTD	Partial Discharge
DLE	Low Energy Discharge
DHE	High Energy Discharge
TF1	Thermal Fault 1 (for t < 300°C)
TF2	Thermal Fault 2 (for 300°C < t < 700°C)
TF3	Thermal Fault 3 (t>700)
NoF	No Fault

The IEEE [86], CIGRÉ (Conseil International des Grands Réseaux Électriques) [87], and the International Electrotechnical Commission (IEC) [85] are reputable international organisations that have developed separate technical guidelines for interpreting DGA results. As seen in the foregoing documents, each fault has a distinct signature in terms of the quantity and combination of the various fault gases. This distinction makes it possible to detect impending or active faults. Furthermore, the particular combination of gases generated depends on the energy level and temperature at the location of the fault. High energy levels tend to produce higher temperatures. High temperatures, in turn, result in an accelerated rate of gas production.

Figure 3-3 shows how temperature influences the production of gases at various temperatures and the faults they are likely to suggest.

3.2.3 Data Exploratory Analysis

An exhaustive analysis of the data was carried out through data exploration. Exploratory Data Analysis (EDA) is a preprocessing procedure used on raw data to obtain additional insight about the data before engaging in model building and

training. During the EDA, the investigator is interested in knowing the shape of the data, the number of features it contains, and the types of variables therein. EDA techniques are applied to raw data to extract its essential characteristics, define feature variables, and obtain guidance on machine learning algorithm selection [136], [137]. In order to fully understand the data, multiple exploratory techniques are used, and the results are aggregated. Figure 3-4 shows the contemporary methods employed in EDA that have been used in this work.

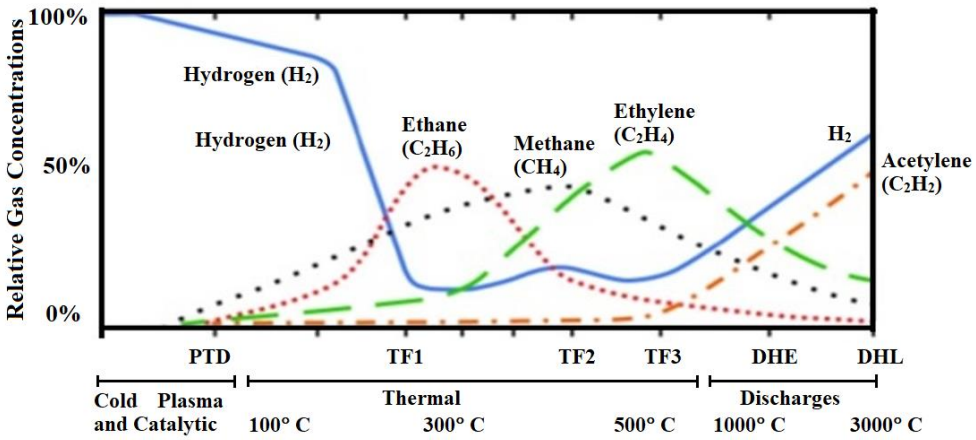

Figure 3-3: Comparative proportion of dissolved gas concentrations in mineral oil as a function of temperature and fault type (Adapted from [86])

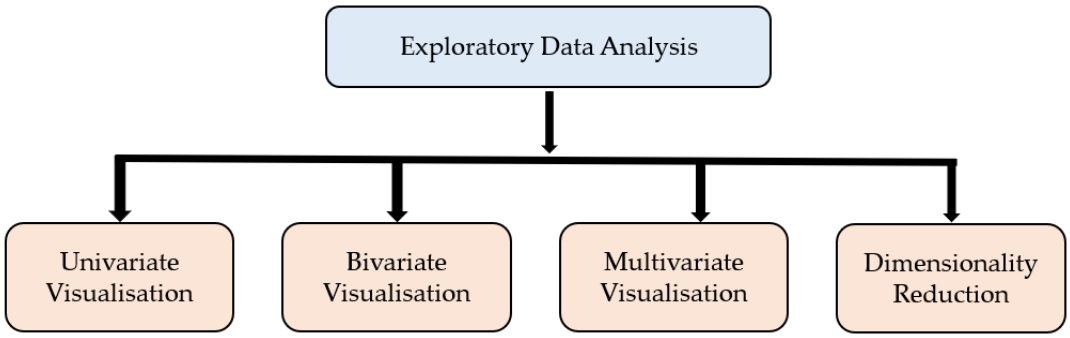

Figure 3-4: Major steps of Exploratory Data Analysis

Univariate visualisation provides statistics for each parameter and is visualised in a one-dimensional space. Bivariate visualisation determines the relationship that exists between each variable in the dataset and the dependent variable. Multivariate visualisation aids in the identification of existing interactions between different fields

in the dataset and examines the variables for correlation. Dimensionality reduction is a technique used to identify the most important predictors so that the model can be built with the fewest number of predictors necessary to maintain high accuracy [137], [138].

Figure 3-5 shows the type and number of variables in the dataset. The variable "Status" is the dependent variable and is of a categorical type, while the rest are integers. The total number of observations in the data set was 2912.

```
<class 'pandas.core.frame.DataFrame'>
RangeIndex:  2912 entries, 0 to 2911
Data columns (total 7 columns):
 #   Column      Non-Null Count  Dtype
---  ------      --------------  -----
 0   Hydrogen    2911 non-null   int64
 1   Methane     2911 non-null   int64
 2   Acetylene   2911 non-null   int64
 3   Ethylene    2911 non-null   int64
 4   Ethane      2911 non-null   int64
 5   CO          2911 non-null   int64
 6   Status      2911 non-null   object
dtypes: int64(6), object(1)
memory usage: 746.9+ KB
```

Figure 3-5: The Independent and Dependent Variables

Primarily, the data was investigated for missing values. Figure 3-6 shows that there are no missing values. Whenever missing values exist, the columns affected show discontinuous gaps. In this case, the columns are continuous, indicating that there are no missing values. Next, a box-and-whisker plot was created, as shown in Figure 3-7. It suggests that the variables acetylene and ethylene have several outliers above the outer whisker, while hydrogen (H2) and carbon monoxide (CO) have no outliers. Outliers are normally handled by prediction or imputation (using the mean, mode, and median), but it is difficult to conclude from the data that the outliers are the result of human or mechanical error [139], [140]. Therefore, the outliers were left as they were. It becomes imperative to handle outliers when it is evident that they result from errors committed during data collection or entry.

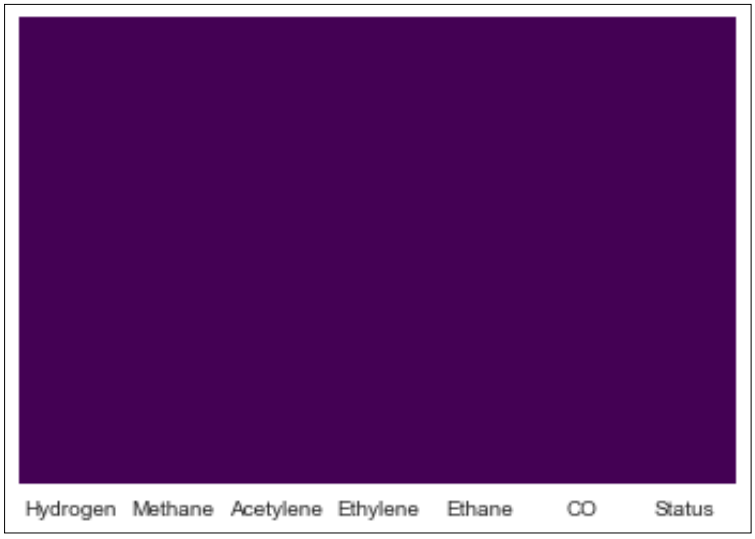

Figure 3-6: Checking for missing values

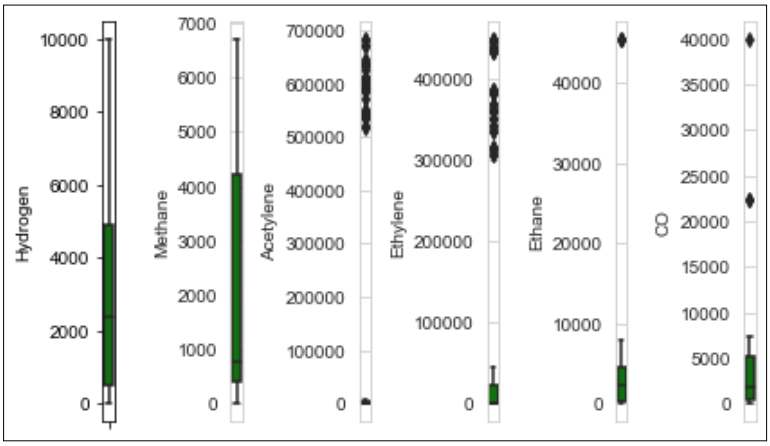

Figure 3-7: Box-and-whisker plot

The correlation matrix or heat map shown in Figure 3-8 establishes the correlation between the various pairs of variables, from which it is determined that the correlation between the two variables, acetylene and ethylene, is high. A keen consideration of Figure 3-3 reveals that this correlation occurs in a coincidental manner because, as the temperature rises, there is a parallel increase in the production of both gases in slightly differing quantities. It is therefore concluded that this correlation does not imply causality [141].

Figure 3-9 investigates the probability distribution of the variables. The distributions of hydrogen, methane, ethylene, ethane, and carbon monoxide appear to be gaussian.

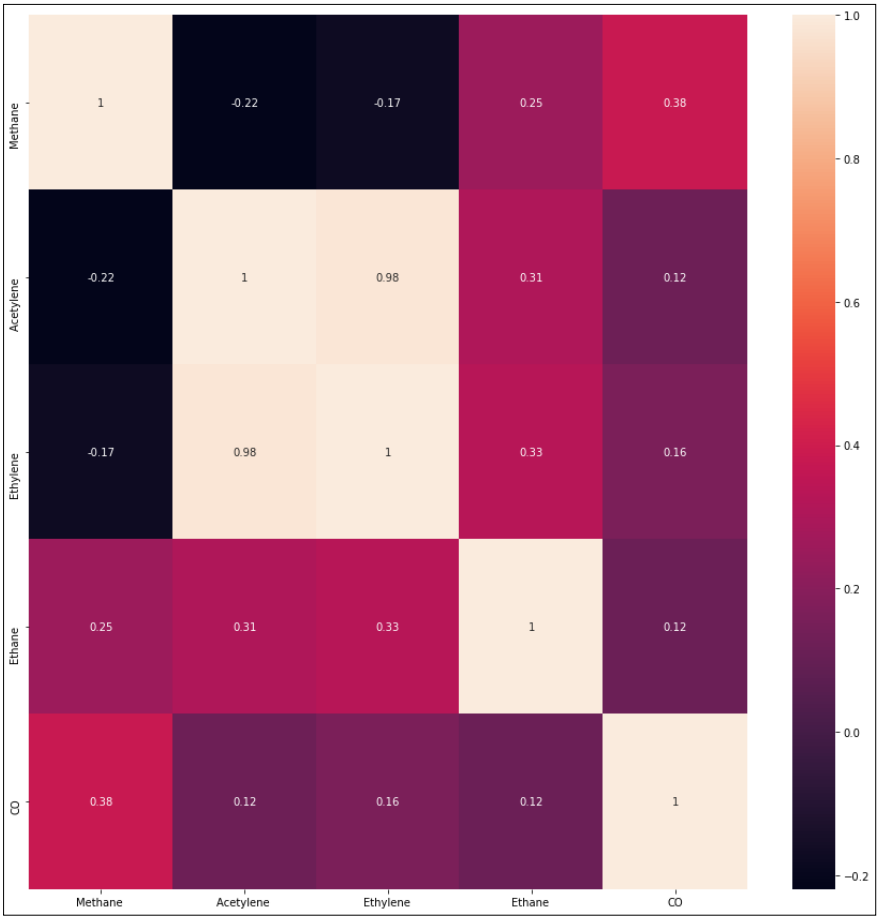

Figure 3-8: The Pearson's correlation coefficient heatmap

Figure 3-10 shows the pairs plot that visualises the distribution of solitary input vectors and the relationships between them. From Figure 3-10, we see that the variable pairs methane and ethane and methane and hydrogen are positively correlated. The same can be said about the variables' methane and carbon monoxide.

3.2.4 Decision Trees (DT)

The decision tree algorithm is a machine learning method that estimates likelihood by developing a tree-like structure that repeatedly splits into smaller and smaller segments until it terminates in nodes called leaf nodes. In a decision tree, data items are classified through an iterative process of repeatedly questioning the features associated with the

items [142], [143]. The questions are enclosed in the nodes, with each interior node pointing to a child node for every probable answer to its queries. In this manner, the queries create a hierarchically encoded tree structure.

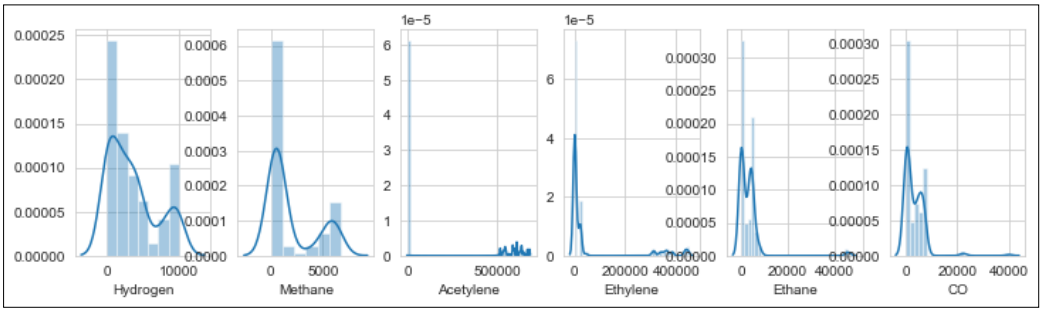

Figure 3-9: The probability distribution of the variables

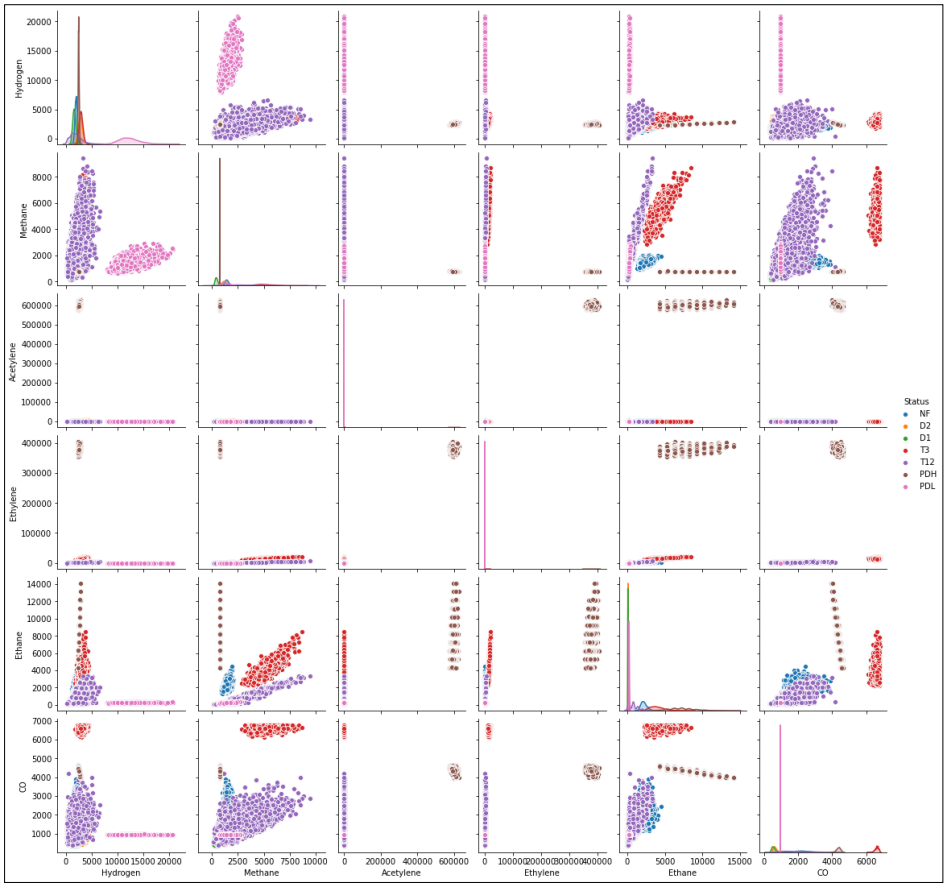

Figure 3-10: Pair-plot of various pairs of variables

The selection of the node on which the decision tree splits is done by examining its impurity. The impurity measures the similarity of the markers on a node and is implemented as the Gini index, or information gain.

By definition, the Gini Index measures the differences in the probability distributions of the dependent attribute values and divides the node in a way that produces the least amount of impurity, while the information gain uses the entropy quantity as its measure of impurity. The node at which a split is caused must result in the greatest amount of information gain. Equation (3-2) gives the formula for information gain, while Equation (3-3) gives the formula for the Gini Index.

$$Gini: Gini\ (E) = 1 - \sum_{j=1}^{c} P^2 \tag{3-2}$$

$$Entropy: H(E) = -\sum_{j=1}^{c} P^2\ log\ P_j \tag{3-3}$$

where *P* prediction models constructed on tree-based algorithms are stable, accurate, and easy to interpret. In addition, they map well to non-linear interactions and are highly adaptive in solving a diverse range of problems, unlike linear models [143].

3.2.5 Naïve Bayes

Naïve Bayes is a principle used in classification algorithms based on the Bayes theorem that states that

$$P(\Phi \mid \Psi) = \frac{P(\Phi \mid \Psi) \cdot P(\Psi)}{P(\Phi)} \tag{3-4}$$

Naïve Bayes works on the assumption that every feature is independent of all others, hence its name, "Naïve Bayes." One strength of the Naïve Bayes algorithm, however, is that it can be trained on very small datasets.

3.2.6 Gradient Boosting

Both regression and classification tasks use Jerome Friedman's gradient boosting technique. It operates by creating a model that comprises an ensemble of frail prediction models from decision trees. As with all other supervised learning algorithms, gradient boosting defines a loss function as shown in Equation (3-5) and attempts to lessen its effect.

$$Loss = MSE = \sum \left(\beta_i - \beta_i^p\right)^2 \tag{3-5}$$

where, β_i = i^{th} target value, β_i^p = i^{th} prediction, $\mathrm{L}\left(\beta_i, \beta_i^p\right)$ is a Loss function

3.2.7 *k* –Near Neighbours (*k*-NN)

k-NN is a pre-trained ML process that works by first learning on a labelled dataset and then classifying new objects by recalling the examples on which it was trained [144], [145]. *k*-NN hinges on the assumption that data points that are similar most often lie close to each other. The *k* in *k*-NN denotes the quantity of nearby neighbours that the classifier retrieves and uses to forecast a new data point. A value for *k* must be chosen iteratively until it is just right for the data. It must be seen as reducing the number of errors encountered while maintaining the algorithms' ability to make accurate predictions [120].

The *k*-Nearest Neighbours classifier algorithm works in the following manner: If *xtrain* is a training set with labels *ytrain*, and given that a new instance *xtest* is to be classified:

1. First, look for the most related occurrences (say, *xNN*) to *xtest* that are in *xtrain*.
2. Obtain the labels *yNN* for all the occurrences in *xNN*.
3. Predict the label for *xtest* by relating the labels to *yNN*.

A sample is categorised by determining the majority vote cast by its *k*-neighbours, with the sample being assigned to the most popular vote. The metric that is

traditionally used is the Euclidean distance, which is calculated as shown in Equation (3-6).

$$D_{m,n} = \sqrt{\sum_{i=1}^{k} (m_i - n_i)^2} \tag{3-6}$$

where *m,n* are two observations in the *Euclidean* space.

The *k*-NN algorithm is easy to implement but performs poorly as the number of predictor variables increases [119].

3.2.8 Random Forests

The random forest, also known as the random decision forest, presents a powerful way of exploring and analysing data with the potential to perform predictive modelling. The random forest is made up of numerous discrete decision trees that create a forest, hence the name "random forest." The fundamental principle underlying the random forest is that individual constituent models cannot outperform numerous delinked trees working as a group. To make a prediction, each classifier in the assembly submits a prediction [146], [147]. The votes are then tallied, and the class that garners the highest number of ballots is presumed to be the prediction of the overall model, as shown in Figure 3-11. Some of the reasons why the random forest is a powerful algorithm are that it does not suffer from overfitting and is highly accurate, maintaining this accuracy even when some of the data is missing.

A random forest is defined as a class predictor made up of an ensemble of autonomous tree structures $\{t(x, \theta_n), n = 1,2, ...\}$ where $\{\theta_n\}$ are random vectors and x is the input vector [148]. A distinctive phenomenon of the random forest is that each tree $\{\theta_n\}$ is independent of all past random vectors $\{\theta_1, ... \ \theta_{n-1}\}$ but has a similar distribution. In creating the tree structures, a random attribute is selected upon which the split takes effect. The pool of potential attributes to split on is kept limited by calculating the first integer less than $\log_2 B + 1$ [147].

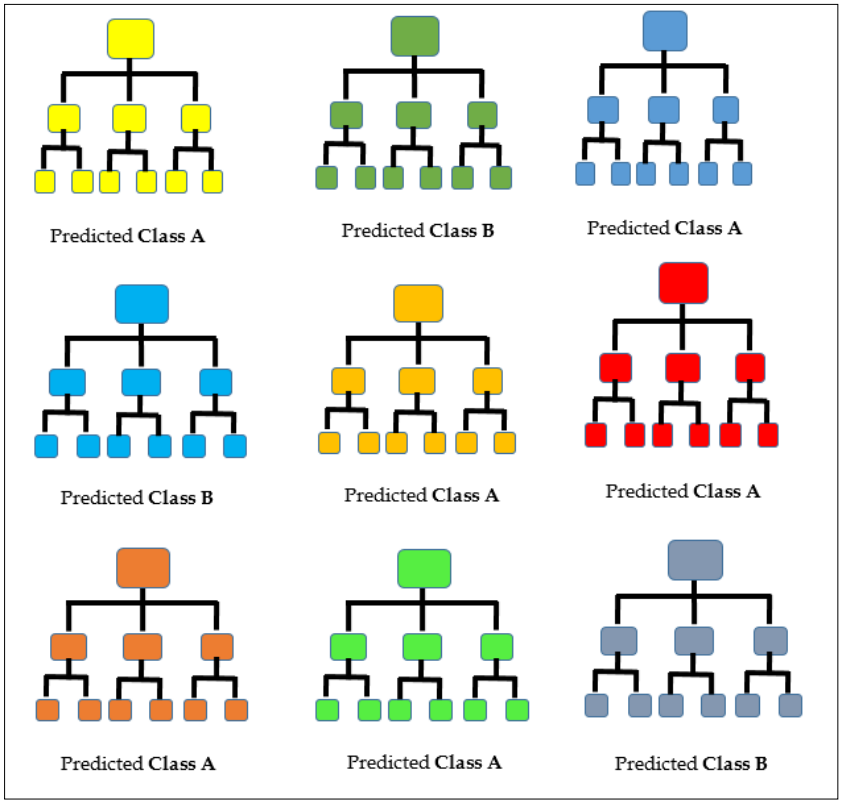

Figure 3-11: Tally: Class A – 6 votes, Class B – 3 votes; Predicted Class A

In growing its trees, the random forest begins by first randomly selecting at each node a small group of input vectors on which to split and then calculating a suitable split point. The best feature to split on is determined randomly.

The random-forest algorithm works by executing the following three steps [49]:

1. The set used for training is chosen. Using an indiscriminate sampling technique, several training sets are selected from the first dataset such that the magnitude of each is equal to that of the original.
2. Construction of a random forest model. For each of the bootstrap training sets, a forest of classification trees is created to produce a similar number of decision trees.
3. Form a simple vote. The training of the random forest can proceed simultaneously because the processes of training its members are independent of each other, thus considerably enhancing its efficiency. To make a

determination based on some sample input, every decision tree submits a vote. The random forest algorithm decides the ultimate category of the submitted sample in accordance with the voting pattern.

3.2.9 KosaNet

KosaNet is designed as an ensemble-based machine-learning technique that improves upon the decision tree algorithm by creating a semblance of an electoral college where decisions are made by a majority vote. KosaNet hinges on the notion that when many separate and independent entities vote in a particular direction, they are highly likely to be correct [149]. The electoral college operates like a democracy, where the minority has its say and the majority gets its way. The vote of the majority constitutes the prediction of the model. To minimize the variance of our predictions, several classifiers modelled on separate sub-samples of the same data set were built. The results of the vote by the separate classifiers are tallied, and the majority vote is determined, which then constitutes the prediction of the model.

Figure 3-12 shows the architecture of KosaNet. The attribute subset selection measure is a data mining technique employed to reduce the amount of data for more effective analysis and prediction of the target variable. There are two primary techniques used for attribute subset selection measures:

1. Gini index
2. Information Gain

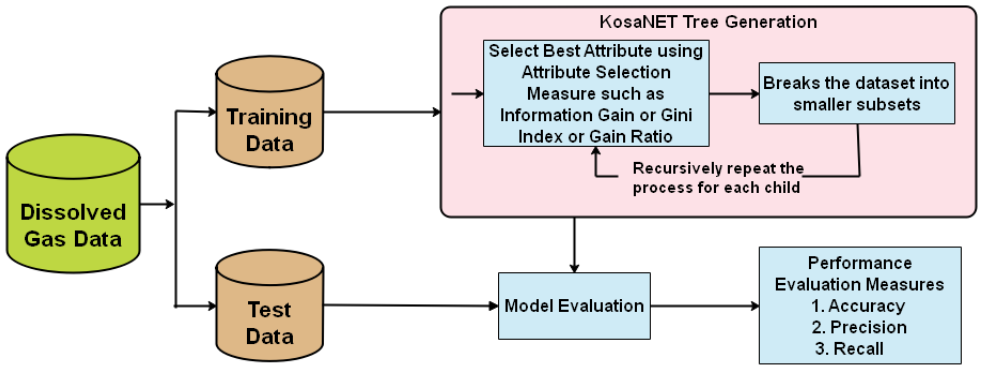

Figure 3-12: KosaNET Architecture

The Gini index, or Gini impurity, refers to the measure that quantifies the likelihood of a variable being incorrectly classified when selected randomly. It determines the degree of impurity in the data, and the data distribution is balanced based on the Gini index. The mathematical formula for the Gini Index is shown in Equation 3-7 [143].

$$Gini = 1 - \sum_{i=1}^{n}(P_i)^2 \quad (3\text{-}7)$$

Where P_i is the probability of an object being classified into a particular class. When the Gini index is used as the selection criteria for the feature that will be used for the root node, the feature that has the lowest Gini index is selected.

The ID3 algorithm, or Information Gain algorithm, relies on the concept of entropy to identify the feature or attribute that provides the most significant information about a class. It aims to reduce the entropy level from the root node to the leaf node by leveraging this approach. The mathematical formula for entropy is shown in Equation 3-8 [143].

$$Gini = 1 - \sum_{i=1}^{n}(P_i)^2 \quad (3\text{-}8)$$

Figure 3-13 shows the components of KosaNET. KosaNET components comprise data I/O, classifier controller, classification, initiate device, and classifier builder components, which run on a CPU. We will now describe in more detail all the system components of KosaNET.

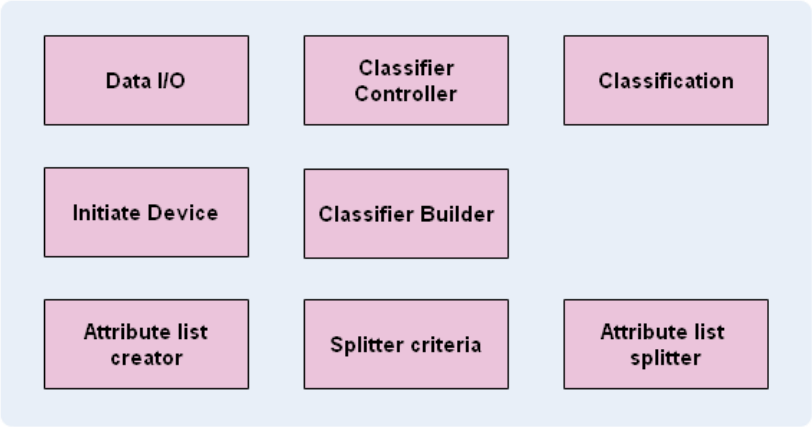

Figure 3-13: KosaNET's Logical Components

3.2.9.1 KosaNET Components

In this section, we discuss the various components of KosaNET.

Data Loading

The initial step in the KosaNET flowchart, as shown in Figure 3-14, involves the host reading input data from a disc. Once the data is read, it is stored in the device's memory. This process includes loading the data from the disc and allocating space for it in the device memory. The allocated space includes the entire training data, storage space for the attribute list, and an internal buffer within the device itself.

Device Initialization

Following the allocation of device memory, the next stage is the initiation of the device. This step involves preparing the device for further processing and ensuring that it is ready to perform its designated tasks.

Initiation of the Classifier's Parameters

Once the device has been initialized, the next step is to establish the user-defined parameters for the KosaNET. These parameters are specific to the classification assessment and include determining the minimum amount of data required for a leaf, specifying the maximum depth of the decision tree, and other relevant settings. These parameter values are crucial for configuring KosaNET to meet the desired classification requirements.

Creation of the Attribute Lists

To generate attribute lists, there are two essential l steps to follow. Firstly, the data is moved to the most appropriate list based on its characteristics. Once the data migration is complete, all the attribute lists need to be sorted for further processing.

Classifier Builder

The classifier builder plays a vital role in two aspects. Firstly, it is responsible for identifying the split point, which involves locating the potential point at which the

attribute lists can be divided. Once a valid split point is found, the second role of the classifier builder is to actually split the attribute lists accordingly.

Classification

The constructed decision tree is stored in the host's local memory. The classifier, which is responsible for making predictions, is built on the host to accommodate scalability requirements. The entire classification process takes place on the host, necessitating sufficient memory resources to handle the task effectively.

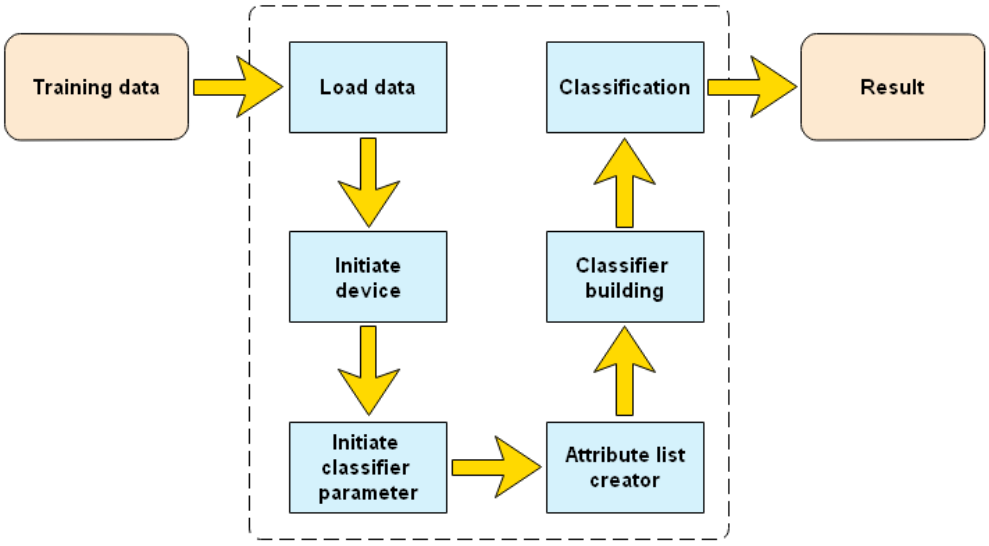

Figure 3-14: A Flowchart for the KosaNET model

Figure 3-14 shows the KosaNET flowchart, which has seven major steps as follows:

1. The training and test data are loaded into the host memory.
2. The devices are initialised. This includes the allocation of memory, copying of training data, and querying device information.
3. Setup of parameters from user input, for instance, the maximum depth of the classifier and the minimum data of a leaf
4. A list of attributes is created on the device, and then each is moved to its corresponding position. Once the data movement is completed, the attribute lists on the device are sorted.

5. In the next step, KosaNET employs an iterative breadth-first scheme instead of the recursive model for building the decision tree algorithm.
6. The classification is performed on the host in a sequential manner.
7. The results of the classification are presented to the host.

The system will continue to iterate until all data is assigned to leaf nodes. For each data segment, the system checks if all the data in that segment shares the same class label, either positive or negative in our system. If all the data in the segment has the same class, a leaf node is created, representing the classification result. If the data in the segment has different classes, the system proceeds with the process of finding a split point for the segment. A leaf node corresponds to the classification result, and the data will be classified accordingly if it reaches that node during the classification process. Once a candidate split point is found, the attribute list is split, and an internal node is created. An internal node can be considered a rule that determines the path for classifying the data.

3.3 Experimentation and Model Evaluation

To implement the KosaNet model, the Python programming environment is used. After the model was implemented, its performance was evaluated. Several metrics were considered for this purpose. This section outlines how the model was implemented and explains the evaluation metrics used in its assessment. Figure 3-15 describes the entire experimental setup, including the predictor gases that were used in the experiment and the models that were evaluated.

3.3.1 Implementation Environment

KosaNet has been implemented in the Python programming environment. Apart from being completely open source, Python boasts a rich set of libraries that support data analytics and analysis [150]. In addition, Python has a comfortable learning curve for programming novices [151]. The specific libraries that were used in conjunction with Python are Matplotlib [152], TensorFlow [153], NumPy [154], Pandas [136], Seaborn [155], Keras [156], and Scikit-learn [157].

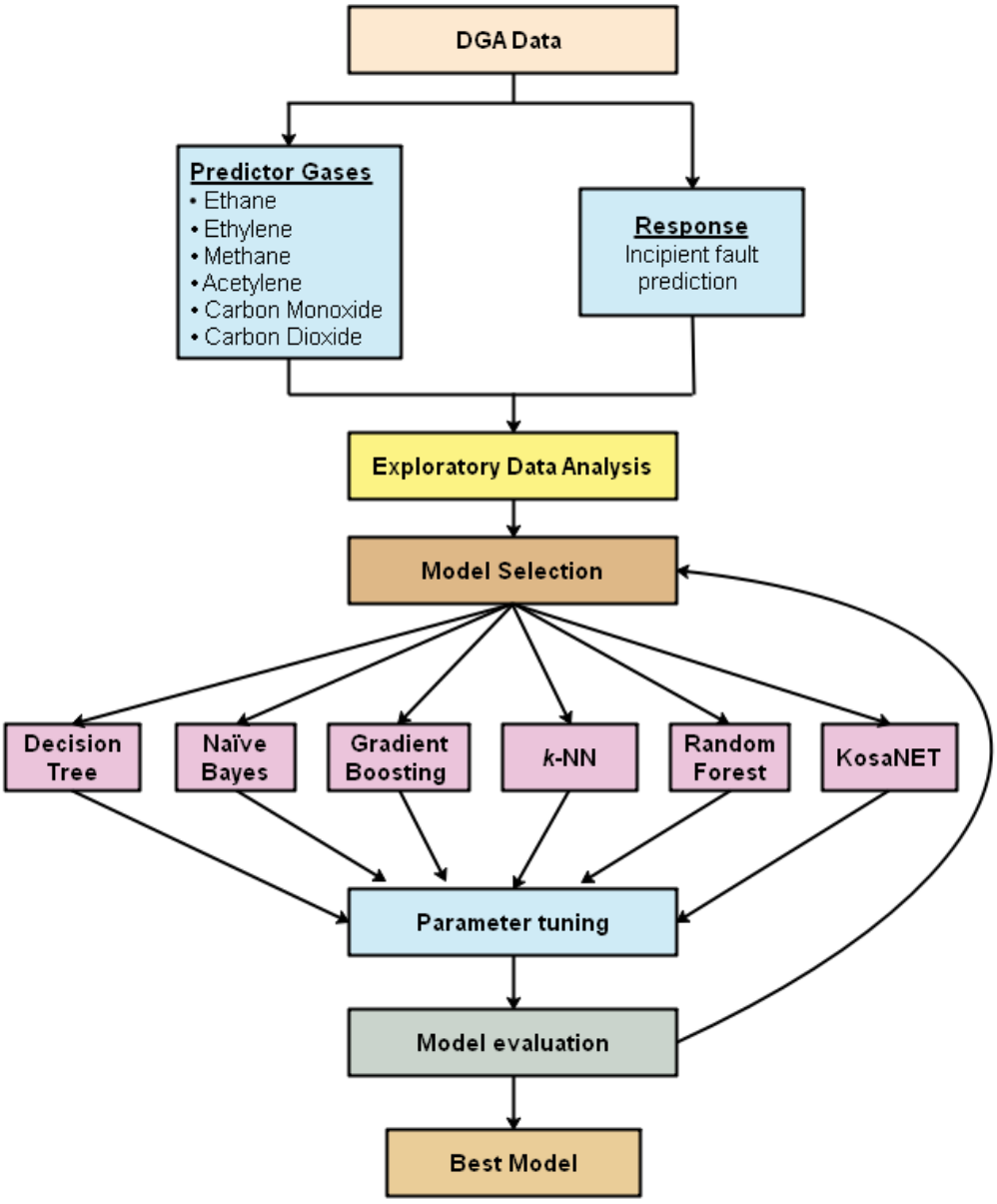

Figure 3-15: Experimental Setup

3.3.2 Classification Evaluation Metrics

Multiple methods exist for the performance evaluation of classifier algorithms. Subsequent sections present a detailed discourse on the evaluation metrics that were employed in this study.

3.3.2.1 Confusion Matrix (CM)

The confusion matrix (CM) is an arithmetically derived means of quantifying how well a model performs during classification. It gives a comprehensive and complete picture of how the classifier performed, where it went wrong, and offers guidance on how to correct the situation. It is basically an *N*-by-*N* dimensional table that compares the "actual" versus the "predicted" entries [158], [159]. In this case, $N = 7$ represents the various classes available in the data set, and it shows the definite positives, definite negatives, projected positives, and projected negatives. The running diagonal represents the values of the correctly predicted instances and is also known as the true positive (TP). The values in the off-diagonal column represent the incorrectly classified instances and manifest as falsely positive or falsely negative. The falsely positive instances are referred to as Type I errors, while the falsely negative instances are Type II errors.

Figure 3-16 shows a confusion matrix for DGA multiclass classification. The confusion matrix allows us to deduce several other evaluation parameters, such as classification accuracy [160], classification error [161], sensitivity [160], precision [162], and the f1-score [163].

		Predicted Class						
		DLE	**DHE**	**NOF**	**PDH**	**PDL**	**THF**	**TH3**
Target Class	**DLE**	TP_{DLE}	$E_{DLE,DHE}$	$E_{DLE,NOF}$	$E_{DLE,PDH}$	$E_{DLE,PDL}$	$E_{DLE,THF}$	$E_{DLE,TH3}$
	DHE	$E_{DHE,DLE}$	TP_{DHE}	$E_{DHE,NOF}$	$E_{DHE,PDH}$	$E_{DHE,PDL}$	$E_{DHE,THF}$	$E_{DHE,TH3}$
	NOF	$E_{NOF,DLE}$	$E_{NOF,DHE}$	TP_{NOF}	$E_{NOF,PDH}$	$E_{NOF,PDL}$	$E_{NOF,THF}$	$E_{NOF,TH3}$
	PDH	$E_{PDH,DLE}$	$E_{PDH,DHE}$	$E_{PDH,NOF}$	TP_{PDH}	$E_{PDH,PDL}$	$E_{PDH,THF}$	$E_{PDH,TH3}$
	PDL	$E_{PDL,DLE}$	$E_{PDL,DHE}$	$E_{PDL,NOF}$	$E_{PDL,PDH}$	TP_{PDL}	$E_{PDL,THF}$	$E_{PDL,TH3}$
	THF	$E_{THF,DLE}$	$E_{THF,DHE}$	$E_{THF,NOF}$	$E_{THF,PDH}$	$E_{THF,PDL}$	TP_{THF}	$E_{THF,TH3}$
	TH3	$E_{TH3,DLE}$	$E_{TH3,DHE}$	$E_{TH3,NOF}$	$E_{TH3,PDH}$	$E_{TH3,PDL}$	$E_{TH3,THF}$	TP_{TH3}

Figure 3-16: Confusion Matrix for DGA Multiclass Classification

3.3.2.2 Classification Accuracy

The classification accuracy gives us a measure of how often the classifier is correct. Equation (3-9) gives the formula for calculating the classification accuracy [164].

$$Classification\ Accuracy = \frac{\sum_x^y trp_x}{\sum_x^y trp_x + \sum_x^y trn_x} \tag{3-9}$$

where *trp* and *trn* are the true positive and true negative values for every class *x* such that $x \in \{x{:}y\}$.

3.3.2.3 Classification Error

The Classification Error provides an indication of how often the classifier is incorrect and is calculated using Equation (3-10) [161].

$$Classification\ Error = \frac{\sum_x^y fap_x + \sum_x^y fan_x}{\sum_x^y trp_x + \sum_x^y trn_x} \tag{3-10}$$

where *trp, trn, fap* and *fan* denote the factual positive, factual negative, erroneous positive, erroneous negative, respectively, for every class *x* such that $x \in \{x{:}y\}$.

3.3.2.4 Averaged Instances Sensitivity

The sensitivity, also referred to as the recall, is an intuitive measure of how sensitive the classifier is to detecting faults whenever they occur. The averaged sensitivity is obtained as shown in Equation (3-11) [160].

$$Averaged\ Sensitivity = \left\{ \sum_{i=1}^{j} \left(\frac{trn_j}{trp_j + \sum_x^y e_{j,x}} \right) \right\} \div j \tag{3-11}$$

where trn_j refers to the true negative rate for class *j*, trp_j is the true positive rate for class *j* and $e_{j,x}$ represents the classification error where class *j* is incorrectly classified as class *x*.

3.3.2.5 Averaged Precision

Average precision answers the question of how often a prediction is correct when a positive value is foretold from the aggregate prediction patterns in an affirmative class. The precision is calculated per class and then averaged as shown in Equation (3-12) [163].

$$Averaged\ \ Precision\ \ = \left\{ \sum_{i=1}^{j} \left(\frac{trp_j}{trp_j + \ \sum_x^y e_{j,x}} \right) \right\} \div j \qquad (3\text{-}12)$$

where trp_j is the true positive rate for class j while $e_{j,x}$ represents the classification error where class j is incorrectly classified as class x.

3.3.2.6 Averaged F_1 Score

The f_1 score measures how accurate a model is on a dataset. It provides a more accurate measure of incorrectly classified cases. The formula for the f_1 score is given in Equation (3-13) [164].

$$Averaged\ F1\ Score = \left\{ \sum_{i=1}^{j} \left(2 \times \frac{P_i\ \times R_i}{P_i\ + R_i} \right) \right\} \div j \qquad (4\text{-}13)$$

where P_i and R_i represent a precision and recall for a class i respectively.

3.4 Evaluation and Results

The results of the evaluation of KosaNet vis-à-vis other multinomial classifier models are presented and discussed on the basis of the metrics discussed previously in Section 4.3. Figure 3-17 shows the confusion matrix that was obtained from the KosaNet model. The label encoder assigned the columns in the following order: DLE, DHE, NoF, PDH, PDL, THF, and TH3. To facilitate further discussion, the confusion matrix has been decomposed as shown in Figure 3-18.

```
Confusion Matrix :
[[1232    0    0    0    0    0    0]
 [   0 1176    0    0    0    0    0]
 [   0    0 1194    0    0    0    0]
 [   0    0    0 1198    0    0    0]
 [   0    0    0    0 1219    0    0]
 [   0    0    0    0    0 1207    0]
 [   0    0    0    0    0    1 1137]]
Accuracy Score : 0.9998804399808704
```

Figure 3-17: Confusion Matrix

In Figure 3-18, an additional row and column for tabulating the total have been included to allow us to compute the evaluation metrics discussed in Section 4.3. The confusion matrix enables us to calculate the classification accuracy, classification error, sensitivity, precision, and the f_1-score [165]. Table 3-2 is an extract of the DGA data in ppm that was used to evaluate the model. Table 3-3 shows how classical techniques compare against the proposed model. The incorrectly labelled classes are marked in red text.

		Predicted Class							
		DLE	DHE	NOF	PDH	PDL	THF	TH3	Total
Target Class	DLE	1232	0	0	0	0	0	0	1232
	DHE	0	1176	0	0	0	0	0	1176
	NOF	0	0	1194	0	0	0	0	1194
	PDH	0	0	0	1198	0	0	0	1198
	PDL	0	0	0	0	1219	0	0	1219
	THF	0	0	0	0	0	1207	0	1207
	TH3	0	0	0	0	0	1	1137	1138
	Total	1232	1176	1194	1198	1219	1208	1137	8364

Figure 3-18: Labelled Confusion Matrix including Row and Column totals

Table 3-2: DGA data extract

Gases Concentration (ppm)							
SN	**Hydrogen**	**Methane**	**Acetylene**	**Ethylene**	**Ethane**	**CO**	**Status**
0	2460	777	614972	376939	6874	4455	DHE
1	2431	782	596579	384308	6840	4404	DHE
2	2514	776	602370	376314	8133	4284	DHE
3	2366	783	602451	369238	5552	4499	DHE
4	2312	787	593503	363152	4347	4544	DHE
5	9393	823	34	12	240	946	DLE
6	14438	1269	30	10	220	959	DLE
7	10606	1084	30	10	240	942	DLE
8	11575	1841	32	10	307	949	DLE
9	9687	1176	31	11	232	951	DLE
10	2352	784	600763	375411	5294	4516	PTD
11	2395	776	594711	381110	6278	4393	PTD
12	2503	775	612427	375907	7283	4394	PTD
13	2476	774	604910	373127	7219	4338	PTD
14	2504	769	602155	379164	7183	4513	PTD
15	2162	3245	53	1854	929	1692	TFT
16	919	2395	49	1398	768	1378	TFT
17	459	1766	28	542	234	1180	TFT
18	324	890	9	365	166	1394	TFT
19	1818	2618	49	1365	818	1462	TFT
20	3163	6428	157	17174	5329	6774	TF3
21	2775	5368	118	14465	4178	6773	TF3
22	3711	5255	224	15158	3058	6692	TF3
23	2371	3723	86	13094	3289	6415	TF3
24	3016	4559	256	12875	3196	6480	TF3
25	1708	1131	1493	1181	2556	1353	NoF
26	1641	1307	1637	1331	2495	2837	NoF
27	1785	1417	1676	1701	2184	1923	NoF
28	1983	1483	1797	1873	1889	2585	NoF
29	1983	1483	1797	1873	1889	2585	NoF

In Table 3-3, a comparison of classification results using key gases, the Duval Triangle, nomography, and KosaNet is made. These results show that the key gas method correctly classified 18 out of 20 gases, or 90%. This performance was

replicated by the Duval triangle method, which also correctly classified 90%. The nomography technique had the least accuracy, attaining only 85%. In comparison, KosaNet attained an accuracy of 95% of accurately classified instances. Table 3-3 provides the results obtained when the model is compared against other algorithms with multi-class classification abilities.

As seen in Table 3-4, the decision tree, Naïve Bayes, gradient boosting, *k*-NN, random forest, and KosaNet realised an accuracy of 68.5%, 70%, 83%, 89.7%, 92.4%, and 99.9%, respectively. This implies that with KosaNet, less than 1 out of 10 labels are incorrectly labelled. With KosaNet, the precision value was high, with the implication that more than nine out of ten labels were incorrectly classified. Similarly, the recall value of 99.9% means that fewer than 1 in 10 DGA readings are incorrectly labelled. The f_1 score, which helps preserve a balance between precision and recall, tends towards one, which is an excellent value for this metric.

3.5 Limitations of KosaNET

One of the problems with the proposed method is that it needs a lab analysis process to figure out how much of each dissolved gas there is. This makes it hard for the method to collect and combine dissolved gas analysis (DGA) data on its own. As a result, the technique does not possess the capability to directly gather real-time or continuous DGA data from the equipment or system being monitored. Instead, it relies on periodic laboratory testing to obtain the necessary data for analysis and interpretation. This limitation hinders the technique's potential for immediate detection and response to evolving fault conditions, as the data collection and analysis are not seamlessly integrated into a real-time monitoring system.

3.6 Summary

This study focuses on utilising machine learning techniques to analyse dissolved gas analysis (DGA) data for early detection of incipient faults in oil-impregnated transformers. Transformers are vital for the transmission and distribution of electrical energy, and the failure of even a single unit can have significant consequences for

consumers and economic activity. Therefore, it is crucial for power utility companies to prioritise the condition monitoring of critical assets.

Table 3-3: Comparison of classification results using Key Gases, Duval Triangle, Nomography and KosaNet

SN	KEY GASES	DUVAL	NOMOGRAPHY	KOSANET	ACTUAL FAULT
0	ARC	D1	TH and PD	DLE	ARC
1	TH	T3	TH	TH3	TH>700°C + CD
2	TH	T3	TH	TH3	TH >700°C
3	TH	T1	TH and PD	THF	TH <300°C
4	ARC	D1	ARC	DHE	ARC + CD
5	ARC	D1	ARC	DHE	ARC + CD
6	TH	T3	TH and PD	TH3	TH >700°C
7	NR	**DT**	**TH**	NoF	NR
8	TH	D1	ARC	DLE	ARC
9	TH	T2	TH	TH3	TH >700°C
10	TH	T1	TH and PD	TH3	TH >700°C + CD
11	NR	T3	**TH**	NR	NR
12	TH + ARC	T3	TH	THF	TH
13	TH	T3	TH	THF	TH
14	**ARC**	**D2**	TH	**NoF**	DP
15	TH	T1	TH	TH3	TH <300°C
16	ARC	DT	DP et TH	DHE	ARC + CD
17	**ARC**	T3	ARC	THF	TH
18	TH	T1	TH	TH3	TH <300°C
19	ARC	T1	**ARC**	TH3	TH >700°C + CD

DGA, a widely used technique for transformer condition monitoring, involves analysing dissolved gases in transformer oil. However, interpreting DGA data to identify incipient faults can be challenging and often relies heavily on the expertise of technical personnel. To address this, the study proposes a novel multinomial classification model called KosaNet, based on decision trees, for accurate and clear interpretation of DGA data.

Table 3-4: Average performance rate for each model

	Decision Tree	Naïve Bayes	Gradient Boosting	*k*-NN	Random Forest	KosaNet
Accuracy	0.685	0.70	0.83	0.8967	0.9241	0.9998
Precision	0.685	0.67	0.83	0.8967	0.9241	0.9998
Recall	0.685	0.80	0.83	0.8967	0.9241	0.9998
F1 Score	0.685	0.73	0.82	0.8851	0.9241	0.9998
Error	0.315	0.30	0.17	0.1033	0.0759	0.0002

The performance of KosaNet is compared to other algorithms capable of multiclass classification, including decision tree, k-NN, random forest, naïve Bayes, and gradient boost. Actual DGA data consisting of 2912 entries is used to evaluate the performance of these algorithms. The investigation reveals that KosaNet exhibits improved DGA classification abilities, particularly when dealing with multinomial data.

In short, the study shows how machine learning, and in particular the KosaNet model, can help make it easier to understand and classify DGA data in oil-impregnated transformers. This approach offers a promising avenue for early detection of incipient faults and improved condition monitoring of critical assets in the power utility sector.

Chapter 4

An Efficient Lora-Enabled Smart Fault Detection and Monitoring Platform for the Power Distribution System Using Self-Powered IoT Devices

4.1 Introduction

The legacy power distribution grid that is still widely in use was never built to enable two-way communication, nor was it made with the ability to facilitate real-time monitoring by the service provider [166], [167]. While highly sophisticated and computerised technologies meticulously monitor electricity generation and transmission, the distribution segment lacks a comparable level of sophistication [168], [169]. Because there is no automated means of monitoring power delivery to consumers, this lack of feedback impedes efficient management of the power distribution grid [32]. In the event of a power failure, the service provider remains completely oblivious to the fact, resulting in a hue and cry from the affected consumers. This lack of feedback also delays the initiation of reparative and restorative activities and interrupts the revenue stream for the power system operator (PSO) [14], [170]. In response to this issue, service providers have had to employ strategies that attempt to keep themselves informed about problems on the distribution side of the network. In Kenya, for instance, Kenya Power Company Plc., the lone purveyor of electricity, encourages its clients to communicate with the company through telephone calls whenever they experience an interruption in power delivery. The power system operator has set up call centres and publicised its telephone and email contacts to be used for this purpose [171]. In order to ascertain the loss of power, Kenya Power clusters the telephone calls according to the areas they originate from, makes a guess at the probable location of the problem, and then sends out a service crew team to find and repair the fault [7]. This arrangement, however, ambitiously assumes that the

client is constantly monitoring the power supply in the affected premises and that the customer is very conversant with troubleshooting the power network. However, even with this arrangement, the time it takes the service provider to learn about an active fault is inordinately long, resulting in prolonged episodes of power blackouts. Every year, Kenya Power customers experience up to 25,000 minutes of power outages [172]. For a growing economy with ambitious goals for the future, this is untenable.

As of June 2021, Kenya had an installed capacity of about 2,813 megawatts generated from various sources as follows: about 29.4% was hydropower, 29.4% was geothermal, 26.6% was thermal, and 11.8% was wind, with solar and biomass closing the list at 1.8% and 1%, respectively [173], [174]. Figure 4-1 is a graphical representation of Kenya's energy generation mix. This energy is distributed to about 7.5 million customers through a distribution and transmission network consisting of about 74,608 kilometres of electric lines.

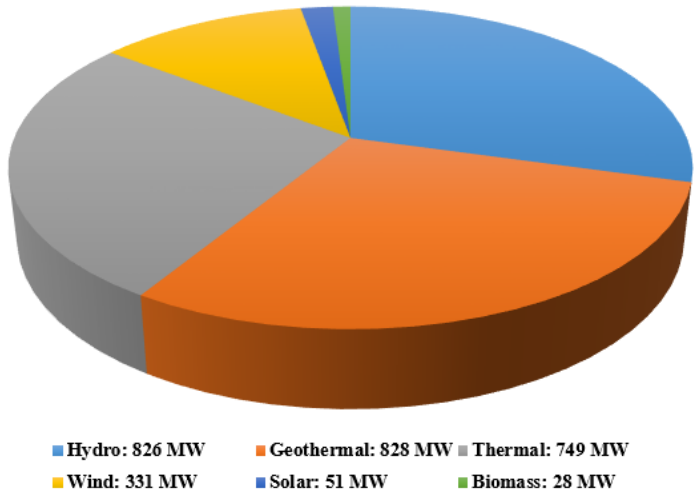

Figure 4-1: Kenya's Energy Generation Mix

Disturbances in the power system are not entirely avoidable. In such a vast and expansive system with so many variables and factors at play, one thing or another will go wrong at any one time, and when this happens, it is important that the incident be immediately brought to the attention of the service provider [175]. The longer it takes to detect and correct a fault, the more damage is done to nearby equipment and

infrastructure, resulting in even more catastrophic failures and costly repairs. The gradual rollout of the Smart Grid (SG) in developed economies is addressing this issue. Due to its ability to integrate power, data, and message exchange to fashion an efficient energy system, the smart grid is seen as a potential solution to the lack of feedback from the electricity grid [176], [177]. However, this solution is not good for developing countries because it is too expensive [178], [179].

Different ways have been suggested in the literature to solve the fault detection and location discovery problem. These include Petri nets [180], [181], fuzzy-based methods [182], [183], artificial neural networks [184], [185], expert systems [186], [187], and analytic models [188], [189]. A variety of approaches have been proposed in the literature to address the fault detection and location discovery problem, including. Although the aforementioned approaches have some very strong points in some respects, they also display certain weaknesses. For example, when it comes to expert systems, establishing and maintaining a knowledge base may be challenging. The ability of artificial neural networks to comprehend reasoning outcomes is still in its infancy; fuzzy theory employs membership functions and fuzzy rules that are susceptible to subjective tendencies; and petri-based methods have poor adaptability and difficulties in online modelling.

In [123], a study that focused on fault diagnosis in power transformers and the role of IoT in power maintenance is reported. Thirty faulty transformers were selected, with 20 of these being used for training while the other 10 were used for testing. For communication, the General Packet Radio Service (GPRS) was used. The researchers studied the rate of accurate detection of the proposed IoT-based power transformer fault analysis method. It was reported that a training error of less than 0.01% was observed, with the model accurately identifying 95.6% of the faults, including those not used in training. In [4], a model that exploits Ohm’s law to detect the fault location is proposed. The model enabled technicians to find the precise location of the fault and assisted service personnel in removing persistent faults, thus reducing the occurrence

of faults and minimising the time of power outages. The system used an Arduino to analyse the distances of the fault incidents with the help of software developed for the purpose. The fault location was relayed using a Wi-Fi module. In [175], a remote IoT surveillance and fault prediction arrangement grounded on custom-made software-defined networking (SDN) is proposed. The methodology, described as an evolution into a smart grid deployment, was based on a tailored software-defined network. The proposed architecture showcased an efficient method of handling imminent interruptions and faults in the power system via reasonably priced and dependable frameworks that predict and deliver live condition monitoring indicators. A prediction accuracy of about 96.1% was attained.

A novel method for precisely locating faults that exploits the various measurements obtainable is proposed in [40], [190]. To determine the position that is closest to the culpable site, the devised method iteratively estimates the fault site. The lines connecting to the chosen site are then scanned in order to pinpoint the problem. A simulation test was conducted on an actual distribution grid, and various failure scenarios were considered to appraise the performance of the suggested technique. The upshot of this appraisal was that the method is accurate and robust even when the measured data is questionable, and it reliably manages measurement mistakes. A novel smart current and voltage observation method is suggested in [190]. The system monitored a 3-phase power grid using an open-source microcontroller, which read currents and voltages from sensors. The readings were then sent wirelessly to an Android application for analysis. The system enabled the monitoring of some basic voltage and power quality aspects. In [191], an algorithm that uses zoning in the power distribution system (PDS) is proposed. It communicated with a cloud server through an edge node and delivered time-harmonised current quantities. A database was used to record all fault incidences that occurred in the power distribution system. Results showed that the procedure was successful at localising the faults in all the test cases conducted.

A mature system that has been extensively used for fault detection for several decades is supervisory control and data acquisition (SCADA) [123]. It is not only used in the power industry but also in several other industrial settings, such as manufacturing, water management and treatment systems, and oil and gas facilities. SCADA is basically a centralised system that monitors and controls a given production environment by gathering relevant data and sending back commands to control certain aspects of the process [192]. Figure 4-2 displays the fundamental components of the SCADA system. Due to the length and breadth of the distribution network, it is often not practically possible to run SCADA over it because of the exorbitant installation costs. Such an installation would cost hundreds of thousands of dollars, cancelling out any potential gains achievable from such action. It is for this reason that many service providers have shied away from a SCADA-monitored distribution grid [6].

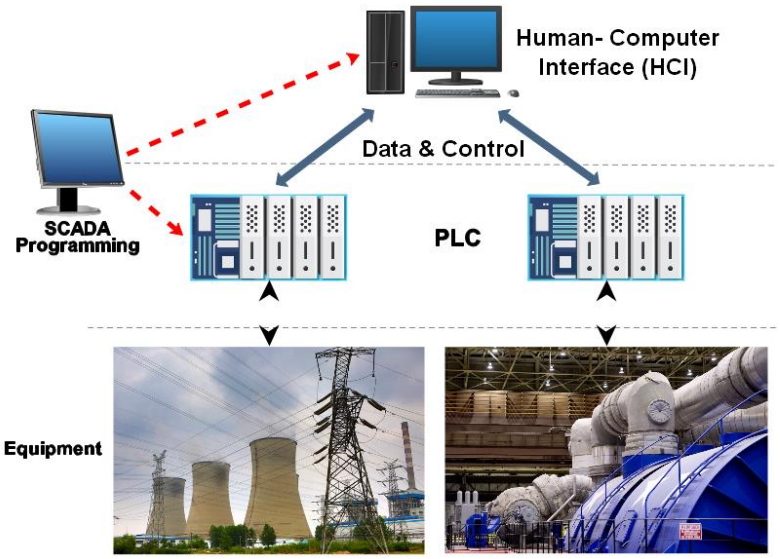

Figure 4-2: Main Components of a SCADA System (Source: Author)

In [193], phasor measurement units (PMUs) have been described as being an integral part of a sophisticated technology for advanced measurement and monitoring of energy transmission and distribution. In contrast to other existing grid measurement methods, PMUs can provide highly accurate and synchronised real-time measurements via Global Positioning System (GPS) signals [194], [195]. PMUs are

typically installed at power substations and work by measuring the amplitude of the voltage and the current at preselected points using current transformers (CTs) and potential transformers (PTs). The phase of the measured quantities along with their time-synchronised signals are also taken and sent to a phasor data concentrator (PDC) for onward transmission to the control centre for further analysis. PMUs are widely used and have been extensively integrated into the transmission and distribution grids. This technology is, however, very expensive and is seldom used on the distribution network.

A suggestion was made in [7] to use smart metre measurements to detect the location of distribution grid faults using a state-approximation-based technique. The suggested technique uses the variable-weight matrix identification method to discover the faulty section. The approach is simple to implement algorithmically and does not require the use of a fault type [7]. An assumption is made that the currents and voltages measured as the fault develops are accessible by the main substation.

Numerous studies have also been conducted on the adoption of intelligent algorithms and machine learning methods for power fault detection and analysis. In [196], it is suggested to use a fuzzy logic controller (FLC) to find faults and an adaptive neurofuzzy inference system (ANFIS) to find out where the fault is. The study focused on how distribution grid incidences can be detected, identified, and located. A fuzzy controller was incorporated into the system to recognise different kinds of faults upon their occurrence. The model was developed in MATLAB, and the results showed that ANFIS attained an accuracy of 51% for identification and 93% for location.

Other researchers have also extensively reported on LPWANs. Song [61] compares the two main technologies in the LPWAN space against GPRS. The study found that, as compared to the coverage areas of ZigBee and Wi-Fi, LPWANs enable considerable connections covering long distances at low cost and are devoid of the requisite maintenance. In [197], a study seeking to understand the abilities and shortcomings of LoRa technology in terms of its throughput, coverage, and scalability is reported. The

study used a combination of measurements from a real-world citywide LoRa deployment and high-fidelity simulations to obtain and analyse the measurement data collected. The results showed that within a radius of about 15 kilometres, three gateways were able to sufficiently cover the area and provide connectivity to about 1,000,000 end devices. The study illustrated the resilience of LoRa, especially in a dense urban environment. In [198], a study on the performance of an IoT application based on LoRaWAN is reported. The experiment sought to obtain insight into the packet loss, RSSI, and SNR values between the transmitting device and the receiving one. Experimentation results showed that when the spreading factor is high, LoRa end devices tend to provide greater immunity against signal fading and multi-path fading.

IoT has today made it possible for miniature, alternatively powered devices to be embedded in the environment, monitoring a diverse range of quantities in various fields such as agriculture, security, manufacturing, environmental monitoring, healthcare, and transportation, just to name a few. This embedding has concomitantly created a need for innovative ways to power these embedded devices. Consequently, the term “energy scavenging” has become relevant in this context. Energy exists in the environment in many different forms and can be harvested for use in low-power-demanding applications [199]. In [200], various latent energy sources in the environment are identified, such as chemical, mechanical, acoustic, solar, and radio frequency (RF). The harvesting of ambient energy coupled with the usage of rechargeable batteries for energy storage is beneficial for Wireless Sensor Network (WSN) operations, opines Dhananjaya [72]. His work further observes that WSNs require energy harvesting to avoid frequent battery replacement and associated costs. Energy harvesting enables on-site charging of rechargeable batteries, which may be cycled hundreds of times before losing their capacity. The battery's life may be prolonged practically forever with the right technology and energy management. As observed in [201], [202], the long-term deployment of IoT devices necessitates some form of energy harvesting. In particular, photovoltaic (PV) cells have been identified as a feasible, low-cost, and long-term energy source for IoT sensors.

4.1.1 IoT, LPWAN, LoRa®, and LoRaWAN®

IoT is a notion that promulgates the idea that millions of independent, ubiquitous, internet-enabled devices can spontaneously and autonomously initiate connectivity with other similarly connected devices and share information at any time, any place, and anywhere [203], [204]. With the widespread adoption of IoT solutions across a wide range of domains [205], the focus has shifted to how these IoT devices can connect from remote and distant locations given that they are battery-powered and severely resource constrained [165], [206]. It is from this perspective that LPWAN, short for "low-power wide-area network," comes into play. The term "LPWAN" refers to communication protocols and technologies that embrace two unique properties: one, they have an enviably small energy demand, and two, they possess the ability to communicate over distances tens of kilometres apart. Due to their low energy demands, LPWAN-compliant devices have the uncanny ability to run for several weeks, maybe even years, on nothing but low-capacity battery cells. As opposed to wireless WANs, which are designed to carry more data using more power, LPWANs have a low data rate that is typically less than 50 kbit/s per channel [68]. The reach of LPWANs varies but can be greater than 15000 metres depending on the specific technology, with payloads of up to 1000 bytes [198], [207]. As such, the term "LPWAN" does not refer to a specific technology but is a generic term used for various long-reach but low-power-consuming networking technologies that come in various shapes, sizes, and flavours [208]. LPWANs can be proprietary or open-standard, and they can use licensed or unlicensed frequency bands [209]. Some examples of LPWAN-compliant technologies include ZigBee, SigFox, Nwave, RPMA, Ingenu, LoRa, NB-IoT, LTE-M, and NB-Fi.

LoRa® is an abbreviation for long range and is the name of a physical layer proprietary LPWAN technology founded on the spread spectrum modulation technique that is plagiaristic of the Chirp Spread Spectrum (CSS). Because of its low power, low bandwidth, and long-range capability, LoRa has emerged as a boon for the IoT, particularly for wide-area data haulage [210]–[214]. LoRa devices offer fascinating

characteristics for IoT use cases that include long-range communication, low power demand, and secure data transfer. It was developed by Cycleo SAS about a decade ago, and later it (Cycleo SAS) was acquired by Semtech [60], [215]. Since then, Semtech has successfully leveraged the wide-area connectivity capabilities of LoRa, so much so that today more than 65 million devices across more than 120 countries are using LoRa [216], [217]. LoRa technology, whose physical layer was patented in July 2014, is popular for many reasons. Not only is it long-range and low-cost, but it makes judicious use of scarcely available power, giving it the ability to operate for many weeks, possibly years, powered by nothing but tiny energy reservoirs [71], [205], [211].

From an architectural point of view, a typical LoRa deployment can be divided into four distinct sections [211], as shown in Figure 4-3. A LoRa network can allow an assorted array of embedded sensors to transmit information to a central gateway, which then forwards the same to an application server via a network server. The end devices, otherwise known as “motes” or “nodes,” are ordinary objects equipped with low-power communication devices. The gateways are the devices that receive and transmit data from and to the motes. The gateways themselves must be connected to the network servers via some kind of backhaul network connection [207], [218]. The network server is the workhorse of the network. The network server manages the gateways and allows the end devices to securely communicate with the cloud. It has all the intelligence to perform security checks, remove duplicate packets, acknowledge packets received from the gateways, and channel packets received to the relevant application server. The application is just some software executed on an Internet server.

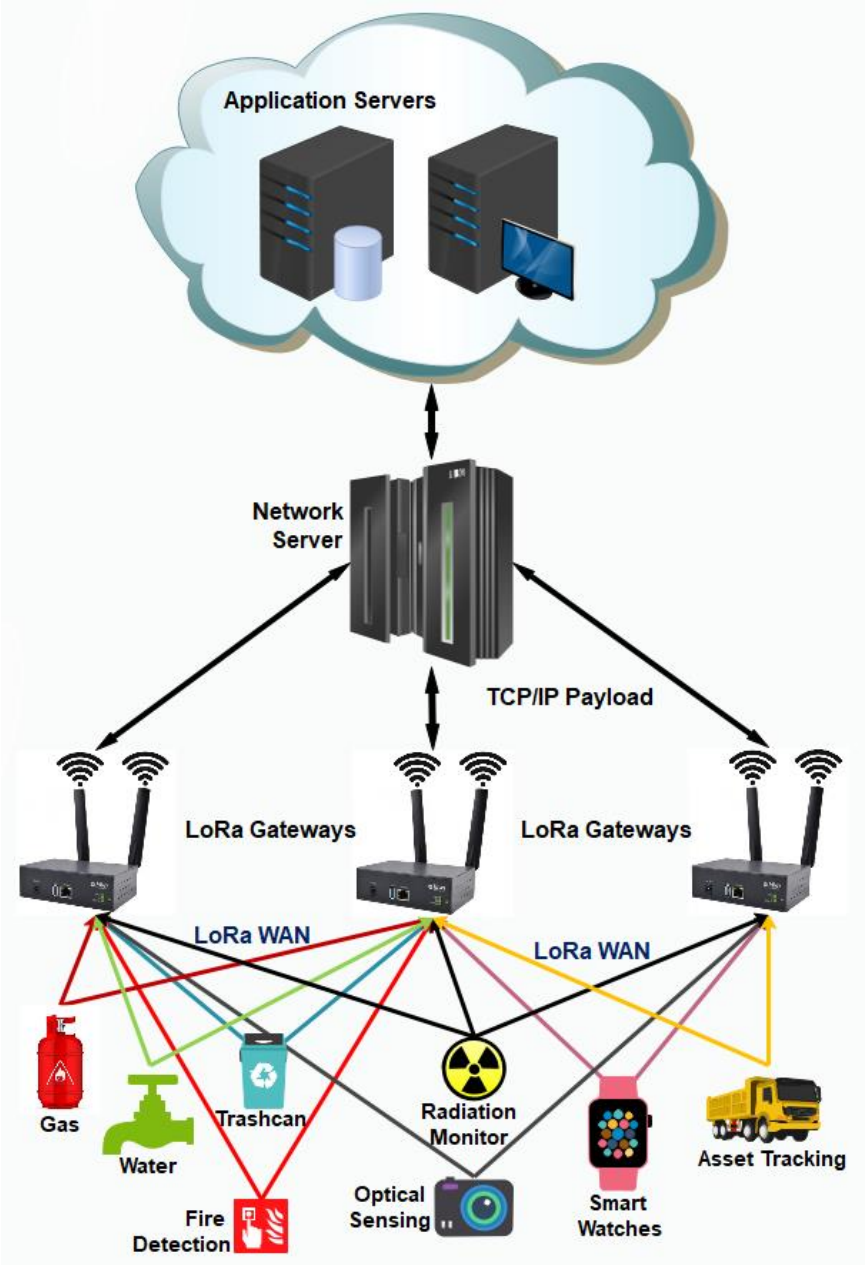

Figure 4-3: Architectural Layout of a LoRaWAN Deployment (Source: Author)

LoRaWAN is an implementation of the adaptive data rate (ADR) algorithm that regulates the communication speed for each node individually. The terminal nodes are permitted to transmit data using any ADR speed over any available channel at any time. Specific rules, however, must be followed, one of which is that the end devices are required to change the channel haphazardly for every broadcast. This ensures the

availability of a variety of frequencies for data transmission. Additionally, the end nodes are required to abide by the range specification's limitations on transmission duty cycles.

The architectural framework of LoRaWAN comprises four major components, as shown in Figure 4-3. These four components are the end nodes; the gateway; the network server; and the application servers. This framework shows how LoRa and LoRaWAN allow dense but widely spread-out networks of edge devices to be connected, thus enabling data collection and monitoring from thousands of nodes in a manageable way. The end nodes are the devices situated at the network boundaries and will usually be equipped with sensory capabilities; the type, design, and function will depend on the specific use case.

Customarily, a low-powered microcontroller is used to build end nodes. This gives the nodes the ability to linger in the environment for many months or years without requiring regular servicing. They will usually be fitted with a means of communication that requires minimal power. The gateways receive and forward data from the end nodes and can therefore be thought of as bridges between the nodes and the network. Because of its primary role in the network, the gateway can also be considered a packet forwarder [211]. The network server joins all the data it receives from the various gateways and uploads it to the application server. Finally, the data collected from the field by the different end nodes must be interpreted either visually or analytically. The application server is responsible for playing this role. In addition, specific actions or triggers may be initiated as a consequence, such as a notification service to inform the resident engineer when a potential issue has arisen or the mere opening of a window or turning on rainwater pumps for agricultural use cases.

LoRa functions in the unregulated and free-to-use unlicensed Industrial, Scientific, and Medical (ISM) radio bands, which are sections of the radio frequency spectrum retained internationally for ISM purposes [210]. The ISM radio bands assigned for use in specific countries differ from one another but are either 433 MHz, 868 MHz, or 915

MHz. In the US, for instance, the frequency sub-band used is 915 MHz, while in the EU, 433 MHz or 868 MHz sub-bands are used. According to regional regulatory agencies' set frequency allocations, other regions of the world will also have them [219]. Even though LoRa functions in the free and unlicensed ISM radio bands, there are regulations on how much power it can transmit, its duty cycle, and sometimes its bandwidth. For instance, in the EU, a duty cycle limit of 1% per sub-band per hour is specified.

LoRa modulation characteristics are premised on three configurable properties that remarkably alter its performance: the coding rate (CDR), the spreading factor (SF), and the bandwidth (BW). The bandwidth is the breadth of the spectrum that a chirp occupies. LoRa provides for a tripartite bandwidth setting of either 125 kHz, 250 kHz, or 500 kHz [199], [220]. The chosen setting will determine the rate at which the transmitter sends data to the receiver. The spreading factor is a significant parameter that determines how many chirps are encoded per symbol and hence the modulation rate. The spreading factor (SF) is chosen such that $SF\epsilon\{7, 8, 9, 10, 11, 12\}$. The chirp rate (*CPR*) is the first derivative of the chirp frequency. Equation (4-1) shows how the three parameters are related [221].

$$CDR = {BW}/{2^{SF}} \tag{4-1}$$

where *CDR* stands for coding rate, SF stands for spreading factor, and BW stands for modulation bandwidth. Equation (4-2) shows how the *SF*, BW, and *CDR* influence the bitrate (*BR*) [221].

$$BR = SF \cdot \frac{BW}{2^{SF}} \cdot DR \tag{4-2}$$

where *SF* stands for spreading factor, *BW* stands for modulation bandwidth, and *CDR* stands for coding rate. The coding rate (*CDR*), expressed as a fraction, denotes the quantity of transmitted bits that carry essential information. The higher the coding rate value, the lower the effective data rate since a data payload is of a prescribed size. LoRa can be configured for four different coding rates, as shown in Equation (4-3).

$$CDR = \frac{4}{(4+EC)} \quad (4\text{-}3)$$

where EC is a value in the set $\{1, 2, 3, 4\}$, and describes how sensitive a receiver should be in detecting and correcting mistakes in the sent message. Using Equation (4-3), it is found that the coding rate can be one of the following $\left\{\frac{4}{5}, \frac{4}{6}, \frac{4}{7}, \frac{4}{8}\right\}$ [216].

There are three classes of end devices defined in the LoRaWAN specification, namely classes A, B, and C. A class A device has extreme savings on available power since every transmit session is initiated by the end-node rather than by the gateway. As such, the end nodes can create and observe a transmit schedule with the lowest duty cycle. After an end node initiates an uplink, the gateway is given an optional downlink opportunity to transmit its own frame if necessary [222]. With a class B device, however, the end node must first synchronise its internal clock with that of the gateway using beacons received from the gateway. During this process of synchronisation, the gateway can create a data transmission and synchronisation schedule with the nodes. Each class B device will therefore utilise the allotted time to transmit uplink frames. Class C devices are perpetually paired with the gateway. This arrangement assumes that power is continuously available and is, in fact, unlimited. Figure 4-4 compares the various classes of devices in terms of their communication latency and how efficiently they utilise energy.

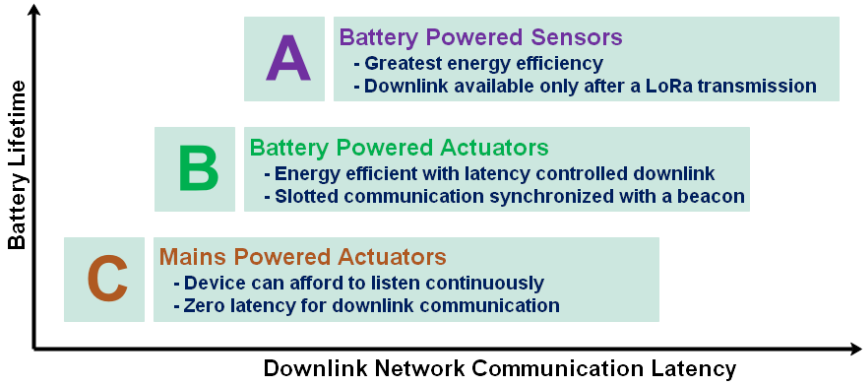

Figure 4-4: A Comparison of Class A, Class B, and Class C Devices (Source: Author)

Most off-the-rack LoRa end nodes are built to comply with the Class A specification. Because LoRa Class A devices use a channel access method similar to ALOHA, there is a small probability that two frames sent by two end nodes using the same spreading factor will collide [211], [223]. However, since a LoRa broadcast has an infinitesimal duty cycle, the probability of frame contention is considerably low. But in Classes B and C, the synchronisation that precedes a transmission renders the communication channel collision-free [224].

Whereas LoRa is a description of the lowest physical layer, the higher layers were initially not defined. This void necessitated the creation of LoRaWAN, which is one of a number of protocols that have been created to define the higher layers of the protocol. It can obtain real-time data from various objects in the environment and is an open, secure, and interoperable worldwide standard for wireless communication. It acts principally as a network layer routing protocol that manages the manner in which end-nodes and gateways communicate, but it is actually a MAC layer protocol based on the cloud. The LoRaWAN standard was proposed by the LoRa Alliance, which is a global association whose member ecosystems developed and maintain the LoRaWAN protocol. The LoRa Alliance, created in 2015, is an open, not-for-profit association with over 500 members who actively support and maintain the LoRaWAN protocol, thus ensuring the interoperability of all LoRaWAN products and technologies. Figure 4-5 shows the LoRa protocol stack. At its lowest level, the physical layer (PHY) is found, which is where LoRa is domiciled. Then, above it, we have the media access control (MAC) layer, whose function is, among other things, to eliminate duplicate receptions and assign frequencies, spread factors, and data rates to the devices. The application layer handles data encryption and decryption as well as encoding and decoding.

4.1.2 Types of Faults

A fault on the electric grid is the sudden and possibly cataclysmic departure of voltages and currents from their rated values that affects usual operations. The equipment of

the power network, including the conductor cables, ordinarily carries voltages and currents that guarantee the safe operation of the system. But when faults happen, they cause current flows that are much higher than usual, which can damage nearby equipment [191].

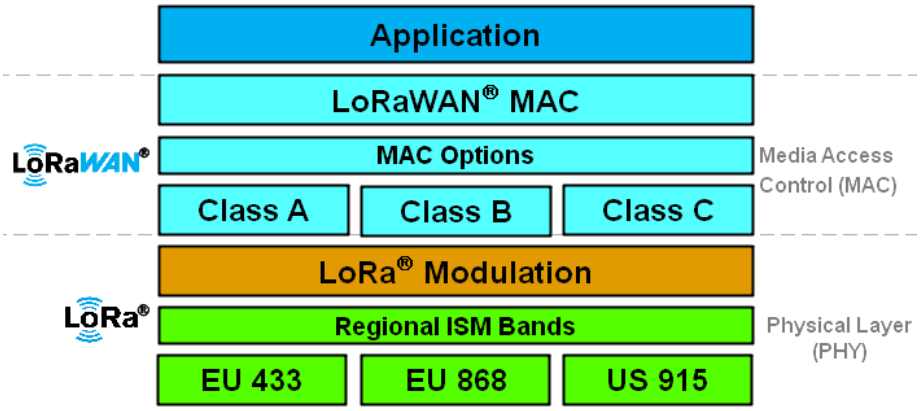

Figure 4-5: The LoRaWAN Protocol Stack (Source: Author)

Faults in the electrical power system can be either symmetrical or non-symmetrical. Symmetrical faults, also known as balanced faults, are very severe. Nevertheless, their occurrence is quite rare. A balanced fault can appear as a line-to-line-to-ground (L-L-L-G) or a line-to-line-to-line (L-L-L), as illustrated in Figures 4-6. Symmetrical faults are estimated to have an occurrence frequency of between 3% and 6%. Since symmetrical faults leave the system in a balanced state, such faults usually result in the colossal destruction of the power equipment [58].

On the other hand, non-symmetrical faults, also known as unbalanced faults, are less severe yet extremely common. When the impedance values of each phase differ, the current flows in those phases are dissimilar. This is what is referred to as an "unbalance" in the system. There are three main manifestations of non-symmetrical faults, namely double line-to-ground (LL-G), line-to-line (L-L), and line-to-ground (L-G) faults [225]. Line-to-ground fault (L-G) is by far the most frequent type of fault in this category and accounts for 65% to 70% of fault manifestations [58]. Figure 4-7 is a diagrammatic representation of non-symmetric faults.

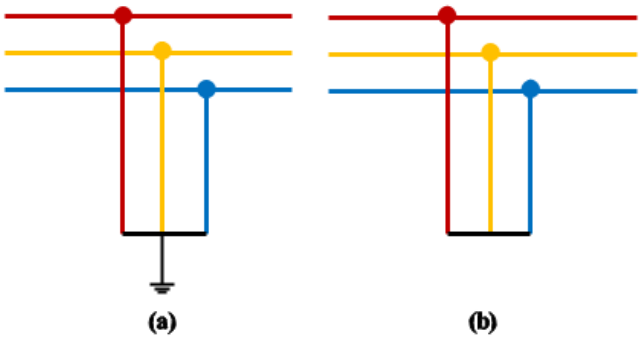

Figure 4-6: Symmetric faults (a) Line-to-Line-to-Line-to-Ground (b) Line-to-Line-to-Line (Source: Author)

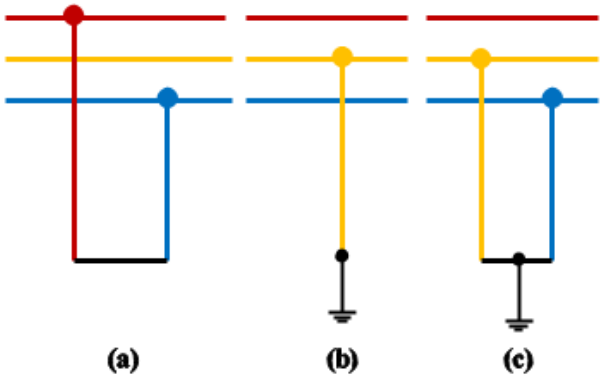

Figure 4-7: Non-symmetric faults (a) Line-to-Line (b) Line-to-Ground (c) Line-to-Line-to-Ground (Source: Author)

4.2 Materials and Methods

4.2.1 The Study Location

This study was conducted in Nakuru County, in the East African country of Kenya. Nakuru is located 189 kilometres north of the city of Nairobi and has an *altitude* of 2217 metres above sea level. Kenya Power (KP) Company Limited has created eight administrative regions, namely: the Central Rift, North Rift, Mt. Kenya, North Eastern, Coast, South Nyanza, Nairobi, and Western regions. Njoro sub-county falls under the Central Rift Region, which has about 1.6 million subscribers.

Nakuru is home to several factories and industries that give the area significant economic importance. The operations of all of these factories rely on a stable supply of electrical energy. As a popular tourist destination, Nakuru is host to several hotels

and resorts that receive many visitors. All these places need to be powered reliably and continuously.

4.2.2 System Design and Construction

The proliferation of miniature sensors that survive on limited energy sources has given impetus to this study's goal of actualizing a LoRaWAN sensor network to monitor the power distribution grid [216]. When constructing IoT devices, the overall goal is to construct devices that will conserve as much power as possible. The designed system comprises a cloud application server, a network server, a LoRa gateway, and field-deplorable sensors. Table 4-1 outlines the various components that were used to build the platform.

The Arduino microcontroller was preferred for this work due to its low power consumption and its versatility in terms of the projects that can be undertaken with it. Along with the little power-consuming hardware, the algorithm that it was developed to run is also power-conserving. Figure 4-8 depicts a flowchart of the algorithm that the microcontroller ran. The algorithm departs from the conventional "polling" technique. The polling technique uses sensors that are configured to continuously take readings at a regular set interval and, as such, is energy-hungry. In contrast, our method uses "interrupts" instead to alert the microcontroller unit of an abnormal situation in the quantity being observed. This means the Arduino microcontroller can be in a state of "deep sleep" most of the time. In a deep sleep state, the microcontroller uses minimal power as opposed to an always-on operation, which is power-consuming. The device is configured such that when an interrupt is detected, the microcontroller wakes up from its state of "deep sleep" and sends an alert to the monitoring and control centre, informing them of an anomaly. This mode of operation is highly energy efficient, especially since we desire the IoT device to conserve as much power as is practically possible without compromising its ability to operate.

Table 4-1: Bill of Materials for the Fault Detection Platform

COMPONENT	PURPOSE
Arduino Mega 2560 Rev3	Microcontroller unit
Dragino LoRa Shield SX1278 chip (868 Mhz)	LoRa transceiver on an Arduino shield
GSM/GPRS SIM900 Module	Global Positioning System (GPS) location information
Micro Gateway RAK7258	LoRaWAN Gateway
Real-Time Clock DS3231	Precise real-time keeping
Solar Panel (5 V, 3.5 W)	Solar energy harvesting
STC013 100A:5mA	Current Transformer
TP 4056 charge module	DC-to-DC Voltage Booster/ Solar Charge Controller

4.2.2.1 Gateway Setup and Configuration

The Micro Gateway RAK7258 was selected for this work. The gateway with Power-over-Ethernet (PoE) capability is managed and configured through the OpenWRT user interface. The MQTT protocol relays data intended for the local server. Given the size and format of the messages, MQTT is appropriate for use in relaying the messages to the server [226]. The data from the sensing devices is aggregated and forwarded to the network server. The RAK7258 Micro Gateway is a full-featured, eight-channel gateway that uses IP to connect to the wireless LoRa network. It is powered by a 12 V - 1 A DC power supply and operates at a frequency of 868 MHz with a listed minimum receiver sensitivity of -142 dBm. Packets are relayed to the local server via an Ethernet backhaul. The gateway message protocol (GMP) is used to send LoRaWAN messages over the wireless interface.

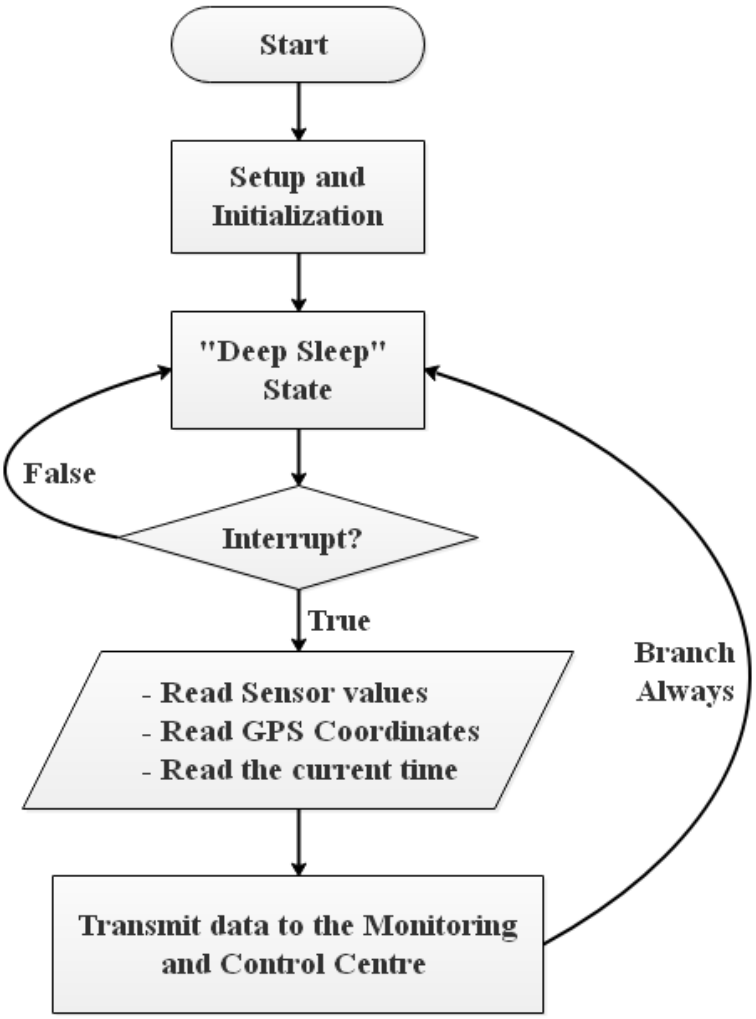

Figure 4-8: A flowchart of the fault-monitoring algorithm (Source: Author)

4.2.2.2 Embedded Electronic Monitoring Device

The Embedded Electronic Monitoring Device (EMMD) was constructed using the open-source hardware Arduino Mega 2650 Rev3 microcontroller (MC). Figure 4-9 shows the layout of the selected Arduino microcontroller, along with its various parts. The microcontroller board was programmed to read from the current transformers (CT) attached to the outbound supply lines of the distribution transformer. The sensors enabled us to determine whether the equipment was energised or not. Since the signal obtained from the sensor was very small, it was first amplified before it was fed to the Arduino microcontroller. Figure 4-10 shows the circuit that was used to amplify the

signal from the current sensor. When no current is detected, the output pin is pulled HIGH, as can be seen. The sensor readings are thereafter forwarded to the LoRa gateway with a time stamp, and the GPS coordinates expressed as a combination of latitude and longitude are appended. The time stamp is obtained from the real-time clock (RTC), and the GPS receiver supplies the GPS coordinates, both of which are attached to the Arduino Mega 2560. Figure 4-11 presents the schematic diagram of the embedded electronic monitoring device (EEMD). Figure 4-12 illustrates the block diagram of the EEMD, and Figure 4-13 is a photo of the assembled EEMD. In order to protect the EEMD from external elements, it was placed inside a protective waterproof casing, as shown in Figure 4-14.

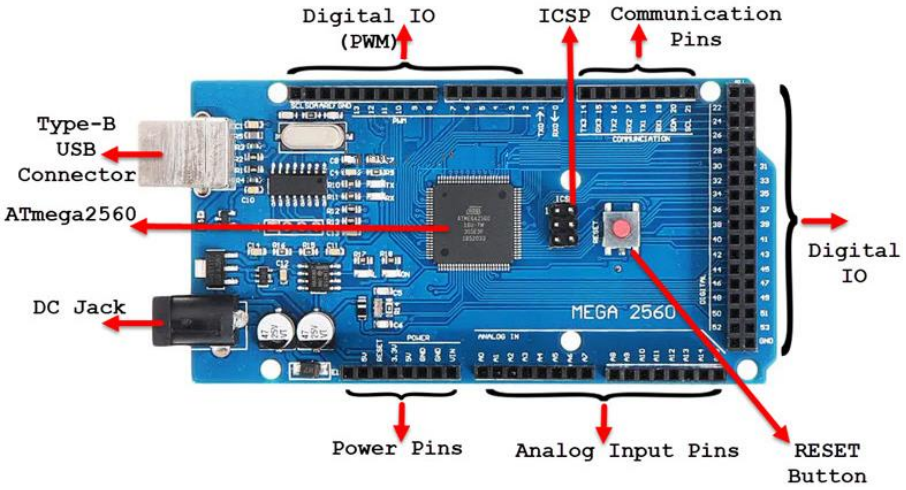

Figure 4-9: Arduino Mega 2560 Microcontroller (Source: Arduino)

4.2.2.3 Harvesting of Solar Energy

The battery life of an embedded device has been cited as its most significant criterion [227]. Considering that the IoT device will be deployed in the field in a remote location to continuously monitor the electrical system, there is a need to eliminate the need for regular maintenance, particularly the necessity for energy replenishment. We therefore built the monitoring device to harvest its own energy from the environment and store it in a rechargeable battery. With the generous insolation available of about 5-7 peak sunshine hours daily, resulting in about 4-6 kWh/m^2, the choice of solar is reasonable [21], [22]. A monocrystalline solar panel, the charge controller TP 4026, and a nickel-

metal hydride (NiMH) battery were selected as shown in Figure 4-15. The solar panel is a 6V/3.5W, and the battery chosen is a 4.8V with a current-ampere-hour rating of 2500 mAh. These components were assembled as shown in Figure 4-16. The TP 4026 charge controller boosts the voltage to 5 volts through an inbuilt DC-to-DC voltage booster.

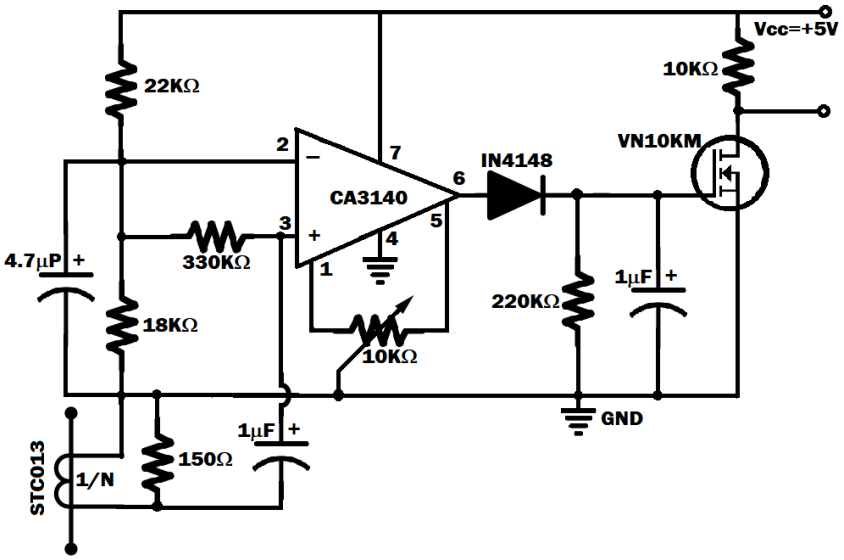

Figure 4-10: Current Transformer connection and interfacing circuitry

The data sheet of the Arduino Mega 2560 recommends a supply voltage of between 7 and 12 volts [228]. However, when this voltage is supplied through the barrel connector, it goes through a linear voltage regulator that reduces it to the 5 volts that is sufficient for the microcontroller unit. This linear voltage reduction by the regulator is wasteful because voltages in excess of 5 volts are not put to any good use but are merely dissipated in the form of heat [229]. With the objective of maximising the available power in mind, we decided to supply the MCU with a constant 5-volt input. Hence, the regulated 5V from the charge controller (TP 4026) was fed directly to the MCU through the 5V pin. This arrangement eliminated the need for the linear voltage regulator and saved the energy that would otherwise have been lost through it.

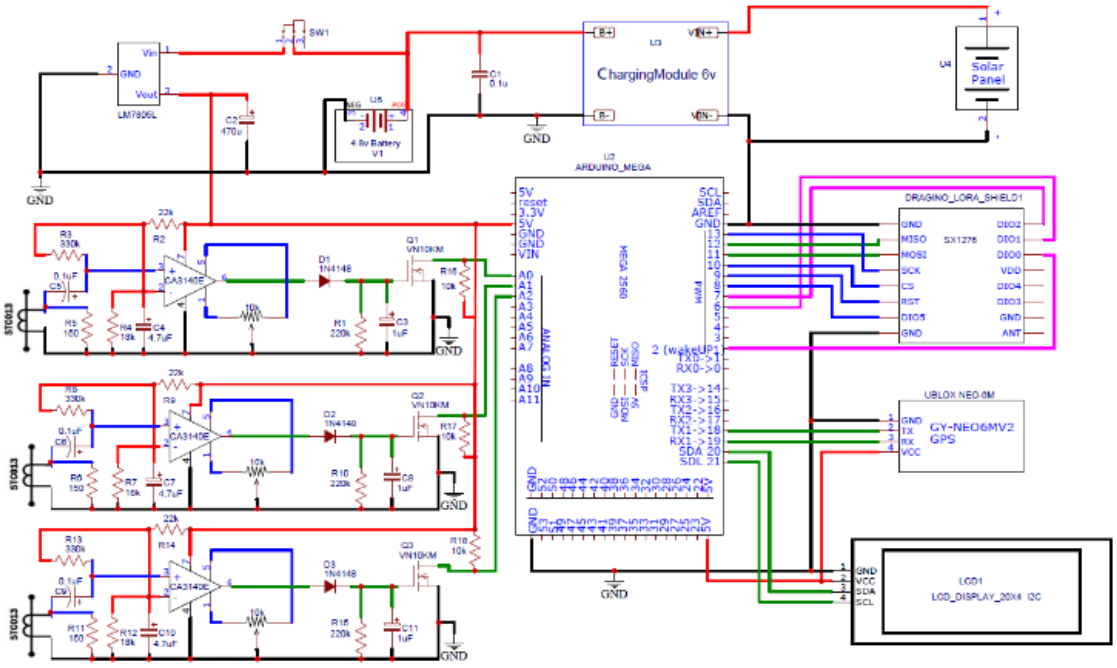

Figure 4-11: Schematic Diagram of the embedded electronic monitoring device

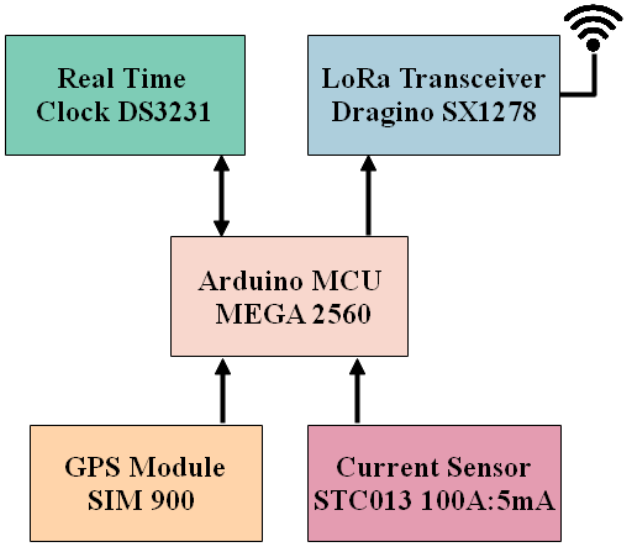

Figure 4-12: Assembly of the EEMD using Arduino MEGA 2560 (Source: Author)

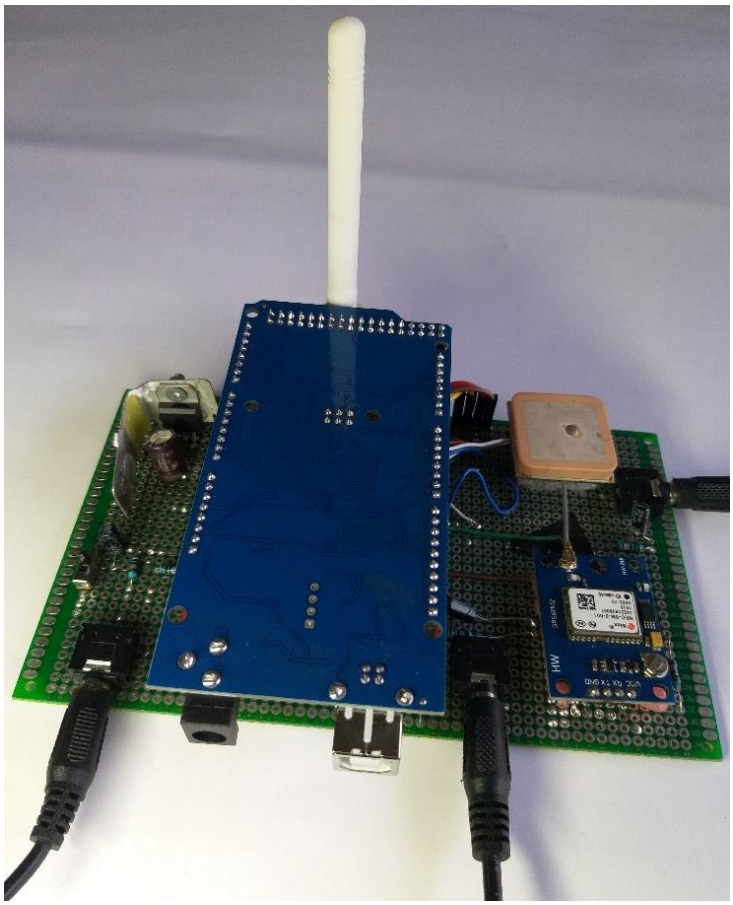

Figure 4-13: The electronic monitoring device with an Arduino board and a LoRa transmitter module (Source: Author)

The charge controller TP4026 uses the Power Point Tracking (PPT) technique and therefore attains high efficiency. Furthermore, the DC-to-DC voltage boost converter not only maintains the voltage constant at 5 volts but also eliminates the need to tap energy directly from the battery terminals. PPT charge controllers exhibit critical advantages over pulse width modulation (PWM) charge controllers. They not only keep the battery from overcharging, but they also boost performance by more than 30% [230]–[232].

Figure 4-14: An EEMD encapsulated in a waterproof protective casing (Source: Author)

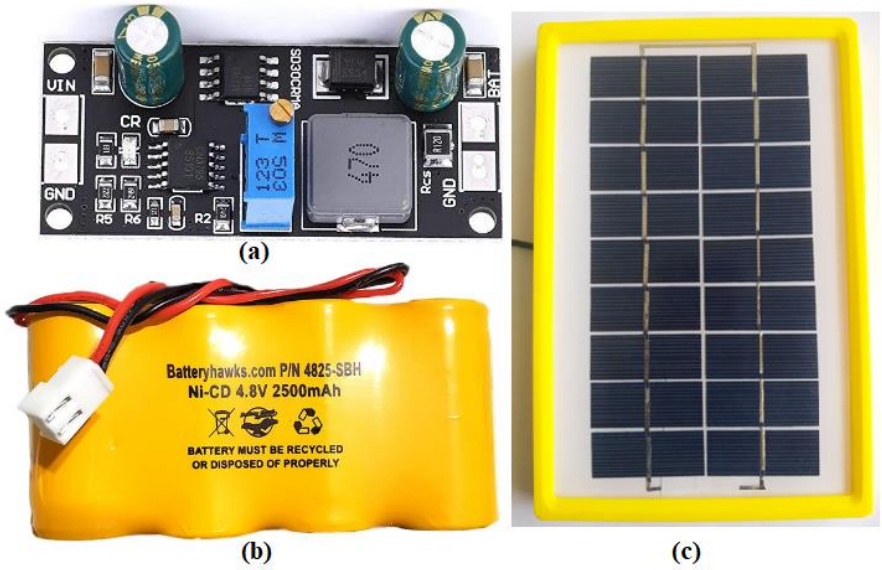

Figure 4-15: Solar Energy Recharge Kit (a) The Charger Controller (b) The Battery (c) The Solar Panel

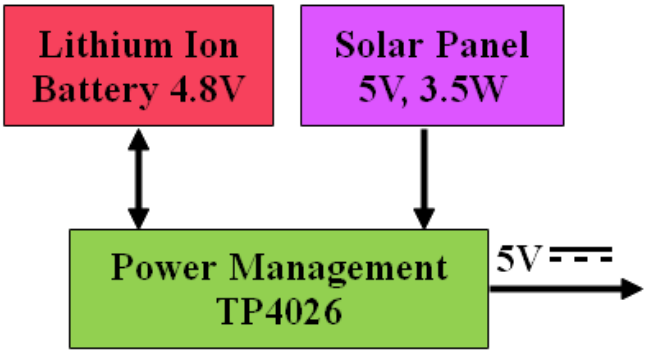

Figure 4-16: A block diagram of the solar recharging circuit

4.2.2.4 Battery Charging Time

In order to determine if the selected solar panel will maintain the battery in a charged condition, we calculate how much time it would take to fully recharge the battery. First, we obtain the maximum charge current using the formula shown in Equation (4-4). The maximum charge current was found to be 729 mA. To cater for system losses estimated to be about 20% and charge controller efficiency of 75%, the effective charging current, C_{eff}, is determined to be 437.5 mA using Equation (4-5).

$$C_i = {}^{W}/_{V} \tag{4-4}$$

$$C_{eff} = {}^{W}/_{V} \times (1 - 80\%) \times 75\% \tag{4-5}$$

where W is the total wattage of the solar panels (3.5W) and V is the battery voltage (4.8V). To cater for inefficiencies in the charging system, a higher battery capacity is assumed and calculated using Equation (4-5). A battery charge efficiency of 85% is taken, and a new value for the battery charge is obtained using Equation (4-6).

$$B_c = C_c \times (85\%)^{-1} \tag{4-6}$$

where B_c is the battery charge capacity and C_c the rated capacity. With C_c being 2500mAh, B_c is determined to be 2941mAh. To determine how much time, it would take to charge the battery, Equation (4-7) was used.

$$t_\tau = {}^{B_c}/_{C_{eff}} \tag{4-7}$$

where t_τ is the time, it takes to fully charge the battery, B_c is the battery charge capacity, and C_{eff} is the effective charging current. Using Equation (4-7), the total time to fully charge (t_τ) is calculated to be 6 hours and 43 minutes. This figure assumes that the battery is fully discharged and that there are no cloudy episodes during the day. However, in reality, the battery is never used until it is completely discharged. Moreover, many batteries have built-in safety limits that, when reached, will automatically trigger a shutdown in order to protect the battery.

4.2.2.5 The Cloud Server and Data Visualisation

The loss of power on a network segment is an emergency that must be promptly addressed. The platform was therefore set to trigger an alarm at the monitoring and control centre. In addition, email and text messages were sent to a preselected email. The power system operator would then be able to send personnel to correct the existing anomaly. The monitoring dashboard showed the GPS location of the transformer, the status of each of the monitored phases of the transformer, and the time the fault was detected. The dashboard is shown in Figure 4-17. Figure 4-18 shows how the fleet of monitoring devices was deployed on the distribution network.

4.3 Experimental Evaluation and Test Results

The experimental findings from the deployment of the EEMDs are reported in this section. The end nodes were assembled, and the sketch was compiled and uploaded to the microcontroller through the IDE. The Things Network (TTN) LoRaWAN server stack was set up to receive data from the end-nodes. For visualisation, the data was sent to Cayenne, which is an online dashboard for IoT applications. A data format conversion was necessary for Cayenne to receive data from TTN. Cayenne enabled the creation of a trigger so that whenever a power outage occurred, an alarm condition was created at the monitoring and control centre.

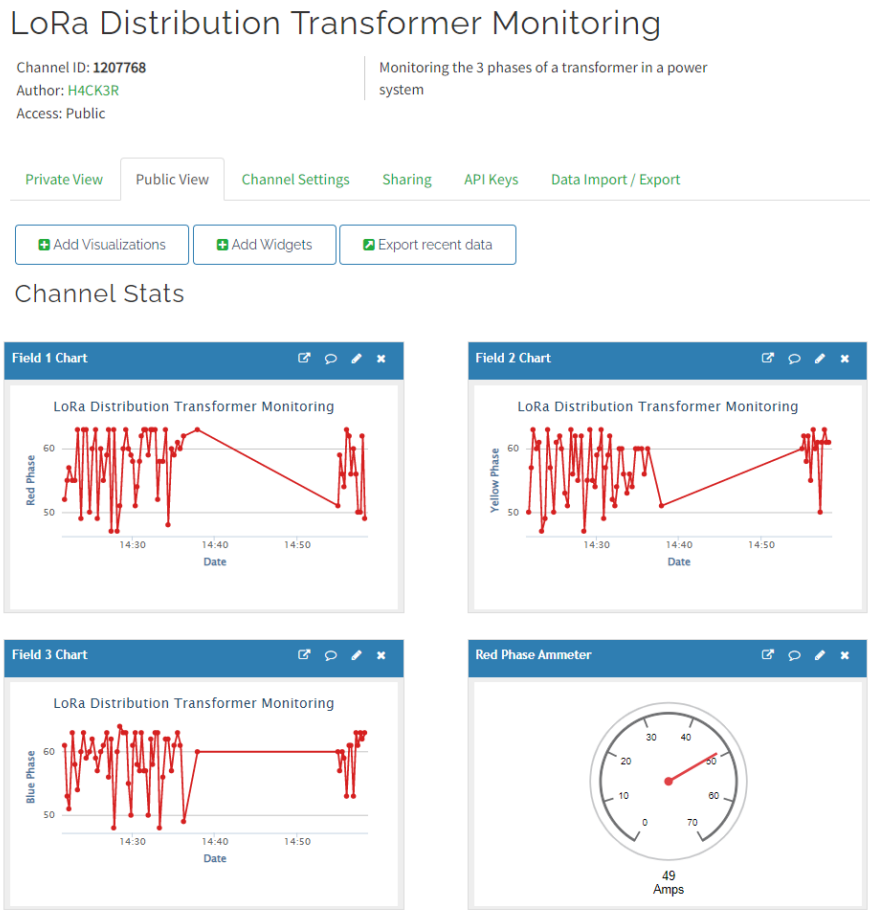

Figure 4-17: Visualization dashboard for distribution transformer monitoring

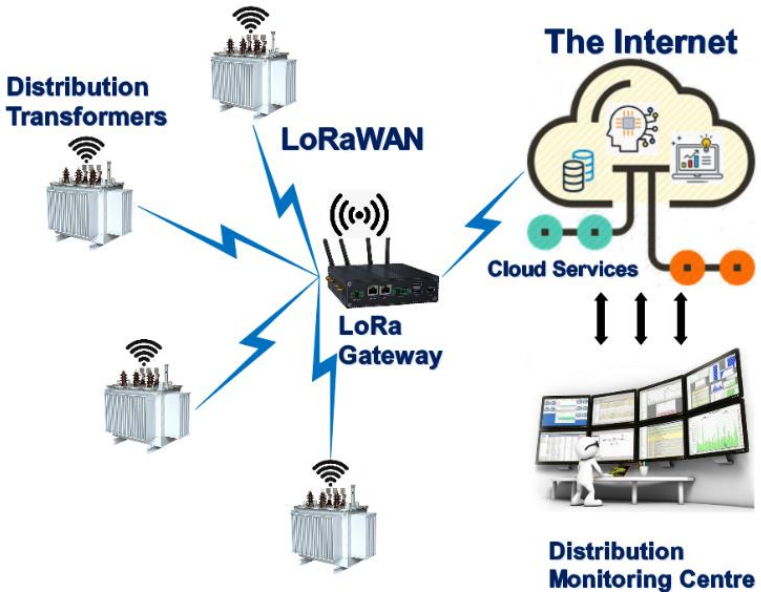

Figure 4-18: Sensor monitoring on the distribution transformers

4.3.1 Platform Deployment

The LoRa-based distribution transformer monitoring platform was piloted between August 7 and September 24, 2021. Six distribution transformers owned and operated by the Kenya Power Company were used for piloting. The transformers themselves were the outdoor, pole-mounted types that were suspended approximately 10 feet above the ground. Figure 4-19 is a picture of the current sensors and the EEMD attached to a distribution transformer, while Figure 4-20 is a satellite map showing the various locations where the specific transformers were located in the area of study. Six EEMDs were installed, one on each distribution transformer, and were set up to communicate with a centralised LoRa gateway. The gateway was placed on the fifth floor of a storied building and was positioned close to a window. It was connected to the local Ethernet and powered by electricity via a 12V AC/DC adaptor.

The embedded electronic monitoring devices were dispatched to the various preselected transformers within the study area, with varying intervening distances between the nodes and the gateway, as shown in Table 4-2.

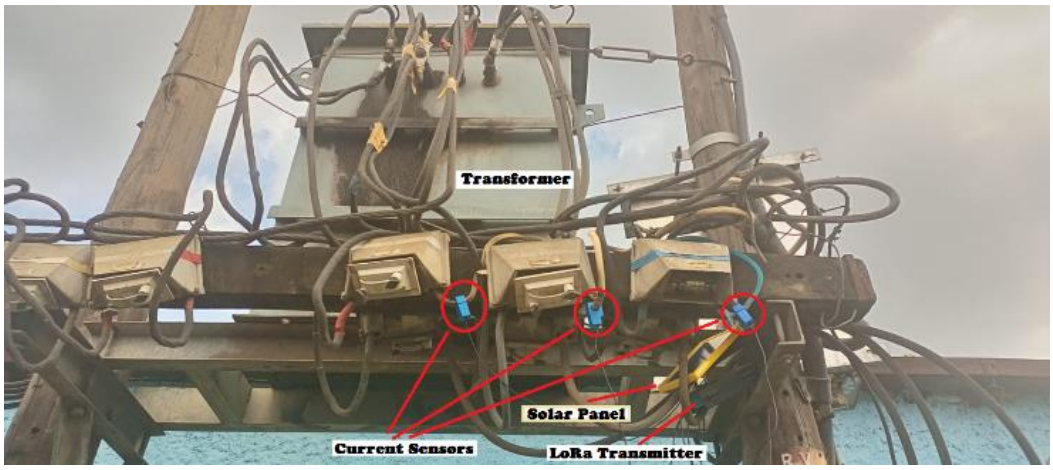

Figure 4-19: A picture showing the current sensors clamped to a distribution transformer (Source: Author)

Figure 4-20: A diagram showing the location of transformers and displacement of the EEMDs from the LoRa gateway (Source: Author)

Table 4-2: Dispersion of the sensors from the gateway

SENSOR ID	GPS COORDINATES	DISTANCE (m)
Node 1	-0.29361, 36.05396	16133
Node 2	-0.37908, 35.96695	3647
Node 3	-0.39804, 35.95815	3744
Node 4	-0.39098, 35.92549	1991
Node 5	-0.36067, 35.92477	1452
Node 6	-0.3318, 35.94698	4939

4.3.2 Data Collection and Message Payload

The data collected by the embedded electronic monitoring devices comprised GPS location information expressed as longitude and latitude, a time stamp, and the current reading of each phase of the transformer. In order to keep the payload small, the timestamp was trimmed to exclude the seconds. This also enabled the LoRa packets generated to conform to the LoRaWAN specifications. This information was then

packaged into a single data structure that enabled us to send different pieces of information as one solitary payload. The total size of the LoRaWAN packet payload was calculated to be 22 bytes, including a 13-byte LoRa packet overhead. Figure 4-21 shows the various parts of a LoRaWAN packet.

Table 4-3 shows the parameters and their settings as they have been used in this study, and Table 4-4 is a subset of the data collected during experimentation.

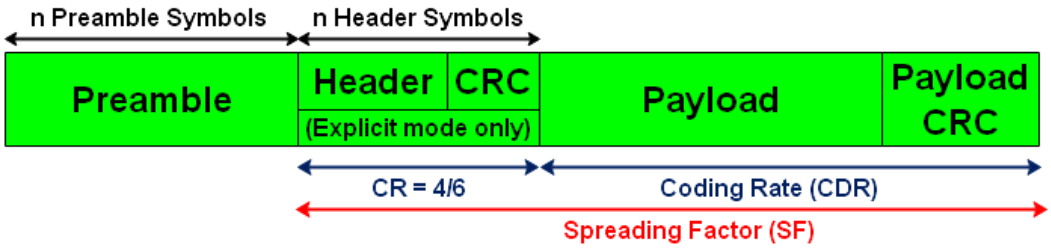

Figure 4-21: LoRaWAN Packet Format

Table 4-3: LoRaWAN Parameter Settings

LoRaWAN Settings		
Parameter	Value	Details
Frequency	EU863-870	Class A
BW	125kHz	Default Configuration
CR	4/6	Coding rate value
SF	{7, 8, 9, 10, 11, 12}	ADR
Tx Payload Size	22 bytes	Used with SF selected

Table 4-4: Experiment sample data from test sites

	Date-Time	GPS Location	I_Y, I_B, I_R	PDT
1	07-08-21 08:12	-0.39804, 35.95815	58,59,52	100.18
2	07-08-21 08:27	-0.39098, 35.92549	54,62,61	98.53
3	07-08-21 08:40	-0.3318, 35.94698	60,57,63	104.64
4	07-08-21 10:23	-0.37908, 35.96695	61,54,53	97.68
5	07-08-21 14:54	-0.36067, 35.92477	63,55,62	96.42
6	08-08-21 08:48	-0.39804, 35.95815	54,59,58	99.12
7	08-08-21 08:57	-0.36067, 35.92477	48,48,50	96.29

8	08-08-21 10:34	-0.37908, 35.96695	59,58,60	100.80
9	08-08-21 11:45	-0.39098, 35.92549	57,49,62	96.75
10	08-08-21 19:20	-0.3318, 35.94698	58,51,63	104.48
11	09-08-21 10:12	-0.3318, 35.94698	63,59,50	104.76
12	09-08-21 13:54	-0.39098, 35.92549	60,56,63	94.06
13	09-08-21 13:57	-0.37908, 35.96695	58,57,53	94.91
14	09-08-21 15:50	-0.39804, 35.95815	63,63,60	96.99
15	09-08-21 17:38	-0.36067, 35.92477	57,60,56	92.22
16	10-08-21 11:09	-0.36067, 35.92477	44,57,52	92.30
17	10-08-21 12:53	-0.39098, 35.92549	52,63,63	98.10
18	10-08-21 15:23	-0.3318, 35.94698	53,57,57	104.92
19	10-08-21 15:25	-0.37908, 35.96695	63,52,59	96.46
20	10-08-21 18:02	-0.39804, 35.95815	55,57,60	97.41
21	11-08-21 09:34	-0.39804, 35.95815	63,54,54	99.68
22	11-08-21 11:53	-0.36067, 35.92477	63,62,55	90.20
23	11-08-21 13:02	-0.39098, 35.92549	59,63,58	94.14
24	11-08-21 16:18	-0.37908, 35.96695	62,60,56	97.03
25	12-08-21 09:01	-0.36067, 35.92477	54,54,59	95.24
26	12-08-21 10:23	-0.39098, 35.92549	54,,51,58	97.85
27	12-08-21 11:01	-0.39804, 35.95815	57,61,63	97.06
28	12-08-21 12:30	-0.3318, 35.94698	62,59,63	105.68
29	12-08-21 19:28	-0.37908, 35.96695	58,61,49	102.85
30	13-08-21 09:12	-0.36067, 35.92477	57,60,61	92.40
31	13-08-21 12:01	-0.39804, 35.95815	60,58,63	100.80
32	13-08-21 12:48	-0.39098, 35.92549	63,59,49	94.86
33	13-08-21 15:59	-0.3318, 35.94698	54,59,53	105.26
34	13-08-21 18:44	-0.37908, 35.96695	50,55,58	96.46
35	14-08-21 07:28	-0.36067, 35.92477	60,49,61	95.20
36	14-08-21 08:20	-0.3318, 35.94698	54,63,61	103.73

37	14-08-21 11:12	-0.39804, 35.95815	49,48,57	96.90
38	14-08-21 12:25	-0.39098, 35.92549	59,63,59	98.36
39	14-08-21 13:30	-0.37908, 35.96695	54,61,48	98.72
40	15-08-21 08:40	-0.37908, 35.96695	48,62,48	100.80
41	15-08-21 10:51	-0.3318, 35.94698	60,58,58	104.92
42	15-08-21 12:46	-0.36067, 35.92477	52,47,62	93.36
43	15-08-21 14:15	-0.39804, 35.95815	57,62,63	97.19
44	15-08-21 16:22	-0.39098, 35.92549	51,57,47	100.46
45	16-08-21 10:23	-0.3318, 35.94698	54,59,61	105.38
46	16-08-21 12:41	-0.36067, 35.92477	58,55,52	94.44
47	16-08-21 15:11	-0.39804, 35.95815	61,62,63	99.56
48	16-08-21 16:01	-0.37908, 35.96695	62,62,63	96.85
49	16-08-21 17:30	-0.39098, 35.92549	61,56,57	97.47
50	17-08-21 10:28	-0.36067, 35.92477	63,61,60	90.68
51	17-08-21 13:34	-0.39804, 35.95815	60,50,59	96.91
52	17-08-21 13:35	-0.37908, 35.96695	58,62,56	97.75
53	17-08-21 17:54	-0.39098, 35.92549	58,53,58	93.56
54	18-08-21 09:31	-0.36067, 35.92477	59,53,61	95.52
55	18-08-21 10:58	-0.39098, 35.92549	50,56,62	98.27
56	18-08-21 11:13	-0.37908, 35.96695	57,60,63	97.07
57	18-08-21 14:42	-0.39804, 35.95815	63,50,54	95.91
58	18-08-21 16:20	-0.3318, 35.94698	60,51,48	106.08
59	19-08-21 09:08	-0.37908, 35.96695	48,60,59	96.96
60	19-08-21 09:18	-0.36067, 35.92477	49,61,49	94.16
61	19-08-21 11:25	-0.39098, 35.92549	56,58,56	102.07
62	19-08-21 15:30	-0.39804, 35.95815	48,57,59	98.64
63	20-08-21 08:21	-0.3318, 35.94698	60,61,61	103.79
64	20-08-21 13:29	-0.39098, 35.92549	63,63,60	95.11
65	20-08-21 13:55	-0.39804, 35.95815	52,63,54	101.92

66	20-08-21 16:45	-0.37908, 35.96695	63,59,57	100.46
67	20-08-21 19:02	-0.36067, 35.92477	47,62,47	93.46
68	21-08-21 09:22	-0.3318, 35.94698	62,60,60	103.42
69	21-08-21 11:57	-0.39804, 35.95815	62,59,63	99.88
70	21-08-21 14:52	-0.3318, 35.94698	61,53,56	106.63
71	21-08-21 15:47	-0.36067, 35.92477	59,63,51	92.58
72	21-08-21 16:39	-0.39098, 35.92549	63,51,58	98.90
73	21-08-21 17:30	-0.37908, 35.96695	50,63,63	99.08

4.3.3 LoRaWAN Configuration and Performance

According to the LoRaWAN documentation, there are several parameters whose values can be set to ensure optimum performance. These parameters are the bandwidth, the coding rate, and the spreading factor. Since the EEMDs are fixed at a stationary point, ADR, or adaptive data rate, was enabled. ADR is an algorithm that assesses the link quality and, based on this assessment, determines the optimal SF. Thus, ADR dynamically and autonomously increases or decreases the data rate to ensure the data rate is optimal. For forward error correction (FEC), a coding rate of 4/6 was chosen because it results in the maximum data transfer per packet. The bandwidth was set at 125 kHz because it affords the medium the highest sensitivity. Receiver sensitivity, expressed in dB, is a measure of the minimum signal strength detectable by a receiver. For best results, this quantity should ideally be very low. The receiver sensitivity (S) is obtained using Equation (4-8) [233].

$$S = TN + 10 \cdot log_{10}(BW) + NF - SNR_{limit} \quad (4\text{-}8)$$

where TN stands for thermal noise (in decibels), BW stands for bandwidth, NF stands for noise factor, and SNR_{limit} stands for the signal-to-noise ratio in decibels.

In order to assess how LoRaWAN performs, a series of packets were sent from each of the nodes (1 to 6), and the average values of the Received Signal Strength Indicator (RSSI), the Packet Reception Rate (PRR), and the Time of the Air (ToA) were

recorded. For Node 1, however, no reception was possible at the gateway. These observations are summarised in Table 4-5.

Table 4-5: Performance of the LoRa transmissions from test sites

NODE ID	PRR (%)	MEAN RSSI (dBm)	MEAN TOA (ms)
Node 1	0	n/a	n/a
Node 2	88.7	-102.6	99.25
Node 3	88.2	-92.9	98.21
Node 4	96.9	-79.1	97.47
Node 5	98.4	-77.8	94.34
Node 6	87.6	-123.2	104.91

4.3.4 Time to Battery Depletion

Energy self-sustenance is a critical aspect of the success of this work. The EEMD described in this work must, by necessity, be able to function for many years without becoming inoperable due to battery drain. In an effort to guarantee longevity, the system was built with the ability to replenish its own power by harvesting solar energy from the environment. This is a critical factor for IoT systems because many of these devices are deployed in far-flung areas that are also hard to reach.

It is also imperative to determine how long the battery will last while continuously powering the EEMD, assuming that there is no replenishment energy for the battery. This will give us an indication as to whether the capacity of the chosen battery is sufficient. The time it would take to completely deplete the battery power source largely depends on the rate at which current is drawn from the battery. In addition, as described earlier, the EEMD spends most of its operational life in deep sleep mode. Due to the low duty cycle of a LoRa send operation, the EEMD spends 99.9% of the time in deep sleep. For this reason, the researchers decided to estimate the life of the battery using only the power consumed during sleep mode. This does not refute the fact that some power is consumed during the awake state, but rather is an appreciation

of the fact that the power consumption when the device is “awake” is infinitesimal in comparison to the deep-sleep power consumption.

The life of a rechargeable battery is estimated based on its rated capacity in ampere-hours (Ah). Using a Fluke 117 digital multimetre, it was determined that the Arduino Mega 2560 used about 29.13 mA when in “Deep Sleep” mode. The interface circuit for the current sensor draws about 5.618 mA. The current consumption during the deep sleep mode for the rest of the components of the EEMD has been extracted from their data sheets and summarized in Table 4-6.

Table 4-6: Current Consumption in the Deep Sleep State

COMPONENT	CURRENT
Arduino Mega 2560 Rev3	29.13mA
LoRa Shield SX1278	215nA
GSM/GPRS SIM900 Module	1.5mA
Sensor Interface Circuit	5.618mA
Real Time Clock DS3231	170µA

Table 4-6 demonstrates that the EEMD's total current draw while in deep sleep mode is 36.4 mA. Using Equation (4-9), and considering a battery with a charge capacity of 2500 mAH, the battery can sustain the EEMD for about 68.65 hours, or 2 days, 20 hours, and 38 minutes. Since the battery can be fully recharged in 6 hours, we conclude that the battery capacity is sufficient for the proposed application.

$$B_{life} = {B_{cap}}/{I_{cur}} \tag{4-9}$$

Where B_{life} is the battery life, B_{cap} is the rated battery capacity, and I_{cur} is the load current.

4.4 Discussion

The LPWAN is the principal component of the wide-area monitoring platform espoused in this work. Six nodes were deployed in the study area to monitor actual

transformers owned and operated by Kenya Power Company Plc. Since the percentage of time the system is available is far greater than the periods of non-availability, a lot of time would have been taken to gather the necessary data for analysis. As a result, we simulated a fault at each site under observation by switching off the current sensor so that the microcontroller receives no input. When the current transformer is isolated, there is no input current to the op-amp CA3140 shown in Figure 4-10, and this will automatically trigger a LoRa uplink transmission. This is the usual behavior of the circuit when a de-energization of the transformer occurs. In addition, the Arduino was programmed to read from the current sensors every 30 minutes for testing purposes. Cumulatively, by this arrangement, we sent about 400 LoRa packets from every node, with each packet representing a fault manifestation. Data was received from all the nodes (2, 3, 4, 5, and 6) except node 1, where the PRR was zero in spite of the best efforts of the researchers to establish communication. In order to demystify this failed attempt, the researchers took the trouble of calculating the Fresnel zone between node 1 and the gateway. The Fresnel zone is an invisible, three-dimensional oval volume of the atmosphere surrounding the straight path connecting the gateway and the end node. Anything lying within this invisible volume, be it a hilltop, a building, a tree, or even the earth's surface, creates an obstacle that can attenuate the transferred signal, even if there is a direct line of sight between two communicating devices. To determine how big this Fresnel zone is, we used Equation (4-10). *R* is calculated at half the distance between Node 1 and the Gateway. From Table 4-2, it is seen that the distance between the LoRa gateway and the transmitting node is 16.1 kilometres. Hence, the mid-distance is about 8.05 kilometres.

$$R = 8.657 \times \sqrt{D/f} \tag{4-10}$$

where *R* is the radius of the Fresnel zone, *D* is the distance, and *f* is the frequency. Using Table 4-2, the value of *D* is calculated at 16.1 kilometres. The radius of the Fresnel zone, *R*, is therefore calculated to be 37.3 meters. This implies that a viable radio link between node 1 and the gateway must have a Fresnel zone with a radius of

37.3 meters midway between the devices. However, because the transmitter is located on distribution transformers that are very close to the ground, it was impossible to achieve such a Fresnel zone. The researchers therefore arrived at the conclusion that the reason the packet reception rate between Node 1 and the gateway is zero is because signal transmission is severely obstructed. As calculated above, it is expected that R should be 37.3 meters for this radio link, but given the height of the transmitter (about 10 feet), this is not possible to achieve. It was therefore concluded that the radio communication path was irreparably compromised by a combination of proximity to the ground, vegetation, and buildings, thus terminally impeding communication. As a result of this, it is observed that for objects close to the ground, and especially when it is not possible to elevate the transmitter any further, the distance between the gateway and the transmitting node should be kept at no greater than five kilometres. This is consistent with the observations made in [223].

The earth's surface was itself within this zone, yet it was not physically possible to raise the antenna any further than ten feet because the distribution transformers are usually placed at that height, suspended on poles. Figure 4-22 shows a Fresnel zone with several obstacles in its path. This is the probable situation that was experienced with Node 1. Even though the gateway was positioned on the fifth floor of a building complex within the study location, this was not sufficient for a transmitter placed very close to the ground and located 16 kilometres away. Despite the fact that LoRa can communicate with transmitters 1,000 kilometres away, Fresnel zone clearance remains a challenge. As the distance increases, the Fresnel zone gets fatter, particularly at its midpoint. For these long distances, it is inevitable that one uses antennas hoisted high above the ground to achieve meaningful communication. Furthermore, the formulae for computing the Fresnel zone do not take into account the curvature of the earth's surface. Therefore, for long-range radio communication technologies, Fresnel zone clearance remains a significant factor to be considered in the establishment of a viable radio link. For the rest of the nodes, a large proportion of the packets sent arrived at the gateway without error and with a packet reception rate greater than 88%. These

findings agree with those of other researchers [73], [209], [234]. This was achieved with a spreading factor of 7, a coding rate of 4/6, and a bandwidth of 125 kHz. This tells us that for the other nodes, the Fresnel zone was clear or not encroached upon to the extent of impeding all communication. The height at which the gateway was placed also contributed to the establishment of a feasible line-of-sight between the communicating devices.

Unlike in the current setup, where faults are located by physically patrolling the length of the distribution cable in the area where a fault is suspected, the proposed method is not only efficient but drastically reduces the duration between the fault occurrence and the receipt of information on the incident at the monitoring and control centre. The prompt receipt of notification of a fault by the monitoring and control centre enables the immediate commencement of reparative activities, resulting in shortened durations of power outages witnessed on the distribution network. This not only has the tangible effect of encouraging economic activity but also enables the power system operator to comply with regulatory demands on quality-of-service provision. The proposed system will also increase consumer contentment and satisfaction. Table 4-7 compares the existing method to the proposed platform in terms of the time taken to notify the Monitoring and Control Centre of the occurrence of a failure. The table shows that the proposed IoT-based platform reduces the time to notify the Monitoring and Control Centre by a factor of 100,000. In addition, it minimizes the time taken by the service crew to locate the faulty site since the GPS location of the EEMD is transmitted as well.

Table 4-7: Comparison of the currently used fault notification system to the proposed IoT-based platform

METHOD	AVERAGE TIME
Telephone notification by customers	200 minutes
IoT-based Platform	0.002 minutes

In the LPWAN space, LoRaWAN has projected itself as having the ability to transmit data to far-flung and remote places using low bandwidth, little energy, and high accuracy. Due to its superior resistance to noise, LoRaWAN technology is a game changer as far as long-range data transmission is concerned. This successful use of LoRaWAN to monitor and find faulted network segments in the existing legacy distribution grid shows that monitoring can be done cheaply with low-cost hardware. Furthermore, this technique imbues the grid with feedback mechanisms and enables the power system operator to address promptly and quickly the incidents that arise on the network. This route circumvents the other, more costly alternatives that would, for instance, demand a complete overhaul of the existing system. This is a viable option for countries in the sub-Saharan Africa (SSA) region where budgetary constraints and cost prohibitions limit further enhancements to the existing electricity network.

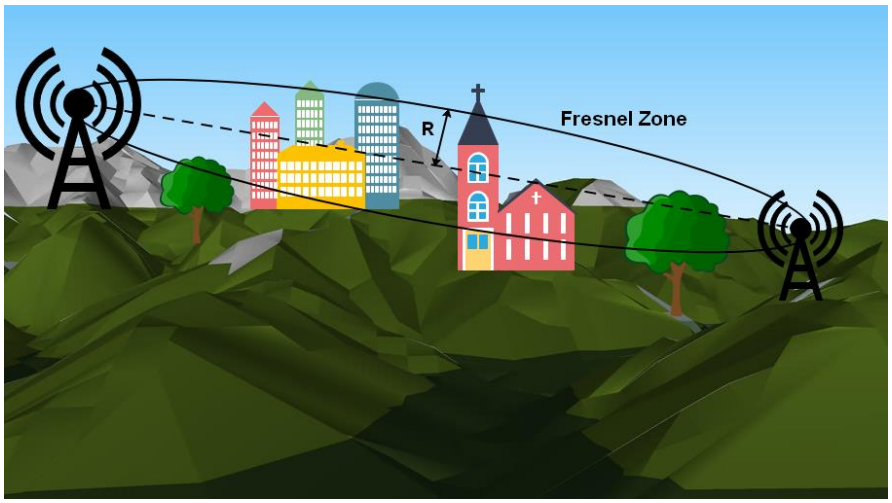

Figure 4-22: The Fresnel zone with several obstacles along the transmission path

4.5 Limitations

During the course of this study, several limitations were identified in the proposed LoRa-based smart fault detection and monitoring platform for the power distribution system. These limitations include:

1. Limited Data Transmission Range: The use of LoRa for long-range data transmission is subject to constraints such as the Fresnel zone and the topology of

the deployment area. This limitation can affect the effective coverage and range of the system. To mitigate this, the researcher elevated the transmitting and receiving devices to improve the transmission range.

2. Lack of Edge Processing Support: The architecture of the system does not support edge processing. Edge processing refers to the capability of processing and analysing data at the edge of the network, closer to the data source. This limitation may hinder real-time data analysis and decision-making capabilities, as data needs to be transmitted to a central processing unit for analysis.
3. Limited data rate: LoRa is designed for low-power, long-range communication, which comes at the cost of limited data rates. LoRa modulation techniques prioritise long-range coverage over high-speed data transmission. As a result, the data rates achievable with LoRa are relatively low compared to other wireless communication technologies.
4. Bandwidth limitations: LoRa operates in unlicensed frequency bands, and the available bandwidth for transmission is limited. This limitation constrains the overall data throughput and the number of devices that can transmit data simultaneously within a given LoRa network.
5. Sensitivity to interference: LoRa operates in the unlicensed spectrum, which means it is susceptible to interference from other devices using the same frequency band. In environments with high levels of interference, the performance of LoRa-based systems can be affected, leading to decreased range and reliability of data transmission.
6. Limited scalability: While LoRa networks can support a large number of devices, there are practical limits to the scalability of a LoRa network. As the number of devices increases, the available bandwidth needs to be shared among more devices, potentially leading to congestion and reduced performance.
7. Latency: LoRa is optimised for low-power, long-range communication, which can result in increased latency. The time it takes for a LoRa message to reach its destination and for a response to be received can be relatively longer compared to

other wireless communication technologies. This latency may not be suitable for applications that require real-time or near real-time responsiveness.

8. Challenging urban environments: In dense urban environments with tall buildings and other obstructions, the performance of LoRa can be significantly affected. Signal propagation can be hindered, resulting in reduced range and reliability of data transmission.
9. Limited bidirectional communication: LoRa is primarily designed for one-way communication from devices to gateways. While it supports bidirectional communication, the uplink and downlink data rates may not be symmetrical. This limitation can impact applications that require frequent and substantial data exchange in both directions.

It is important to acknowledge these limitations, as they can impact the overall performance and functionality of the proposed platform. Further research and development efforts may be needed to address these limitations and enhance the capabilities of the system.

4.6 Summary

This study addresses the challenges of transient stability and supply disturbances in power distribution systems, with a particular focus on sub-Saharan Africa. The demand for improved reliability and dependability in power delivery has sparked interest among researchers in developing advanced technological solutions for fault detection and location determination at medium- and low-voltage levels. Managing distribution networks, including identifying faulty segments, is a recurring challenge for power system operators, especially considering the vast length of these networks, which span hundreds to thousands of kilometres.

To tackle these challenges, the study proposes, designs, and implements a cost-effective IoT platform based on LoRaWAN technology for monitoring distribution networks. The research is conducted in Nakuru County, Kenya, using an active distribution network owned and managed by Kenya Power Company. Experimental

results demonstrate that the proposed platform can generate a trigger at the network monitoring centre within approximately 100 ms of a fault occurrence, enabling swift initiation of necessary repair actions. The platform proves to be well-suited for developing countries, where financial constraints and budget limitations often hinder the transformation of legacy grids into fully functional smart systems.

In summary, this study presents an IoT-based solution utilising LoRaWAN technology for monitoring distribution networks, addressing the challenges of fault detection and location determination. The platform's practical evaluation showcases its effectiveness in enabling rapid response and repair actions, even in resource-constrained settings. By leveraging IoT technologies, power distribution systems can be transformed into more responsive, communicative, attractive, and robust entities, enhancing service reliability and meeting the demands of a modern energy landscape.

Chapter 5

Condition Monitoring of Oil-Immersed Transformers Using AI Edge Inference for Incipient Fault Prediction: A Case Study

5.1 Introduction

Energy is a vital resource in today's modern world, whose copious availability has a direct bearing on the performance of an economy as well as societal development. Energy consumption and spatial econometrics are intricately intertwined and inseparably interwoven. The development and enhancement of the quality of human life require an abundant, efficient, and stable energy supply. Over the last decade, Kenya's energy supply and consumption have witnessed rapid and steady growth, which is attributed to a power-demanding economy growing in leaps and bounds. Improvements in electrical fixtures and facilities, such as voltage, frequency, and current, are primarily responsible for these advancements.

However, the frequency with which the distribution transformers owned and operated by Kenya Power Plc fail is a cause for concern. A convergence of different factors, either acting together or separately, conspires to affect the reliability of transformer units in operation. In 2020 alone, 3866 transformers out of the more than 69,000 on the distribution network failed. Cumulatively, these failures result in hundreds of thousands of power outages every year, disrupting industrial activity, endangering the lives of hospitalised patients, and frustrating consumers. Evidently, power system operators (PSOs) are faced with the challenge of how to safely operate equipment that is nearing the end of its operational lifespan.

An overwhelming number of machine learning platforms that have been proposed in recent literature have been cloud-centric [235]. The widespread and ever-growing adoption of Internet of Things (IoT) technology in cross-cutting domains has catalysed

research on novel smart monitoring and sensing techniques [236]. When IoT devices fitted with transducers are deployed using low-power, long-range networking technologies, the result is powerful platforms with smart actuation and transduction capabilities. IoT devices installed in remote locations primarily collect data from such deployments. This data collection capability from the network periphery has spurred renewed interest from contemporary researchers in edge computation. Edge computing is a relatively new paradigm for distributed data processing in which users' information is acquired and processed at the network's fringe, as close as possible to where the data is collected. In previous studies, we proposed a multinomial gas analysis classifier for the identification of developing faults in oil-filled transformers [14], and work is ongoing on a LoRa-enabled proactive fault detection and monitoring platform for the power distribution system employing self-powered IoT devices. In this chapter, we propose to devolve from the cloud-centric processing model to an edge-based computational environment. We demonstrate that machine learning can be deployed on an edge device for the purpose of monitoring the condition of oil-immersed transformers. Specifically, the tinyML platform is used in this work for the stated objective.

5.2 AI Edge Inference for Condition Monitoring

In the last twenty years, there has been a strong movement within the field of engineering towards the development of methods for developing and constructing machines that can think and behave in the same manner as a human brain. To put it another way, one of the most prominent trends in technology today is the programming of robots to gain intelligence. The discipline of science that investigates this endeavour is known as "artificial intelligence" (AI), and it may be thought of as a subfield of computer science [237], [238]. Due to the recent increase in research concentration on this topic, the field has been subdivided into numerous subfields, as shown in Figure 5-1.

Condition monitoring of transformers makes it possible to detect incipient problems early. AI has been used to perform predictive maintenance, but inference at the edge is

a relatively novel concept [239]. AI edge inference is ideal for the real-time application of predictive maintenance. With AI edge inference, artificial intelligence and computational capacity are brought closer to data sources. Thus, only the outputs of inference models produced on the edge nodes are delivered to the centralised cloud servers, rather than the entire raw data acquired from the hardware of IoT devices. Because the obtained data is processed on decentralised edge nodes, centralised servers' network bandwidth and computing resources will be reduced. Edge AI approaches reduce communication costs and latency while also improving dependability, scalability, data security, and privacy [240].

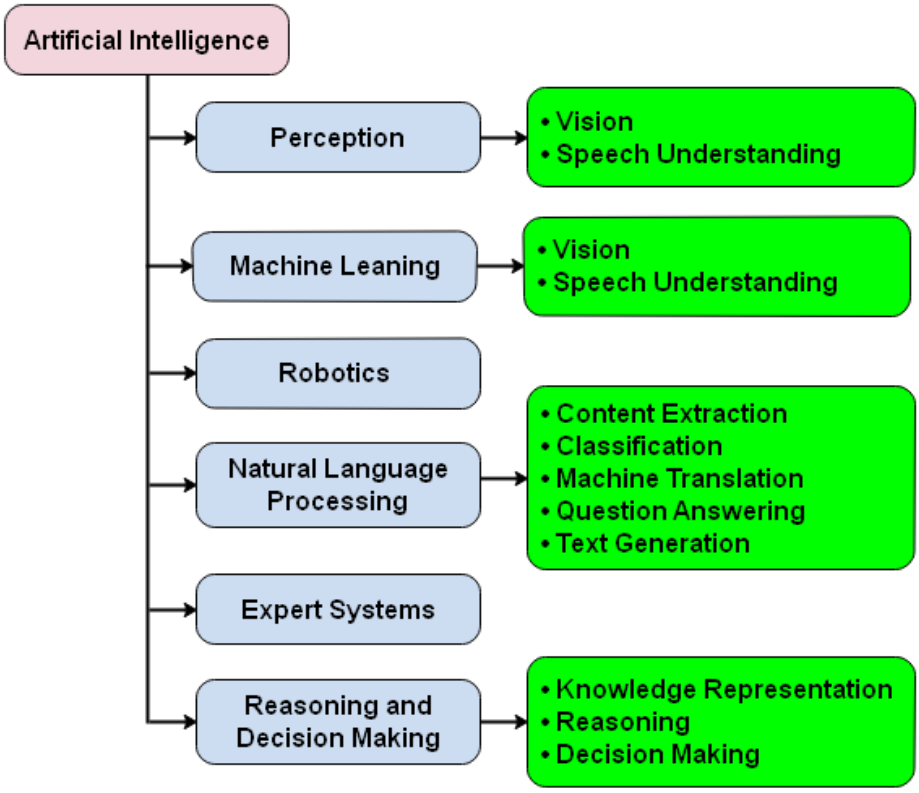

Figure 5-1: Categories of Artificial Intelligence

With this concept in mind, a machine-trained model can be developed and deployed to the edge to eliminate the need for cloud-based inference [241]. This method has a number of advantages over reactionary and preventative maintenance procedures, including the early identification of catastrophic failures and increased equipment availability. AI inference at the edge enables businesses to make better judgements,

enhancing fundamental business operations through improved performance and the quality of strategic decision-making. By averting major breakdowns, optimising the mean time between failures (MTBF), and decreasing unforeseen problems, predictive maintenance minimises the mean time to repair (MTTR) and the frequency of repairs, thus increasing the equipment's useful life. As a result, earnings are higher, maintenance and manufacturing expenses are lower, and productivity is more sustainable. The effective deployment of a predictive maintenance programme can result in a 25 percent to 30 percent reduction in maintenance expenditures and a 1000 percent return on investment [239].

Recently, multiple research studies have been conducted on the transference of processing tasks to the edge from the cloud. For real-time monitoring of tea processing, reference [242] presented a deep learning machine learning model deployed to the edge and fog environments. The technology, which is fuelled by solar energy, solves the problems of inconsistent grid power and intermittent Internet access. According to the study, in comparison to cloud and fog-based systems, the edge-computing paradigm had the lowest latency. Furthermore, the TeaNet model that was evaluated yielded highly precise and accurate results. To reduce the expense of widespread deployment, [243] shows a model prototype and develops an edge-based offline water-bone cholera detection tool that can be plugged into existing taps. In comparison to real cloud categorization, simulated results demonstrated high accuracy in edge inference. Reference [244] investigated the possible detection of respiratory diseases using edge AI. The study provided a prototype design for an STM32-based offline portable tool that embedded a tinyML model for respiratory illness prediction locally. It was effectively proven through simulated testing that the inference accuracy of the edge AI to forecast chronic obstructive pulmonary disease (COPD) is comparable to the ideal precision when inferencing in the cloud.

5.3 Prototyping of TinyML

In this section, we discuss the development and compilation of the proposed systems' library, as well as modelling and simulation.

5.3.1 TinyML Library Generation and Compilation for Embedded Inference

The machine learning (ML) process begins with a dataset for training. The data consists of samples collected from the gas sensors to detect emitted gases. The next step is to train a tinyML model tailored for embedded processors using a dataset and an appropriate machine learning framework. The resulting model is then converted into a software library for the target board. In this work, we have used an Arduino-based Microcontroller Unit (MCU), which can later be used with an alternative microprocessor architecture and deployed with the assistance of a suitable development platform before deployment on either the target board or through simulation. In the context of a simulator, the performance of the tiny model will be measured by inputting a file containing the test data and making a comparison between the inference results and those achieved by machine learning inference from the cloud during training. Figure 5-2 shows the edge AI tool stack. The procedure starts with a dataset of DGA parameters for gas level readings that Kenya Power Plc has gathered over time. The data is then used to train a lightweight machine-learning model that is optimised for embedded computing applications. Using an IDE, the AI model is subsequently built for the target CPU and bundled as a software library. Edge Impulse was chosen as the framework for this. Edge Impulse is a new, non-proprietary platform that is rapidly gaining popularity for machine learning models targeted at the edge. The Arduino IDE, which has been developed in C and C++, is a multi-platform programme that is useful for creating and loading programmes onto microcontroller boards that are Arduino-compliant.

5.3.2 Validation of TinyML in Predicting Transformer Failure

The prototype tool stack has been tested for the prediction of incipient transformer defects from dissolved gases. This section talks about the simulation that can be inferred

from the virtual embedded board after the sample dataset and the edge AI Tiny Model training architecture have been introduced.

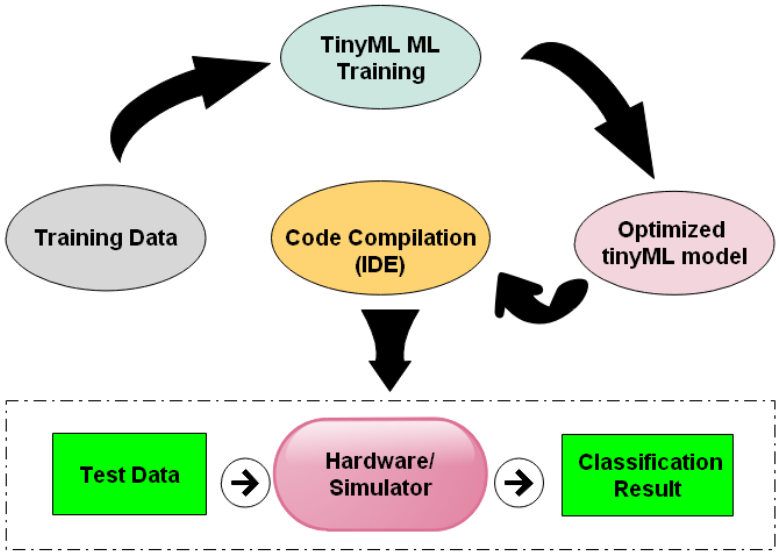

Figure 5-2: The Edge AI Tool stack

5.3.3 The Dataset

The dataset represents dissolved gas analysis (DGA) data gathered from transformers run by Kenya Power plc on Kenya's power network. The data consists of six predictor variables and one dependent variable. The predictor variables represent the values (in *parts per million*) of the gas's hydrogen, ethylene, methane, ethane, acetylene, and carbon monoxide, while the dependent variable indicates the status of the transformer. The six types of faults are identified based on energy discharges (whether high or low), thermal faults and their observed temperatures, and partial discharge.

5.3.4 Model training architecture

This section presents the architectural model for training in tinyML. The first step in the digital signal processing (DSP) block is the application of the feature processing technique. After understanding the data, it is determined whether further mathematical techniques are required. This involves the extraction of raw features before they are fed to the neural network. The pre-processed data stream is then fed into two training streams: the first for identifying anomalous observations and the other for categorising

the observations. Figure 5-3 shows the model training architecture for the tinyML platform. We began by uploading a dataset of samples collected for DGA analysis in comma-separated file format. This dataset was used for training, but prior to this, features were retrieved from the submitted data such that meaningful information would be extracted and utilised in training the fault prediction model. The resulting features were mapped into clusters. The diagram in Figure 5-4 shows the visualised clusters obtained from the DSP block. It shows that since the classes are distinctly separated, the training is expected to perform well. Otherwise, one would be forced to go back and assess the data. The observations are then sent to two parallel blocks used for machine learning training, resulting in an accurate model. One block is used to detect anomalous observations, such as gas samples that are not among the selected parameters, and the second is for inferring transformer health. The K-means anomaly detection-learning block is employed for anomaly identification. This approach employs a threshold value to detect anomalies by assessing whether the distance between a data point and the closest centroid exceeds the threshold value. The threshold value and model cluster count were set to 0.30 and 32, respectively. Two training runs were conducted on a four-layer neural network (NN) classifier, each with a different number of training epochs. With a confidence rate of 0.60 and a learning rate of 0.0005, satisfactory results were obtained after 50 epochs. The resulting model has a loss of 4.78 percent and a validation accuracy of 82.6 percent for an optimized model. Further examination of an unoptimised tinyML model reveals an increase to 99% accuracy. Figure 5-5 depicts the validation set's confusion matrix.

Every row in Figure 5-6 represents a set of features. For example, the highlighted row in Figure 5-6 represents the output of one set of features, which is represented in Figure 5-7 as [1410, 4187, 85, 2220, 1334, 1198] for class thermal fault (low temperature). That is, the prediction is 1.00 for that particular set of features. To prove that the model can perform as a tinyML model on an embedded device, we selected features and compared the outputs from the online live classification to the targeted embedded device. The features selected in Figure 5-7 represent the online live cloud platform, and Figure 5-8

shows that the same features are copied to the embedded targeted device for the class of thermal fault (low temperature). Figure 5-9 shows the output from the serial monitor, showing an inference time of 1 ms. This output is compared to the live classification output of Figure 5-6, which proves that predictions on the cloud platform are similar to those of an embedded device. The results on the serial display are marginally different in terms of how its scorecard works with less than 1 ms of inference time, 46408 bytes of RAM, and 120888 bytes of flash on the Arduino.

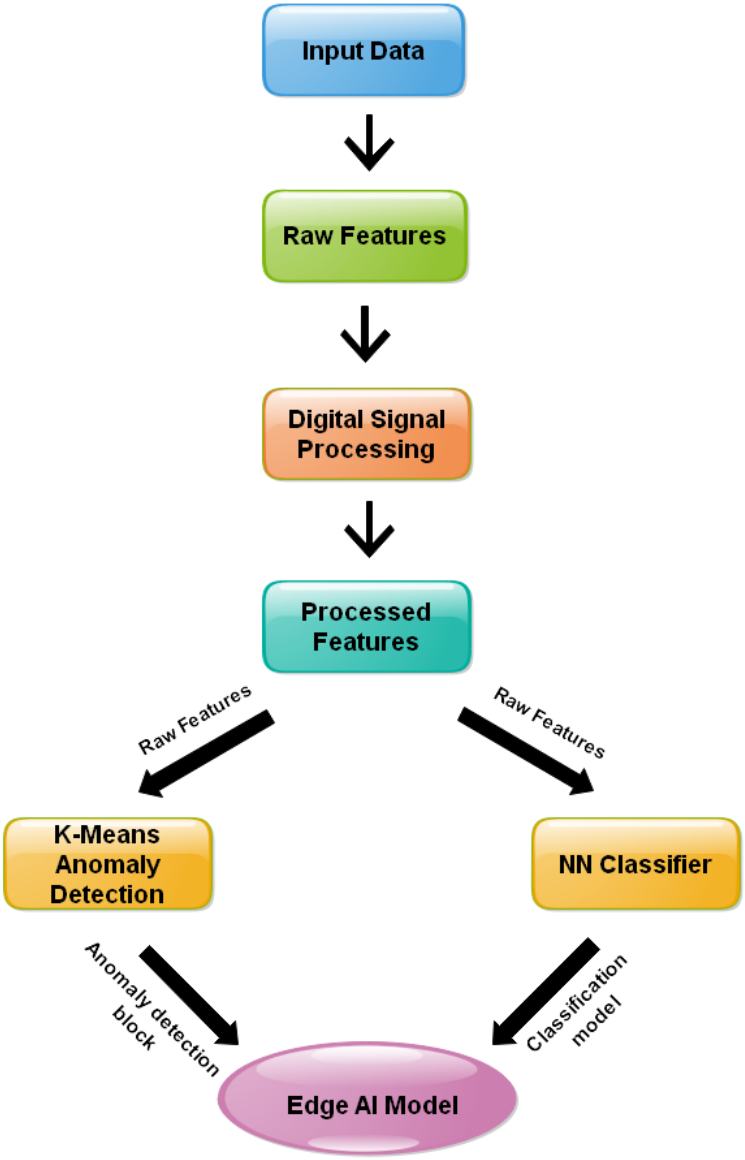

Figure 5-3: Digital signal processing block

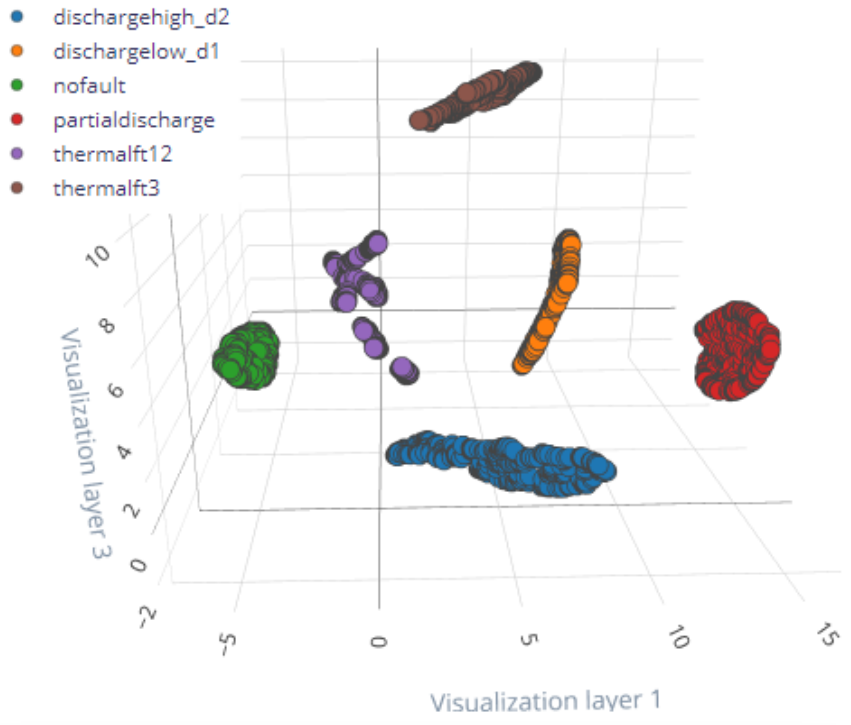

Figure 5-4: The categorization of the training set illustrating the classification of the sample training data

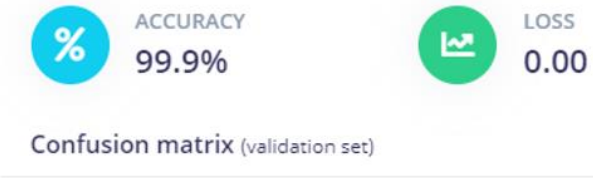

Confusion matrix (validation set)

	HIGH ENERGY DISCHARGE	LOW ENERGY DISCHARGE	NO FAULT	PARTIAL DISCHARGE	THERMAL FAULT LOW	THERMAL FAULT HIGH
LOW ENERGY DISCHARGE	99.6%	0.4%	0%	0%	0%	0%
HIGH ENERGY DISCHARGE	0%	100%	0%	0%	0%	0%
NO FAULT	0%	0%	100%	0%	0%	0%
PARTIAL DISCHARGE	0%	0%	0%	100%	0%	0%
THERMAL FAULT LOW	0%	0%	0%	0%	100%	0%
THERMAL FAULT HIGH	0%	0%	0%	0%	0%	100%
F1 SCORE	1.00	1.00	1.00	1.00	1.00	1.00

Figure 5-5: Validation set accuracy and confusion matrix

TIMESTAMP	HIGH ENERGY DISCHARGE	LOW ENERGY DISCHARGE	NO FAULT	PARTIAL DISCHARGE	THERMAL FAULT LOW	THERMAL FAULT HIGH	ANOMALY
0	0	0	0	0	1.00	0	0.12
1000	0	0	0	0	1.00	0	0.12
2000	0	0	0	0	1.00	0	0.12
3000	0	0	0	0	1.00	0	0.13
4000	0	0	0	0	1.00	0	0.06

Figure 5-6: An image of live classification on edge impulse

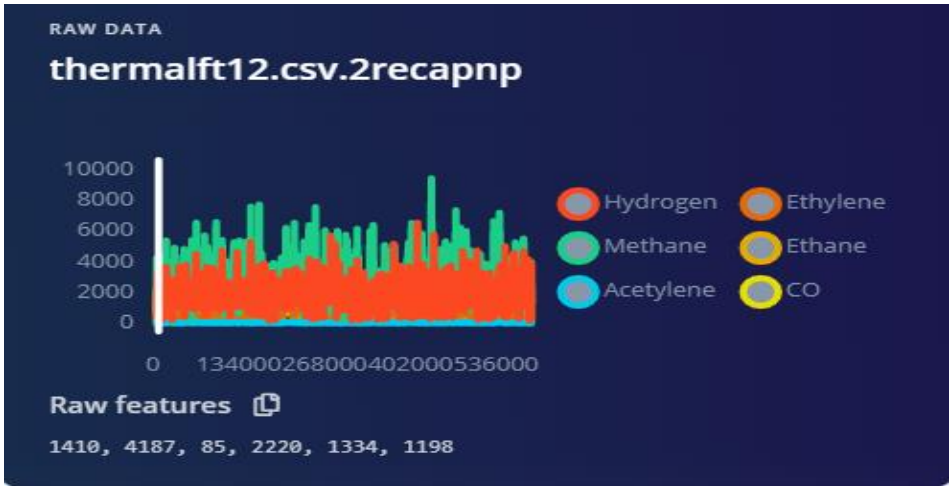

Figure 5-7: Selected features from the Cloud platform

5.4 Results obtained from the embedded board

The results of the simulation were compared to those obtained during live classification. It was evident that the results were very similar to those shown in Figures 5-6 and 5-10. Figures 5-11 and 5-9 show that the AI edge platform predicts the resource usage of the board, which is accurately achieved when the model is deployed on an actual board. It is recommended that non-optimised model optimisations be performed, as the model will still achieve optimum performance despite its smaller size compared to an optimised model. Optimising the model to occupy the minimum space on the board leads to lower accuracy. The embedded device displayed the same accuracy in this instance as the Edge impulse platform (Figures 5-6 and 5-10).

```
static const float features[] = {1410, 4187, 85, 2220, 1334, 1198
    // copy raw features here (for example from the 'Live classification' page)
    // see https://docs.edgeimpulse.com/docs/running-your-impulse-arduino
};
```

Figure 5-8: Selected features input on the Arduino code

Figure 5-9: Edge impulse estimations

```
Edge Impulse standalone inferencing (Arduino)
run_classifier returned: 0
Predictions (DSP: 0 ms., Classification: 0 ms., Anomaly: 0 ms.):
[0.00000, 0.00000, 0.00000, 0.00000, 1.00000, 0.00000, -0.426]
    dischargehigh_d2: 0.00000
    dischargelow_d1: 0.00000
    nofault: 0.00000
    partialdischarge: 0.00000
    thermalft12: 1.00000
    thermalft3: 0.00000
    anomaly score: -0.426
```

Figure 5-10: Output from Serial Monitor

```
Sketch uses 120888 bytes (12%) of program storage space. Maximum is 983040 bytes.
Global variables use 46408 bytes (17%) of dynamic memory, leaving 215736 bytes for local variables. Ma
Device       : nRF52840-QIAA
Version      : Arduino Bootloader (SAM-BA extended) 2.0 [Arduino:IKXYZ]
Address      : 0x0
Pages        : 256
Page Size    : 4096 bytes
Total Size   : 1024KB
Planes       : 1
Lock Regions : 0
Locked       : none
Security     : false
Erase flash

Done in 0.001 seconds
Write 120896 bytes to flash (30 pages)
[==============================] 100% (30/30 pages)
Done in 4.982 seconds
```

Figure 5-11: Compilation embedded hardware specifications

5.5 Limitation

In this phase of the study, several limitations associated with using tinyML and Edge Impulse devices were encountered:

1. Limited computational power: Edge devices typically have limited computational resources compared to cloud-based platforms. This limitation may restrict the complexity and size of the machine learning models that can be deployed on these devices.
2. Memory constraints: Edge devices often have limited memory capacity, which can pose challenges when storing and running machine learning models. Complex models with large parameter sizes may not fit within the memory limitations of the device.
3. Power constraints: Edge devices are often battery-powered or have limited power availability. Running resource-intensive machine learning models continuously can drain the device's power quickly, leading to a reduced operational lifespan or frequent recharging requirements.
4. Limited data processing capabilities: Edge devices may have limited processing capabilities, such as slower CPUs or low-performance GPUs, compared to powerful servers in cloud environments. This limitation can impact the speed and efficiency of data processing and model inference on the device.
5. Training data availability: Training machine learning models typically requires large amounts of labelled data. Acquiring diverse and representative datasets for training models directly on edge devices can be challenging due to limited storage capacity or connectivity constraints.
6. Model updates and maintenance: Updating and maintaining machine learning models deployed on edge devices can be more challenging compared to cloud-based deployments. Ensuring timely updates, bug fixes, and model improvements on a large number of edge devices distributed across various locations can be complex and resource-intensive.

7. Scalability and deployment logistics: Deploying and managing machine learning models on a large scale across numerous edge devices can be logistically challenging. Coordinating updates, ensuring compatibility, and managing the distributed deployment of models require careful planning and infrastructure considerations.

Despite these limitations, tinyML and Edge Impulse devices offer valuable opportunities for deploying machine learning models at the edge, enabling real-time and localised inference. With advancements in hardware and software technologies, many of these limitations are being addressed, making edge computing and tinyML increasingly viable for a wide range of applications.

5.6 Summary

This study focuses on the application of machine learning for condition monitoring of oil-immersed power transformers by analysing dissolved gases in transformer oil. Monitoring dissolved gases is a widely used technique for assessing the health of power transformers. The research explores the use of machine learning models deployed on edge devices for efficient and accurate condition monitoring.

Through simulated experiments, the study demonstrates that machine learning models deployed at the edge can achieve a high level of accuracy comparable to cloud-based platforms. The selected technique exhibits an overall accuracy of 99.9%, indicating its effectiveness in anticipating incipient faults. This approach enables timely assessment, addressing, and action on detected issues before they escalate and lead to transformer failure.

The research highlights the potential of tinyML, a resource-restricted machine learning approach, for training models on embedded devices. The results of the simulations show that embedded inference is possible and that machine learning models can be used to find problems early in transformers.

Overall, the study underscores the value of machine learning and edge computing in enhancing the condition monitoring and management of oil-immersed power

transformers. By leveraging these technologies, power utilities can proactively address developing issues, improve reliability, and prevent costly downtime.

Chapter 6

Conclusion, Recommendation and Future Work

6.1 Introduction

This chapter summarises the key research findings and then provides a conclusion, recommendations, and suggestions for future studies. Additionally, this chapter points out the inferences to be drawn from the study's findings for empirical, theoretical, and managerial policies and practises. Lastly, the chapter concludes with a discussion of the research's limitations and potential future directions.

6.2 Summary of Major Findings and Recommendations

The primary goal of this study was to investigate how the Internet of Things (IoT) can be used to monitor the electrical power system for faults and aid in the identification of the precise location where a malfunction has taken place. In the foregoing chapters, we have introduced the background to fault detection on the power transmission system (PTS) in the context of sub-Saharan Africa.

In Chapter 1, we outlined the research problem along with the specific objectives of the study. Our study was a case study that focused on Kenya Power (KP), an electricity service provision company engaged in the distribution and retail of electrical energy in Kenya. The overarching aim of this study was to investigate how the Internet of Things (IoT) can be used to monitor the electrical power grid for faults and identify the precise location where a malfunction has taken place. The research questions were framed as follows:

1. *How can cloud-based machine-learning models use DGA data to enhance the prediction of incipient faults in oil-immersed power transformers?*
2. *How can automated fault monitoring on the electrical power system using an Internet of Things platform be used to reduce the duration of power blackouts?*

3. *How can the deployment of autonomous edge-based machine-learning models enhance the detection of incipient faults in oil-immersed electrical transformers?*

The Internet of Things (IoT) technology was essential to the successful resolution of the research problem as well as the accomplishment of the study objectives.

In Chapter 2, a review of both theoretical and empirical scientific studies is undertaken. The underpinning technologies in support of this work were the Internet of Things (IoT) and LoRa®. Additionally, the research gaps were examined in previous empirical literature related to this study. This research study relied on both primary and secondary data sources. Primary data was collected through field experiments, and secondary data on dissolved gas analysis was obtained from the utility company, Kenya Power. The data collected related to seven gases: ethane (C_2H_4), ethylene (C_2H_4), oxygen (H_2), methane (CH_4), acetylene (C_2H_4), nitrogen (H_2), and hydrogen. Because nitrogen (N_2), and oxygen (H_2) are non-fault gases, they were not studied further. Hydrogen gas (H_2), hydrocarbons ($H_2, CH_4, C_2H_4, C_2H_4$), and carbon oxides ($CO_2, CO$) were thereafter studied further using explorative data analysis (EDA) techniques. The techniques used comprised both univariate graphical and non-graphical and multivariate graphical and multivariate. The explorative data analysis revealed the need for further interventions to improve the quality and reliability of the data for building machine learning models. Variable pairs, methane and ethane, and methane and hydrogen, were found to be coincidentally positively correlated. In addition, the gases acetylene, ethylene, ethane, and carbon monoxide had outliers. The data was then used for the first objective of the study. The study was guided by three research questions. The first research question was to develop a prediction model that makes use of DGA data to predict and forecast faults in the power distribution system. The data set with gas values was the basis upon which a prediction model was developed. The platform that was used to develop the machine learning models was the Python Integrated Development Environment (IDE). The machine learning algorithms decision trees, naïve bayes, gradient boost, *k* nearest neighbour, and random forest, which had multinomial

capability, were tested with the data set but were found to have low accuracy scores of 92% or lower.

In Chapter 3, the first objective of this study, which was to build a machine learning model that uses historical data to predict an ongoing fault, is addressed. The decision tree algorithm, which is a supervised approach to machine learning, was chosen for this purpose. The decision tree algorithm, which is based on classification and regression trees, was found to be especially good for this task because, unlike other classification algorithms, it uses the information gain and the Gini index to choose which attributes to use. The information gain is the measurement of changes in entropy after the segmentation of a dataset based on an attribute and essentially calculates how much information a feature provides us about a class, while the Gini impurity is the probability of incorrectly classifying random data points in the dataset if they were labelled based on the class distribution of the dataset. These two attributes imbue the decision tree algorithm with a powerful mechanism for performing classification duties. The mechanism is powerful because it relies on several metrics to perform a split. Based on the value of the information gain, a node is split to build the decision tree. The decision tree algorithm always tries to maximise the value of information gained, and a node or attribute with the highest information gain is split first.

Chapter 4 tackles the second objective, where an electronic monitoring device with sensors attached is assembled and embedded into the power distribution grid. In order to facilitate communication, LoRa technology was used. LoRa was selected because it is ideal for IoT deployments, especially where long-range data transmission is required. It was practically demonstrated that the platform is able to transmit information to the control centre within 200 ms, which is a significant departure from the prevailing situation where information about faults in remote systems takes hours and sometimes days to reach the control centre. This delay in notification of ongoing faults has contributed immensely to prolonged episodes of power blackouts.

In Chapter 5, the third objective of this study is tackled. Whereas in Chapter 4, the fault monitoring model was stationed in the cloud, in Chapter 5, the model is moved closer to its point of data generation. Tiny Machine Learning (TinyML) was used to create a miniaturised model that can be deployed on resource-constrained platforms such as Arduino. Moving the model closer to the point of generation yielded several tangible benefits. First, there was a tangible reduction in bandwidth usage. This is because more processing is being conducted at the edge rather than in the cloud. Secondly, the system experienced reduced levels of latency. The result demonstrated that, in terms of performance, the system attained performance metrics compared to their cloud-based counterparts.

The reliable, safe, and efficient functioning of the power grid requires effective condition monitoring and timely intervention to resolve issues detected. The transformer is not only indispensable but also one of the most important and costliest pieces of equipment in the system, and its failure can cause large disruptions in the power supply. Transformers immersed in oil have been in use for many decades now and have been proven to be more effective than their dry-type counterparts. In addition to serving as a cooling agent, oil also serves as an insulator when used with solid insulation. A very dangerous condition of the transformer arises from the generation of fault gas as a result of incipient faults and the ageing of the insulation materials. By looking at the types, amounts, and ratios of dissolved gases in the transformer oil on a regular basis, you can learn about problems that may be starting to happen inside the transformer. The use of the dissolved gas analysis (DGA) method is widely acknowledged as a practical way for determining a transformer's fault states. The transformer oil is a crucial information carrier that offers insight into any transformer malfunction and enables the use of the most appropriate repair measures in a timely manner. But a successful gas-in-oil analysis is crucial, and its success depends on how well the DGA procedure is carried out.

The fundamental objective of this doctoral thesis was to build and prototype an internet-of-things-based platform for the power distribution system that is capable of predicting

faults and discovering their location. Using machine learning algorithms, the proposed prototype data collection device for fault monitoring with an instantaneous date and time log-in feature gives a new way to find, identify, and classify faults on the transmission line network. In this work, machine learning algorithms for fault detection, classification, and location techniques have been realised. The techniques used depend on the current and voltage signals from the sensors. The features were extracted from the current and voltage signals by using a machine-learning decision tree, the support vector machine, k-nearest neighbours (*k*-NN), and the proposed model KosaNET. The feature vector is then given as input to the machine learning algorithms. The capabilities of machine learning algorithms in pattern classification were utilised. Simulation studies were performed for each of the algorithms, and the performance of the scheme with different system parameters and conditions for fault detection was investigated. The test result shows that the accuracy obtained for fault classification by KosaNET was found to be better compared to the decision tree, *k*-NN, and SVM with respect to accuracy at 99.5% and the training time response at 0.000999928 seconds. KosaNET was tested with data sets with wide variations in the operating conditions of the power system network, including load variation, and it provided accurate results. The robustness and accuracy of the proposed model showed the potential of KosaNET for protecting the distribution transformer in a large power network.

6.3 Implications of Research Findings

This study makes original contributions to the corpus of knowledge in the areas of the Internet of Things, fault monitoring of the electricity power system, long-range data transmission, and DGA data analysis using machine learning techniques. The themes of these contributions are empirical research, theoretical knowledge, and policy and practise. Figure 6-1 provides a summarised visual depiction of the contributions of this study. We now highlight our contribution in each of these thematic areas.

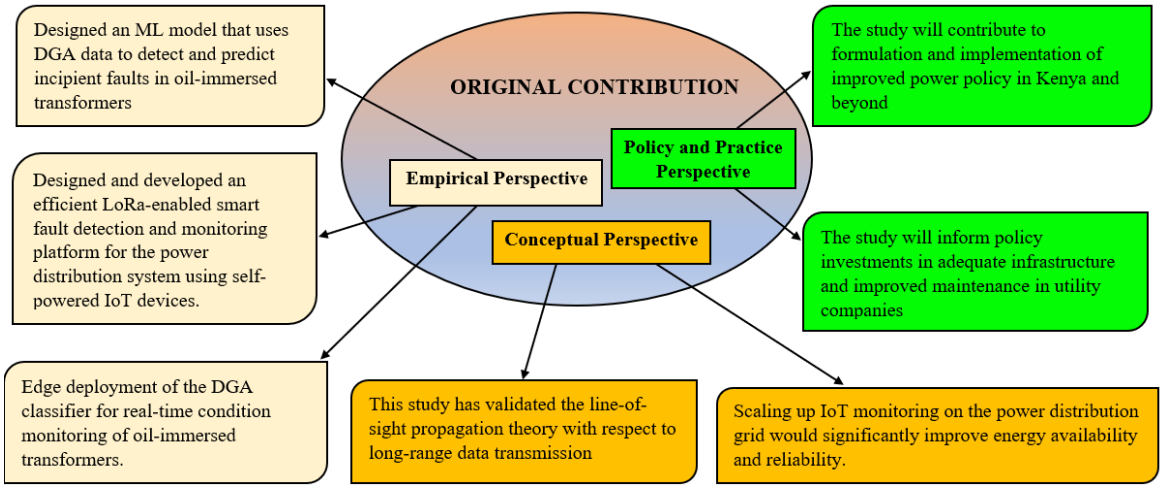

Figure 6-1: Original contributions of the study

6.3.1 Contribution to Empirical Research

In relation to empirical research, this study makes a contribution in three main ways. Firstly, the study designed KosaNET, which is a machine learning model that uses DGA data to detect and predict incipient faults in oil-immersed transformers. In this phase of the study, the problem of practical relevance was how to detect incipient faults in oil-immersed power transformers early, before a catastrophic state is attained. The cloud-based model, founded on the decision tree algorithm, was developed in a Python programming environment using decision trees. Decision trees are highly interpretable and robust. The amount of uncertainty at a single node was quantified using a metric called the Gini impurity, and the amount by which a question reduces that uncertainty was quantified using a metric called information gain. Secondly, we have developed an efficient LoRa-enabled smart fault detection and monitoring platform for the power distribution system using self-powered IoT devices. Arduino microcontrollers with sensors attached were programmed and embedded in transformers that were identified to participate in the study. In addition to the sensors, LoRa transmitters were also connected to the Arduino microcontrollers. The embedded device was designed to be maintenance-free and energy-independent and was able to renew its power from solar energy stored in a rechargeable battery. Lastly, this study deployed the DGA classifier to the edge environment for real-time condition monitoring of oil-immersed

transformers. As a result, this study lends credence to the idea that frequent electric power outages adversely affect financial losses for business entities. As a result, the top management of utility firms should implement interventions that would mitigate power outages in order to comply with the recommendations of this study.

6.3.2 Contribution to Conceptual Research

With respect to conceptual or theoretical knowledge, this interdisciplinary study has intertwined the Internet of Things (IoT) with the power distribution system and extended the applicability and predictive power of machine learning for fault monitoring. The results of this study indicate that the upscaling of IoT monitoring on the power distribution grid would greatly enhance the availability and reliability of energy provision. Secondly, this study has validated the line-of-sight propagation theory with respect to long-range data transmission. We have made recommendations on best practises that can be put to immediate use by other researchers. Specifically, we have observed that the transmitters and the receiver operate at their best when they are stationed high above the ground so as to create a perfect clearance for the Fresnel zone.

6.3.3 Contribution to managerial practise and policy

The research findings of this study will be beneficial to numerous stakeholder categories. These include the government, regulators, and electric utility companies that produce and distribute electricity. The research will aid in the creation and application of better power policies in Kenya. Understanding the value of fault monitoring in the power distribution network helps policymakers make informed decisions about the design and construction of adequate infrastructure that will prevent avoidable power outages. Furthermore, the study will inform policy investments in adequate infrastructure and improved maintenance in utility companies to ensure highly available power supply and maintenance in utility companies to ensure highly available power supply and efficiency as well as provide information to power utility companies that will inform their investment priorities. It will also give information to power utilities that will support their investment in supplying power to businesses at all times. The study

provides the Energy and Petroleum Regulatory Authority (EPRA), responsible for regulating the electricity and petroleum sectors, with valuable information to enhance the protection of power users, specifically manufacturing companies. These insights aim to mitigate the negative impact of power outages on their productivity. When power outages occur because of the utilities' omissions or commissions, the regulator may implement punitive mechanisms. This should reduce the number of power outages and the harm they cause to consumers. The Energy Act of 2019 provides excellent protection for consumers against the negative effects of poor electricity quality and power outages. Subsidiary legislation and regulations should specify practical ways of implementing the law. Kenya's blueprint for economic development has been identified as relying heavily on the manufacturing sector. According to Vision 2030, the nation will change from a developing to a middle-income country by the year 2030. The three main pillars of economic, social, and political development will support the realisation of the vision. Manufacturing is anticipated to be the sector that contributes most to the economic pillar. The "Big 4 Agenda," which identified four sectors of Kenya's economy for prioritisation and improved facilitation in order to transform the economy, also forms the foundation of the government's economic agenda. Manufacturing, universal healthcare, food security, and affordable housing are among these sectors. The manufacturing sector is a crucial component for the country's achievement of economic growth, as stated explicitly in government policies. Therefore, its success must be protected in every way through appropriate business facilitation and the provision of adequate infrastructure. For the majority of manufacturing processes, electricity is a crucial input. However, due to its effective delivery, performance won't be impacted by inadequate power distribution.

6.4 Limitations

The research study focuses on IoT technology but highlights the challenges of the costly and limited availability of IoT devices and sensors, which require special arrangements to obtain. Supervised machine learning techniques were used in the study due to the availability of labelled data. The research specifically focuses on the power distribution

grid in Kenya, although it acknowledges potential institutional bias and the need to consider global, regional, and local perspectives. The Dissolved Gas Analysis (DGA) technique faces limitations such as restricted data collection, a lack of real-time monitoring, and integration challenges. The LoRa-based Smart Fault Detection and Monitoring Platform faces limitations related to data transmission range, edge processing support, bandwidth, scalability, latency, and communication capabilities. TinyML devices have limitations in computational power, memory capacity, power constraints, data acquisition, model updates, scalability, and deployment management. Ongoing research and development efforts aim to address these limitations and improve the capabilities of the proposed techniques and devices.

Despite the limitations, tinyML and Edge Impulse devices offer opportunities for real-time and localised inference at the edge, with advancements in hardware and software technologies making them increasingly viable for various applications.

6.5 Propositions for Future Work

This study makes several suggestions for additional study, including the following:

- **To study the influence induced by mechanical disturbances and other natural variables.**

  The first proposal for future studies is to further investigate the influences induced by mechanical disturbances and other natural variables on transformer failures. Future researchers may be able to explore new possibilities in automated and autonomous power grid monitoring, including self-healing mechanisms, using the data and analysis provided by this research.

- **To develop expanded models for estimating the residual life of transformers.**

  Secondly, the results of this study can also be useful in developing expanded models for estimating the residual life of transformers and asset management decisions using data from dissolved gas analysis (DGA).

- **To investigate how other long-range data transmission techniques compare with LoRa, which has been used in this study.**

  Lastly, it has been demonstrated that the Fresnel zone exerts a significant amount of influence on the data transmission that occurs between two communicating nodes. The Fresnel zone is one of a series of confocal, prolate ellipsoidal regions of space that are located between and around a transmitter and a receiver. This study has practically evaluated the effect of the Fresnel zone on LoRa data transmission. In this context, antenna height has been demonstrated to be a significant variable in microwave data reception. Instead of tinkering with the transmitter power or the antenna gain, a much better alternative would be to increase the antenna height in order to minimise interference from the foreground. Future studies could be conducted on how NB-IoT compares with LoRa as far as data transmission is concerned. In addition, further research could be conducted on improving antenna design and placement for IoT devices.

REFERENCES

[1] O. K. Kareem, A. I. Adekitan, and A. Awelewa, "Power distribution system fault monitoring device for supply networks in Nigeria," *Int. J. Electr. Comput. Eng.*, vol. 9, no. 4, pp. 2803–2812, 2019, doi: 10.11591/ijece.v9i4.pp2803-2812.

[2] A. Bahmanyar and A. Estebsari, "A Practical Integrated Fault Location Method for Electrical Power Distribution Networks," in *Proceedings - 2018 IEEE International Conference on Environment and Electrical Engineering and 2018 IEEE Industrial and Commercial Power Systems Europe, EEEIC/I and CPS Europe 2018*, 2018, pp. 1–5. doi: 10.1109/EEEIC.2018.8494491.

[3] I. Srivastava, S. Bhat, and A. R. Singh, "Fault diagnosis, service restoration, and data loss mitigation through multi-agent system in a smart power distribution grid," *Energy Sources, Part A Recover. Util. Environ. Eff.*, pp. 1–26, 2020, doi: 10.1080/15567036.2020.1817190.

[4] R. Navaneetha Krishna, N. Shyamsundar, and C. Venkatesan, "IoT Based Transmission Line Fault Monitoring System," *Int. J. Res. Anal. Rev.*, vol. 7, no. 3, pp. 1–5, 2020, doi: 10.13140/RG.2.2.20627.91685.

[5] S. Zare, Y. Ghafarifar, and M. Hashemi, "Assessment of Smart Grid Communication Infrastructures Requirements and Challenges," in *International conference on electricity distribution*, 2014, no. 0069, pp. 11–12. doi: 10.7563/cired0096.4523_23.

[6] I. Allafi and T. Iqbal, "Low-Cost SCADA System Using Arduino and Reliance SCADA for a Stand-Alone Photovoltaic System," *J. Sol. Energy*, vol. 2018, no. 3140309, pp. 1–8, 2018, doi: 10.1155/2018/3140309.

[7] S. Jamali, A. Bahmanyar, and E. Bompard, "Fault location method for distribution networks using smart meters," *Measurement*, 2017, doi: 10.1016/j.measurement.2017.02.008.

[8] KPLC, "During an outage." https://www.kplc.co.ke/content/item/553/during-an-outage (accessed Jun. 16, 2022).

[9] Nation, "Nairobi West residents angered by Kenya Power's inefficiency," *Daily Nation*, 2016. https://www.youtube.com/watch?v=NXaDWmLqkN4 (accessed Jul.

04, 2022).

[10] A. O. Ifelebuegu and P. Ojo, “Renewable Energy in Africa: Policies, Sustainability, and Affordability,” *Energy in Africa*, pp. 199–221, 2019, doi: 10.1093/7.6.476.

[11] S. O. Maende and M. U. Alwanga, “The Cost of Power Outages on Enterprise Performance in Kenya,” *Int. J. Res. Innov. Soc. Sci.*, vol. IV, no. Iii, pp. 1–5, 2020.

[12] N. W. Wanjiku, “Effects of electric power outage dynamics on the performance of manufacturing firms in Kenya,” University of Nairobi, 2021.

[13] M. C. Nyangwaria and P. Munene, “Relationship between Power Supply Interruptions and Financial Performance of Manufacturing Companies in Machakos County,” *J. Hum. Resour. Leadersh.*, vol. 3, no. 3, pp. 1–26, 2019.

[14] G. Odongo, R. Musabe, and D. Hanyurwimfura, “A multinomial DGA classifier for incipient fault detection in oil-impregnated power transformers,” *Algorithms*, vol. 14, no. 4, 2021, doi: 10.3390/a14040128.

[15] G. Odongo, R. Musabe, D. Hanyurwimfura, and A. Bakari, “An efficient LoRa-enabled smart fault detection and monitoring platform for the power distribution system using self-powered IoT devices,” *IEEE Access*, vol. PP, p. 1, 2022, doi: 10.1109/ACCESS.2022.3189002.

[16] G. Y. Odongo, R. Musabe, D. Hanyurwimfura, and A. Bakari, “Condition Monitoring of Oil-immersed Transformers Using AI Edge Inference for Incipient Fault Prediction: A case study,” in *2022 PowerAfrica Conference*, 2022, p. 5. doi: doi.org/10.1109/PowerAfrica53997.2022.9905325.

[17] R. M. Larik, M. Wazir Mustafa, and S. Hussain Qazi, “Smart Grid Technologies in Power Systems: An Overview,” *Res. J. Appl. Sci. Eng. Technol.*, vol. 11, no. 6, pp. 633–638, 2015, doi: 10.19026/rjaset.11.2024.

[18] W. Tian, “A Review of Smart Grids and Their Future Challenges,” *MATEC Web Conf.*, vol. 173, 2018, doi: 10.1051/matecconf/201817302025.

[19] J. Xiao, G. Zu, X. Gong, and C. Wang, “Model and Topological Characteristics of Power Distribution System Security Region,” *J. Appl. Math.*, 2014.

[20] P. Schavemaker and L. van der Sluis, *Electrical Power System Essentials*. New York: John Wiley & Sons Ltd., 2008.

[21] B. Albert, K. Kendagor, and R. J. Prevost, “Energy Diversity and Development in Kenya,” *Joint Force Quarterly*, vol. 70, pp. 94–99, 2013.

[22] International Renewable Energy Agency, “A Renewable Energy Roadmap Report,” *IRENA*, 2023. https://www.irena.org/publications (accessed Jan. 02, 2022).

[23] H. Huangfu and W. Zeng, “Transmission Line Fault Location and Intelligent Inspection System based on GPS and GIS,” in *2019 2nd International Conference on Mechanical, Electrical and Material Application (MEMA)*, 2017, vol. 32, no. 12, pp. 1068–1075. doi: 10.1088/1757-899X/740/1/012142.

[24] M. E. El-Hawary, *Introduction to Electrical Power Systems*. Hoboken: John Wiley & Sons, Inc, 2008.

[25] G. Ma, L. Jiang, K. Zhou, and G. Xu, “A Method of Line Fault Location Based on Traveling Wave Theory,” *Int. J. Control Autom.*, vol. 9, no. 2, pp. 261–270, 2016, doi: 10.14257/ijca.2016.9.2.25.

[26] H. Jia, “An Improved Traveling-Wave-Based Fault Location Method with Compensating the Dispersion Effect of Traveling Wave in Wavelet Domain,” *Math. Probl. Eng.*, vol. 2017, pp. 1–11, 2017, doi: 10.1155/2017/1019591.

[27] S. Adhikari, N. Sinha, and T. Dorendrajit, “Fuzzy logic based on-line fault detection and classification in transmission line,” *Springerplus*, vol. 5, no. 1002, pp. 1–14, 2016, doi: 10.1186/s40064-016-2669-4.

[28] M. Vimal, A. L. Vaghamshi, and D. Matang, “Simulation and Analysis of transmission line fault detection and location using fuzzy logic,” *Int. J. Technol. Res. Eng.*, vol. 4, no. 8, pp. 1463–1470, 2017, doi: https://doi.org/10.9390/0408718.

[29] R. Escudero, J. Noel, J. Elizondo, and J. Kirtley, “Microgrid fault detection based on wavelet transformation and Park’s vector approach,” *Electr. Power Syst. Res.*, vol. 152, pp. 401–403, 2017, doi: 10.1016/j.epsr.2017.07.028.

[30] J. Gopinath, A. V Manirathnam, K. M. Kumar, and C. Murugan, “High Impedance Fault Detection and Location in a Power Transmission Line Using ZIGBEE,” *Int. J. Innov. Res. Sci. Eng. Technol.*, vol. 5, no. 2, pp. 2586–2591, 2016, doi: 10.15680/IJIRSET.2016.0502187.

[31] K. Agbesi and F. A. Okai, “Automatic Fault Detection and Location in Power

Transmission Lines using GSM Technology," *Int. J. Adv. Res. Sci. Eng.*, vol. 5, no. 01, pp. 193–207, 2016, doi: doi.org/10.4380/v7650878.

[32] A. Parejo, E. Personal, D. F. Larios, J. I. Guerrero, A. García, and C. León, "Monitoring and Fault Location Sensor Network for Underground Distribution Lines," *Sensors*, vol. 19, no. 576, 2019, doi: 10.3390/s19030576.

[33] J. Lin, B. Zhu, P. Zeng, W. Liang, H. Yu, and Y. Xiao, "Monitoring power transmission lines using a wireless sensor network," *Wirel. Commun. Mob. Comput.*, vol. 15, pp. 1799–1821, 2015, doi: http://dx.doi.org/10.1002/wcm.2458.

[34] T. Zhihai *et al.*, "An accurate fault location method of smart distribution network," in *China International Conference on Electricity Distribution, CICED*, 2014, vol. 2014-Decem, no. Ciced, pp. 916–920. doi: 10.1109/CICED.2014.6991842.

[35] B. Samuel and J. Ct, "Identification of Faults in Medium Underground Cables System: Rwanda Case Study," *Int. J. Adv. Res. Electr. Electron. Instrum. Eng.*, vol. 6, no. 6, pp. 1–7, 2017, doi: 10.1088/2278-8875/1/012017.

[36] S. Sahana, H. Kumar, A. S, V. H, T. Sudha, and P. Kumar, "Analysis of fault detection and its location using microcontroller for underground cables," *Int. Res. J. Eng. Technol.*, vol. 04, no. 06, 2017, doi: doi.org/2395-0072/a22038.

[37] C. Haseltine and E. E. S. Eman, "Prediction of power grid failure using neural network learning," in *Proceedings - 16th IEEE International Conference on Machine Learning and Applications, ICMLA 2017*, 2018, pp. 505–510. doi: 10.1109/ICMLA.2017.0-111.

[38] I. Ullah *et al.*, "Predictive maintenance of power substation equipment by infrared thermography using a machine-learning approach," *Energies*, vol. 10, no. 12, 2017, doi: 10.3390/en10121987.

[39] Y. Tang, H. Cui, and Q. Wang, "Prediction model of the power system frequency using a cross-entropy ensemble algorithm," *Entropy*, vol. 19, no. 10, 2017, doi: 10.3390/e19100552.

[40] A. Mukherjee, P. K. Kundu, and A. Das, "Transmission Line Faults in Power System and the Different Algorithms for Identification, Classification and Localization: A Brief Review of Methods," *J. Inst. Eng. Ser. B*, vol. 102, no. 4, pp. 855–877, 2021,

doi: 10.1007/s40031-020-00530-0.

[41] B. L. Theraja and A. K. Theraja, *A Textbook of Electrical Technology*, vol. 1. Uttar Pradesh, India: S Chand & Co Ltd, 1999.

[42] J. Faiz and R. Heydarabadi, "Diagnosing power transformers faults," *Russ. Electr. Eng.*, vol. 85, no. 12, pp. 785–793, 2014, doi: 10.3103/S1068371214120207.

[43] N. Kumari, S. Singh, R. Kumari, R. Patel, and N. A. Xalxo, "Power System Faults: A Review," *Int. J. Eng. Res. Technol.*, vol. 4, no. 02, pp. 1–2, 2016, doi: 10.1007/z12649-0294-05129-6.

[44] L. R. Almobasher and Ibrahim Omar Habiballah, "Review of Power System Faults," *Int. J. Eng. Tech. Res.*, vol. 9, no. 11, pp. 61–64, 2020, doi: 10.17577/IJERTV9IS110036.

[45] I. K. Bálint Németh, Szilvia Laboncz, "Condition Monitoring of Power Transformers using DGA and Fuzzy Logic," in *IEEE Electrical Insulation Conference*, 2009. doi: 10.1109/EIC.2009.5166373.

[46] J. D. Glover, M. S. Sarma, and T. J. Overbye, *Power System Analysis and Design*, vol. 4, no. 1. Stamford, CT: Global Engineering, 2012.

[47] A. L. Sheldrake, *Handbook of Electrical Engineering For Practitioners in the Oil , Gas and Petrochemical Industry*. West Sussex, England: John Wiley & Sons, Ltd, 2003.

[48] C. Bayliss, *Transmission and Distribution Electrical Engineering*. Burlington, MA, UK: Elsevier Academic Press, 1996.

[49] M. Kaur and S. Kalra, "A Review on IoT Based Smart Grid," *Int. J. Energy, Inf. Commun.*, vol. 7, no. 3, pp. 11–22, 2016, doi: 10.14257/ijeic.2016.7.3.02.

[50] S. Oprea, B. G. Tudorica, A. Belciu, and I. Botha, "Internet of Things, Challenges for Demand Side Management," *Informatică Econ.*, vol. 21, no. 4, pp. 59–72, 2017, doi: 10.12948/issn14531305/21.4.2017.05.

[51] G. Kulkarni, "Enabling Technologies, Protocols, and Applications: A Detailed Survey on IoT," *Int. J. Adv. Res. Ideas Innov. Technol.*, vol. 3, no. 2, pp. 1091–1098, 2017.

[52] M. S. Mahdavinejad, M. Rezvan, M. Barekatain, P. Adibi, P. Barnaghi, and A. P.

Sheth, “Machine learning for internet of things data analysis: a survey,” *Digit. Commun. Networks*, vol. 4, no. 3, pp. 161–175, 2018, doi: 10.1016/j.dcan.2017.10.002.

[53] M. G. Kibria, K. Nguyen, G. P. Villardi, O. Zhao, K. Ishizu, and F. Kojima, “Big Data Analytics, Machine Learning, and Artificial Intelligence in Next-Generation Wireless Networks,” *IEEE Access*, vol. 6, pp. 32328–32338, 2018, doi: 10.1109/ACCESS.2018.2837692.

[54] A. S. Hashmi and T. Ahmad, “Big Data Mining: Tools & Algorithms,” *Int. J. Recent Contrib. from Eng. Sci. IT*, vol. 4, no. 1, pp. 36–40, 2016, doi: 10.3991/ijes.v4i1.5350.

[55] V. Bolón-Canedo, B. Remeseiro, K. Sechidis, D. Martinez-Rego, and A. Alonso-Betanzos, “Algorithmic challenges in Big Data analytics,” in *European Symposium on Artificial Neural Networks, Computational Intelligence and Machine Learning (ESANN 2017)*, 2017, pp. 519–528.

[56] T. Melia, A. Cooke, and S. Grayson, “Machine Learning Techniques for Automatic Sensor Fault Detection in Airborne SHM Networks,” in *8th European Workshop on Structural Health Monitoring (EWSHM 2016)*, 2016, no. July, pp. 5–8.

[57] J. Li, Q. Zhang, K. Wang, J. Wang, T. Zhou, and Y. Zhang, “Optimal Dissolved Gas Ratios Selected by Genetic Algorithm for Power Transformer Fault Diagnosis Based on Support Vector Machine,” *IEEE Trans. Dielectr. Electr. Insul.*, vol. 23, no. 2, pp. 1198–1206, 2016, doi: 10.1109/TDEI.2015.005277.

[58] M. Jung, O. Niculita, and Z. Skaf, “Comparison of Different Classification Algorithms for Fault Detection and Fault Isolation in Complex Systems,” *Procedia Manuf.*, vol. 19, pp. 111–118, 2018, doi: 10.1016/j.promfg.2018.01.016.

[59] Internet Engineering Task Force, “Low-Power Wide Area Network (LPWAN) Overview,” *IETF*, 2018. https://www.rfc-editor.org/rfc/pdfrfc/rfc8376.txt.pdf (accessed Jan. 01, 2022).

[60] K. Mekki, E. Bajic, F. Chaxel, and F. Meyer, “A comparative study of LPWAN technologies for large-scale IoT deployment,” *ICT Express*, vol. 5, no. 1, pp. 1–7, 2019, doi: https://doi.org/10.1016/j.icte.2017.12.005.

[61] Y. Song, J. Lin, M. Tang, and S. Dong, “An Internet of Energy Things Based on Wireless LPWAN,” *Engineering*, vol. 3, no. 4, pp. 460–466, 2017, doi: 10.1016/J.ENG.2017.04.011.

[62] C. F. Hernández *et al.*, “Indoor Performance Evaluation of LoRa 2.4 GHz,” in *IEEE Wireless Communications and Networking Conference*, 2023. doi: 10.25300/MISQ/2015/39.3.02.

[63] N. Naik, “LPWAN Technologies for IoT Systems: Choice Between Ultra Narrow Band and Spread Spectrum,” *4th IEEE Int. Symp. Syst. Eng. ISSE 2018 - Proc.*, 2018.

[64] R. K. Singh, P. P. Puluckul, R. Berkvens, and M. Weyn, “Energy consumption analysis of LPWAN technologies and lifetime estimation for IoT application,” *Sensors (Switzerland)*, vol. 20, no. 17, pp. 1–22, 2020, doi: 10.3390/s20174794.

[65] D. M. Hernandez, G. Peralta, L. Manero, R. Gomez, J. Bilbao, and C. Zubia, “Energy and coverage study of LPWAN schemes for Industry 4.0,” *Proc. 2017 IEEE Int. Work. Electron. Control. Meas. Signals their Appl. to Mechatronics, ECMSM 2017*, 2017, doi: 10.1109/ECMSM.2017.7945893.

[66] M. S. Danladi and M. Baykara, “Low Power Wide Area Network Technologies: Open Problems, Challenges, and Potential Applications,” *Rev. Comput. Eng. Stud.*, vol. 9, no. 2, pp. 71–78, 2022, doi: 10.18280/rces.090205.

[67] M. E. Elkhatib, J. Hernandez-Alvidrez, and A. Ellis, “Fault Analysis and Detection in Microgrids with High PV Penetration,” 2017.

[68] V. Reddy, K. Jitesh, S. Ashif, C. V. Ravikumar, and B. Kalapraveen, “LPWAN technologies for IoT deployment,” *Int. J. Electr. Eng. Technol.*, vol. 11, no. 3, pp. 285–296, 2020, doi: 10.1109/PERCOMW.2018.8480255.

[69] B. S. Chaudhari and M. Zennaro, *Introduction to low-power wide-area networks*. INC, 2020. doi: 10.1016/B978-0-12-818880-4.00001-6.

[70] C. L. Narayana, R. Singh, and A. Gehlot, “Performance evaluation of LoRa based sensor node and gateway architecture for oil pipeline management,” *Int. J. Electr. Comput. Eng.*, vol. 12, no. 1, pp. 974–982, 2022, doi: 10.11591/ijece.v12i1.pp974-982.

[71] T. Bouguera, J. F. Diouris, J. J. Chaillout, R. Jaouadi, and G. Andrieux, “Energy

consumption model for sensor nodes based on LoRa and LoRaWAN," *Sensors (Switzerland)*, vol. 18, no. 7, pp. 1–23, 2018, doi: 10.3390/s18072104.

[72] M. R. Mamatha Dhananjaya, "A survey of energy harvesting sources for embedded systems," *Int. J. Adv. Eng. Manag. Sci.*, vol. 3, no. 1, pp. 442–447, 2017, doi: 10.1109/SECON.2008.4494336.

[73] O. H. Kombo, S. Kumaran, and A. Bovim, "Design and Application of a Low-Cost, Low- Power, LoRa-GSM, IoT Enabled System for Monitoring of Groundwater Resources with Energy Harvesting Integration," *IEEE Access*, vol. 9, pp. 128417–128433, 2021, doi: 10.1109/ACCESS.2021.3112519.

[74] C. R. Valenta and G. D. Durgin, "Ultra-low-power energy harvesting using power-optimized waveforms," *Wirel. Power Transf.*, vol. 3, no. 1, pp. 1–8, 2016, doi: 10.1017/wpt.2015.13.

[75] J. Henkel, S. Pagani, H. Amrouch, L. Bauer, and F. Samie, "Ultra-Low Power and Dependability for IoT Devices (Invited paper for IoT technologies)," in *Design, Automation & Test in Europe Conference & Exhibition*, 2017, pp. 954–959. doi: 10.23919/DATE.2017.7927129.

[76] M. A. Bandurin, I. F. Yurchenko, and V. A. Volosukhin, "Remote monitoring of reliability for water conveyance hydraulic structures," *Mater. Sci. Forum*, vol. 931 MSF, pp. 209–213, 2018, doi: 10.4028/www.scientific.net/MSF.931.209.

[77] S. Nunoo and E. K. Mahama, "Investigation into Remote Monitoring of Power Transformers using SCADA," *Int. J. Energy Eng.*, vol. 3, no. 6, pp. 213–219, 2013, doi: 10.5963/ijee0306002.

[78] M. Jouhari, E. M. Amhoud, N. Saeed, and M.-S. Alouini, "A Survey on Scalable LoRaWAN for Massive IoT: Recent Advances, Potentials, and Challenges," *J. Low Power Electron. Appl.*, vol. 13, no. 1, pp. 1–30, 2022, doi: 10.3390/jlpea12306006.

[79] A. Banafa, "The Industrial Internet of Things (IIoT): Challenges, Requirements, and Benefits," in *Introduction to Internet of Things (IoT)*, 2023.

[80] S. Li, L. Da Xu, and S. Zhao, "The Internet of Things: A Survey," *Inf. Syst. Front.*, vol. 17, no. 2, pp. 243–259, 2015, doi: 10.1007/s10796-014-9492-7.

[81] S. A. Wani, A. S. Rana, S. Sohail, O. Rahman, S. Parveen, and S. A. Khan,

"Advances in DGA based condition monitoring of transformers: A review," *Renew. Sustain. Energy Rev.*, vol. 149, Oct. 2021, doi: 10.1016/j.rser.2021.111347.

[82] S. Nilakanta, K. Borah, and S. Chatterjee, "Results in Optics Review on monitoring of transformer insulation oil using optical fiber sensors," *Results Opt.*, vol. 10, no. January, p. 100361, 2023, doi: 10.1016/j.rio.2023.100361.

[83] Y. C. Huang, C. M. Huang, and H. C. Sun, "Data mining for oil-insulated power transformers: An advanced literature survey," *Wiley Interdiscip. Rev. Data Min. Knowl. Discov.*, vol. 2, no. 2, pp. 138–148, 2012, doi: 10.1002/widm.1043.

[84] S. Bustamante, M. Manana, A. Arroyo, P. Castro, A. Laso, and R. Martinez, "Dissolved Gas Analysis Equipment for online monitoring of transformer oil: A review," *Sensors (Switzerland)*, vol. 19, no. 19, pp. 4–12, 2019, doi: 10.3390/s19194057.

[85] IEC-60599, *Mineral Oil-Filled Electrical Equipment in Service – Guidance on the Interpretation of Dissolved and free gases Analysis*. IEC, 2015.

[86] IEEE-C57.104, *IEEE Guide for the Interpretation of Gases Generated in Mineral Oil-Immersed Transformers*. 2019.

[87] CIGRE-SC.15, *Recent developments on the interpretation of dissolved gas analysis in transformers*, vol. 296, no. June. 2006.

[88] R. Baskerville, "Genres of Inquiry in Design-Science Research: Justification and Evaluation of Knowledge Production," *MIS Q.*, vol. 39, no. 3, pp. 541–564, 2015.

[89] I. Horváth, "Comparison of Three Methodological Approaches of Design Research," in *International Conference on Engineering Design (ICED'07)*, 2007, pp. 1–11.

[90] J. G. Teixeira, L. Patrício, K.-H. Huang, E. Nóbrega, and L. Constantine, "The MINDS Method: Integrating Management and Interaction Design Perspectives for Service Design," *J. Serv. Res.*, vol. 20, no. 3, 2016, doi: https://doi.org/10.1177/109467051668.

[91] L. V. Lapão, M. M. Da Silva, and J. Gregório, "Implementing an online pharmaceutical service using design science research," *BMC Med. Inform. Decis. Mak.*, vol. 17, no. 1, pp. 1–14, 2017, doi: 10.1186/s12911-017-0428-2.

[92] K. Peffers, T. Tuunanen, M. A. Rothenberger, and S. Chatterjee, "A design science

research methodology for information systems research," *J. Manag. Inf. Syst.*, vol. 24, no. 3, pp. 45–77, 2007, doi: 10.2753/MIS0742-1222240302.

[93] J. R. Venable and R. Baskerville, "Eating our own cooking: Toward a more rigorous design science of research methods," *Electron. J. Bus. Res. Methods*, vol. 10, no. 2, p. 142, 2012, doi: 10.1109/TDEI.2012.64907485.

[94] T. Enninga *et al.*, *Service Design – insights from nine case studies*. 2013.

[95] J. Y. Mao, K. Vredenburg, P. W. Smith, and T. Carey, "The state of user-centered design practice," *Commun. ACM*, vol. 48, no. 3, pp. 105–109, 2005, doi: 10.1145/1047671.1047677.

[96] A. Chammas, M. Quaresma, and C. Mont'Alvão, "A Closer Look on the User Centred Design," *Procedia Manuf.*, vol. 3, no. Ahfe, pp. 5397–5404, 2015, doi: 10.1016/j.promfg.2015.07.656.

[97] W. Visser, "Simon : Design as a Problem-Solving Activity," *Collect. Parsons Paris Sch. art Des. 2010, Art + Des. Psychol.*, vol. 2, pp. 11–16, 2011.

[98] A. Dresch, D. P. Lacerda, and J. A. V. Antunes, *Design science research: A method for science and technology advancement*. London, UK: Springer Cham Heidelberg, 2015. doi: 10.1007/978-3-319-07374-3.

[99] J. vom Brocke, A. Hevner, and A. Maedche, "Introduction to Design Science Research," in *Design Science Research. Cases*, Cham, Switzerland: Springer International Publishing AG, 2020, pp. 1–13. doi: 10.1007/978-3-030-46781-4_1.

[100] A. K. Carstensen and J. Bernhard, "Design science research–a powerful tool for improving methods in engineering education research," *Eur. J. Eng. Educ.*, vol. 44, no. 1–2, pp. 85–102, 2019, doi: 10.1080/03043797.2018.1498459.

[101] L. L. Grigsby, *Electric Power Generation, Transmission, and Distribution*, 3rd ed. Boca Raton, Florida, United States: CRC Press, 2012.

[102] C. Ndungu, J. Nderu, L. Ngoo, and P. Hinga, "A Study of the Root Causes of High Failure Rate of Distribution Transformer - A Case Study," *Int. J. Eng. Sci.*, vol. 6, no. 2, pp. 14–18, 2017, doi: 10.9790/1813-0602021418.

[103] A. K. Abotsi, "Power Outages and Production Efficiency of Firms in Africa," *Int. J. Energy Econ. Policy*, vol. 6, no. 1, pp. 98–104, 2016, doi: 10.2139/ssrn.2729838.

[104] H. C. Sun, Y. C. Huang, and C. M. Huang, “A review of dissolved gas analysis in power transformers,” *Energy Procedia*, vol. 14, no. 2011, pp. 1220–1225, 2012, doi: 10.1016/j.egypro.2011.12.1079.

[105] S. Ranjan, P. L. Narayana, and M. Kirar, “Dissolved Gas Analysis based Incipient Fault Diagnosis of Transformer: A Review,” *Impending Power Demand Innov. Energy Paths*, vol. 3, no. 1, pp. 325–332, 2015, doi: 10.1049/ipd-iep.2015.0085.

[106] S. Chakravorti, D. Dey, and B. Chatterjee, *Recent Trends in the Condition Monitoring of Transformers: Theory, Implementation and Analysis*, vol. 67. 2013. doi: 10.1007/978-1-4471-5550-8.

[107] R. Turkar *et al.*, “Design and fabrication of a Single-phase 1KVA Transformer with automatic cooling system,” *Int. Res. J. Eng. Technol.*, vol. 05, no. 04, pp. 679–682, 2018.

[108] L. Nickelson, *Electromagnetic Theory and Plasmonics for Engineers*. Singapore, Republic of Singapore: Springer Singapore, 2019. doi: 10.1007/978-981-13-2352-2.

[109] M. Hartnack, “Rising Power Outage Cost and Frequency is Driving Grid Modernization Investment,” *Guidehouse Insights*, 2018. https://guidehouseinsights.com/news-and-views/rising-power-outage-cost-and-frequency-is-driving-grid-modernization-investment (accessed Dec. 12, 2022).

[110] Africa Energy Series: Kenya Special Report, “Invest in the Energy sector of Kenya,” 2020.

[111] S. Apte, R. Somalwar, and A. Wajirabadkar, “Incipient Fault Diagnosis of Transformer by DGA Using Fuzzy Logic,” *Proc. 2018 IEEE Int. Conf. Power Electron. Drives Energy Syst. PEDES 2018*, pp. 1–5, 2018, doi: 10.1109/PEDES.2018.8707928.

[112] R. Soni, S. Joshi, V. Lakhiani, and A. Jhala, “Condition Monitoring of Power Transformer Using Dissolved Gas Analysis of Mineral Oil: A Review,” *Int. J. Adv. Eng. Res. Dev.*, vol. 3, no. 02, 2015, doi: 10.21090/ijaerd.e1009510.

[113] M. Bage, P. S. Bisht, and A. Khanna, “Transformer Fault Diagnosis Based on DGA using Classical Methods,” *Int. J. Eng. Res. Technol.*, vol. 4, no. 02, pp. 1–7, 2016, doi: 10.1109/ACCESS.2021.3102415.

[114] T. Manoj, C. Ranga, S. S. M. Ghoneim, U. M. Rao, and S. A. M. Abdelwahab, "Alternate and Effective Dissolved Gas Interpretation to Understand the Transformer Incipient Faults," *IEEE Trans. Dielectr. Electr. Insul.*, 2023, doi: 10.1109/TDEI.2023.3237795.

[115] A. Abu-Siada, "Improved consistent interpretation approach of fault type within power transformers using dissolved gas analysis and gene expression programming," *Energies*, vol. 12, no. 4, 2019, doi: 10.3390/en12040730.

[116] R. A. Prasojo, H. Gumilang, Suwarno, N. U. Maulidevi, and B. A. Soedjarno, "A fuzzy logic model for power transformer faults' severity determination based on gas level, gas rate, and dissolved gas analysis interpretation," *Energies*, vol. 13, no. 4, 2020, doi: 10.3390/en13041009.

[117] H. Malik, R. Sharma, and S. Mishra, "Fuzzy reinforcement learning based intelligent classifier for power transformer faults," *ISA Trans.*, vol. 101, pp. 390–398, 2020, doi: 10.1016/j.isatra.2020.01.016.

[118] K. Chatterjee, S. Dawn, V. K. Jadoun, and R. K. Jarial, "Novel prediction-reliability based graphical DGA technique using multi-layer perceptron network & gas ratio combination algorithm," *IET Sci. Meas. Technol.*, vol. 13, no. 6, pp. 836–842, 2019, doi: 10.1049/iet-smt.2018.5397.

[119] Y. Benmahamed, Y. Kemari, M. Teguar, and A. Boubakeur, "Diagnosis of Power Transformer Oil Using KNN and Naïve Bayes Classifiers," *2018 IEEE 2nd Int. Conf. Dielectr. ICD 2018*, no. 3, pp. 1–4, 2018, doi: 10.1109/ICD.2018.8468532.

[120] D. V. Tanfilyeva, O. V. Tanfyev, and Y. V. Kazantsev, "K-nearest neighbor method for power transformers condition assessment," *IOP Conf. Ser. Mater. Sci. Eng.*, vol. 643, no. 1, 2019, doi: 10.1088/1757-899X/643/1/012016.

[121] H. A. Illias, X. R. Chai, A. H. A. Bakar, and H. Mokhlis, "Transformer incipient fault prediction using combined artificial neural network and various particle swarm optimisation techniques," *PLoS One*, vol. 10, no. 6, pp. 1–16, 2015, doi: 10.1371/journal.pone.0129363.

[122] H. A. Illias and W. Z. Liang, "Identification of transformer fault based on dissolved gas analysis using hybrid support vector machine-modified evolutionary particle

swarm optimisation," *PLoS One*, vol. 13, no. 1, pp. 1–15, 2018, doi: 10.1371/journal.pone.0191366.

[123] Y. Liu, B. Song, L. Wang, J. Gao, and R. Xu, "Power transformer fault diagnosis based on dissolved gas analysis by correlation coefficient-DBSCAN," *Appl. Sci.*, vol. 10, no. 13, 2020, doi: 10.3390/app10134440.

[124] N. Pattanadech, K. Sasomponsawatline, J. Siriworachanyadee, and W. Angsusatra, "The conformity of DGA interpretation techniques: Experience from transformer 132 units," *Proc. - IEEE Int. Conf. Dielectr. Liq.*, vol. 2019-June, no. Icdl, pp. 1–4, 2019, doi: 10.1109/ICDL.2019.8796588.

[125] D. Borcard, F. Gillet, and P. Legendre, *Numerical Ecology with R*. Manhattan, NY, USA: Springer International Publishing AG, 2018. doi: 10.1007/978-1-4419-7976-6.

[126] Suchandan Das, A. Paramane, S. Chatterjee, and U. M. Rao, "Sensing Incipient Faults in Power Transformers Using Bi-Directional Long Short-Term Memory Network," *IEEE Sensors Lett.*, vol. 7, no. 1, pp. 1–4, 2023, doi: 10.1109/LSENS.2022.3233135.

[127] E. Baker, S. V. Nese, and E. Dursun, "Hybrid Condition Monitoring System for Power Transformer Fault Diagnosis," *Energies (Switzerland)*, vol. 16, no. 1151, pp. 1–11, 2023.

[128] N. Bin and A. Bakar, "A New Technique to Detect Loss of Insulation Life in Power Transformers," Curtin University, 2016. [Online]. Available: https://pdfroom.com/books/a-new-technique-to-detect-loss-of-insulation-life-in-power-transformers/Oor5WGjA5qD

[129] N. Abu Bakar, A. Abu-Siada, and S. Islam, "A review of dissolved gas analysis measurement and interpretation techniques," *IEEE Electr. Insul. Mag.*, vol. 30, no. 3, pp. 39–49, 2014, doi: 10.1109/MEI.2014.6804740.

[130] M. Golkhah, S. S. Shamshirgar, and M. A. Vahidi, "Artificial neural networks applied to DGA for fault diagnosis in oil-filled power transformers," *J. Electr. Electron. Eng. Res.*, vol. 3, no. 1, pp. 1–10, 2011, doi: 10.5897/JEEER.9000006.

[131] N. Ravichandran and V. Jayalakshmi, "Investigations on power transformer faults

based on dissolved gas analysis," *Int. J. Innov. Technol. Explor. Eng.*, vol. 8, no. 6, pp. 296–299, 2019.

[132] M. Duval, "A review of faults detectable by gas-in-oil analysis in transformers," *IEEE Electr. Insul. Mag.*, vol. 18, no. 3, pp. 8–17, 2002, doi: 10.1109/MEI.2002.1014963.

[133] E. Sisic, "Chromatographic analysis of gases from the transformer," *Transformers Magazine*, vol. 2, no. 1, pp. 36–41, 2015.

[134] ASTM-D923-15, "Standard Practices for Sampling Electrical Insulating Liquids," ASTM International, West Conshohocken, PA, 2015.

[135] ASTM-D3612-02, *Standard Test Method for Analysis of Gases Dissolved in Electrical Insulating Oil by Gas Chromatography*, vol. 05. 2017.

[136] A. Kumar, *Master Data Science and Data Analysis with Pandas*. Birmingham, UK: Packt Publishing Ltd, 2020.

[137] D. T. Larose and C. D. Larose, *Discovering Knowledge in Data: An Introduction to Data Mining*. Hoboken, New Jersey, USA: John Wiley & Sons, Inc, 2014.

[138] H. Garg, *Mastering Exploratory Analysis with Pandas*. Birmingham, UK: Packt Publishing Ltd, 2018.

[139] D. Niederhut, "Safe handling instructions for missing data," *Proc. 17th Python Sci. Conf.*, no. Scipy, pp. 56–60, 2018, doi: 10.25080/majora-4af1f417-008.

[140] D. Bertsimas, C. Pawlowski, and Y. D. Zhuo, "From predictive methods to missing data imputation: An optimization approach," *J. Mach. Learn. Res.*, vol. 18, pp. 1–39, 2018, doi: 10.5555/3122009.3242053.

[141] K. Devroop, "Correlation versus Causation: Another Look at a Common Misinterpretation," in *Annual Meeting of the Southwest Educational Research Association*, 2000, pp. 1–15.

[142] A. Basuki and Suwarno, "Online dissolved gas analysis of power transformers based on decision tree model," in *4th IEEE Conference on Power Engineering and Renewable Energy, ICPERE 2018 - Proceedings*, 2018, pp. 1–6. doi: 10.1109/ICPERE.2018.8739761.

[143] W. Buntine, "Learning classification trees," in *Artificial Inteligence frontiers in*

statistics, London, UK: Chapman and Hall/CRC, 2020, pp. 182–201.

[144] Z. Zhang, "Introduction to machine learning: K-nearest neighbors," *Ann. Transl. Med.*, vol. 4, no. 11, 2016, doi: 10.21037/atm.2016.03.37.

[145] S. B. Imandoust and M. Bolandraftar, "Application of K-Nearest Neighbor (KNN) Approach for Predicting Economic Events : Theoretical Background," *Int. J. Eng. Res. Appl.*, vol. 3, no. 5, pp. 605–610, 2013, doi: 10.1007/978-3-030-80216-5_7.

[146] X. Gao, J. Wen, and C. Zhang, "An Improved Random Forest Algorithm for Predicting Employee Turnover," *Math. Probl. Eng.*, 2019, doi: 10.1155/2019/4140707.

[147] H. Sug, "Applying randomness effectively based on random forests for classification task of datasets of insufficient information," *J. Appl. Math.*, 2012, doi: 10.1155/2012/258054.

[148] L. Breiman, "Random Forests," *Mach. Learn.*, vol. 45, pp. 5–32, 2001, doi: 10.1023/A:1010933404324.

[149] A. Bakhtouchi, "A Tree Decision Based Approach for Selecting Software Development Methodology," in *2018 International Conference on Smart Communications in Network Technologies (SaCoNeT)*, 2018, pp. 211–216.

[150] E. Williams, *Python for Data Science*. Sebastopol, CA, USA: O'Reilly Media, Inc., 2019.

[151] Z. A. Shaw, *Learn Python 3 the Hard Way*. Boston, USA: Addison-Wesley, 2017.

[152] R. Johansson, *Numerical Python*. Berkeley, California: Apress Berkeley, CA, 2018. doi: doi.org/10.1007/978-1-4842-4246-9.

[153] A. Géron, *Machine Learning with Scikit-Learn, Keras, and TensorFlow*, 2nd ed., vol. 53, no. 9. Sebastopol, CA, USA: O'Reilly Media, Inc., 2019.

[154] I. Idris, *NumPy: Beginner's Guide*, Third Edit. Holborn, London: Packt Publishing, 2015.

[155] M. Waskom, "Seaborn: Statistical Data Visualization," *J. Open Source Softw.*, vol. 6, no. 60, p. 3021, 2021, doi: 10.21105/joss.03021.

[156] F. J. J. Joseph, S. Nonsiri, and Annop, "Keras and TensorFlow: A Hands-On Experience," in *Advanced Deep Learning for Engineers and Scientists*, no.

November, Springer Berlin Heidelberg, 2021, pp. 85–111. doi: 10.1007/978-3-030-66519-7.

[157] A. Géron, *Hands-on Machine Learning whith Scikit-Learing, Keras and Tensorfow*. 2019.

[158] J. Xu, Y. Zhang, and D. Miao, "Three-way confusion matrix for classification: A measure driven view," *Inf. Sci. (Ny).*, vol. 507, no. August, pp. 772–794, 2020, doi: 10.1016/j.ins.2019.06.064.

[159] E. Beauxis-Aussalet and L. Hardman, "Simplifying the visualization of confusion matrix," in *Belgian/Netherlands Artificial Intelligence Conference*, 2014, no. November 2014, pp. 133–134.

[160] P. Cichosz, "Assessing the quality of classification models: Performance measures and evaluation procedures," *Cent. Eur. J. Eng.*, vol. 1, no. 2, pp. 132–158, 2011, doi: 10.2478/s13531-011-0022-9.

[161] M. Hossin; and S. M.N, "A Review on Evaluation Metrics for Data Classification Evaluations," *Int. J. Data Min. Knowl. Manag. Process*, vol. 5, no. 2, pp. 01–11, 2015, doi: 10.5121/ijdkp.2015.5201.

[162] Q. Gu, L. Zhu, and Z. Cai, "Evaluation Measures of the Classification Performance of Imbalanced Data Sets," *Comput. Intell. Intell. Syst. ISICA 2009. Commun. Comput. Inf. Sci.*, vol. 51, pp. 461–471, 2009, doi: https://doi.org/10.1007/978-3-642-04962-0_53.

[163] R. Bikmetov, M. Y. A. Raja, and T. U. Sane, "Infrastructure and applications of Internet of Things in smart grids: A survey," in *2017 North American Power Symposium (NAPS)*, 2017. doi: 10.1109/NAPS.2017.8107283.

[164] L. A. Staeheli and D. Mitchell, "The Relationship Between Precision-Recall and ROC Curves," in *Proceedings of the 23 rd International Conference on Machine Learning*, 2006, pp. 546–559. doi: 10.4135/9780857021113.n29.

[165] P. Flach, "Performance Evaluation in Machine Learning: The Good, the Bad, the Ugly, and the Way Forward," in *Proceedings of the AAAI Conference on Artificial Intelligence*, 2019, vol. 33, pp. 9808–9814. doi: 10.1609/aaai.v33i01.33019808.

[166] N. A. Hidayatullah, A. C. Kurniawan, and A. Kalam, "Power Transmission and

Distribution Monitoring using Internet of Things (IoT) for Smart Grid," *IOP Conf. Ser. Mater. Sci. Eng.*, vol. 384, no. 012039, pp. 1–8, 2018, doi: 10.1088/1757-899X/384/1/012039.

[167] D. Baimel, S. Tapuchi, and N. Baimel, "Smart Grid Communication Technologies-Overview, Research Challenges and Opportunities," in *International Symposium on Power Electronics, Electrical Drives, Automation and Motion, SPEEDAM 2016*, 2016, pp. 116–120. doi: 10.1109/SPEEDAM.2016.7526014.

[168] Y. Saleem, N. Crespi, M. H. Rehmani, and R. Copeland, "Internet of Things-aided Smart Grid: Technologies, Architectures, Applications, Prototypes, and Future Research Directions," *IEEE Access*, vol. 7, pp. 62962–63003, 2019, doi: 10.1109/ACCESS.2019.2913984.

[169] J. Yuan, J. Shen, L. Pan, C. Zhao, and J. Kang, "Smart grids in China," *Renew. Sustain. Energy Rev.*, vol. 37, pp. 896–906, 2014, doi: 10.1016/j.rser.2014.05.051.

[170] G. Rigatos, "Condition Monitoring of the Electric Power Transmission and Distribution System," in *Intelligent Renewable Energy Systems*, Springer International Publishing Switzerland, 2016, pp. 463–505. doi: 10.1007/978-3-319-39156-4_10.

[171] J. Taneja, "Measuring Electricity Reliability in Kenya," *Energy Policy*, vol. 12, p. 6, 2018, doi: 10.3403/30077701.

[172] P. Nduhuura, M. Garschagen, and A. Zerga, "Impacts of electricity outages in urban households in developing countries: A case of Accra, Ghana," *Energies*, vol. 14, no. 3676, 2021, doi: 10.3390/en14123676.

[173] M. Takase, R. Kipkoech, and P. K. Essandoh, "A comprehensive review of energy scenario and sustainable energy in Kenya," *Fuel Commun.*, vol. 7, p. 100015, 2021, doi: 10.1016/j.jfueco.2021.100015.

[174] D. Owiro, G. Poquillon, K. S. Njonjo, and C. Oduor, "Situational Analysis of Energy Industry, Policy and Strategy for Kenya. Institute of Economic," Institute of Economic Affairs (IEA), Nairobi, 2021. [Online]. Available: https://ieakenya.or.ke/download/situational-analysis-of-energy-industry-policy-and-strategy-for-kenya/

[175] A. K. Al Mhdawi and H. S. Al-Raweshidy, “A Smart Optimization of Fault Diagnosis in Electrical Grid Using Distributed Software-Defined IoT System,” *IEEE Syst. J.*, vol. 14, no. 2, pp. 2780–2790, 2020, doi: 10.1109/JSYST.2019.2921867.

[176] A. Sallam and O. Malik, “Microgrids and Smart Grids,” in *Electric Distribution Systems*, Second Edi., Boca Raton, FL: John Wiley & Sons, Inc, 2019, pp. 553–580. doi: 10.1002/9781119509332.ch20.

[177] T. Hilorme, L. Sokolova, O. Portna, L. Lysiak, and N. Boretskaya, “Smart grid concept as a perspective for the development of Ukrainian energy platform,” *IBIMA Bus. Rev.*, vol. 2019, no. Article ID 923814, pp. 1–13, 2019, doi: 10.5171/2019.923814.

[178] T. Baležentis and D. Štreimikiene, “Sustainability in the electricity sector through advanced technologies: Energy mix transition and smart grid technology in China,” *Energies*, vol. 12, no. 1142, pp. 1–21, 2019, doi: 10.3390/en12061142.

[179] R. Kappagantu and S. A. Daniel, “Challenges and issues of smart grid implementation: A case of Indian scenario,” *J. Electr. Syst. Inf. Technol.*, vol. 5, no. 3, pp. 453–467, 2018, doi: 10.1016/j.jesit.2018.01.002.

[180] N. Pamuk and Y. Uyaroglu, “The fault diagnosis for power system using Fuzzy Petri Nets,” *Prz. Elektrotechniczny*, vol. 88, no. 7a, pp. 99–102, 2012.

[181] M. Tan, J. Li, S. Zhao, and X. Cheng, “Method of power grid fault diagnosis using intuitionistic fuzzy petri nets with inhibitor arcs,” in *Proceedings of 2019 IEEE 8th Data Driven Control and Learning Systems Conference (DDCLS)*, 2019, pp. 568–573. doi: 10.1109/DDCLS.2019.8908886.

[182] A. J. Lekie, D. C. Idoniboyeobu, and S. L. Braide, “Fault Detection on Distribution Line Using Fuzzy Logic,” *Int. J. Sci. Eng. Res.*, vol. 9, no. 12, pp. 490–503, 2018, doi: 10.1007/978-981-16-8721-1_3.

[183] T. Wu, G. Tu, Z. Q. Bo, and A. Klimek, “Fuzzy set theory and fault tree analysis based method suitable for fault diagnosis of power transformer,” in *Proceedings of the 2007 International Conference on Intelligent Systems Applications to Power Systems (ISAP)*, 2007, pp. 1–5. doi: 10.1109/ISAP.2007.4441664.

[184] M. R. Zaidan, “Power System Fault Detection, Classification and Clearance by

Artificial Neural Network Controller," in *Proceedings of the 2019 Global Conference for Advancement in Technology (GCAT)*, 2019, pp. 1–5. doi: 10.1109/GCAT47503.2019.8978400.

[185] M. Jamil, S. K. Sharma, and R. Singh, "Fault detection and classification in electrical power transmission system using artificial neural network," *Springerplus*, vol. 4, no. 334, pp. 1–13, 2015, doi: 10.1186/s40064-015-1080-x.

[186] H. J. Cho and J. K. Park, "An expert system for fault section diagnosis of power systems using fuzzy relations," *IEEE Trans. Power Syst.*, vol. 12, no. 1, pp. 342–348, 1997, doi: 10.1109/59.574957.

[187] G. Xiong, D. Shi, and J. Chen, "A New Approach to Fault Diagnosis of Power Systems Using Fuzzy Reasoning Spiking Neural P Systems," *Math. Probl. Eng.*, vol. 2013, 2013, doi: 10.1109/PESMG.2013.6672758.

[188] F. S. Wen and C. S. Chang, "Probabilistic approach for fault-section estimation in power systems based on a refined genetic algorithm," *IEE Proc. Gener. Transm. Distrib.*, vol. 144, no. 2, pp. 160–168, 1997, doi: 10.1049/ip-gtd:19970802.

[189] F. Wen, C. S. Chang, and W. Fu, "New approach to alarm processing in power systems based on the set covering theory and a refined genetic algorithm," *Electr. Mach. Power Syst.*, vol. 26, no. 1, pp. 53–67, 1998, doi: 10.1080/07313569808955807.

[190] M. J. Mnati, A. Van den Bossche, and R. F. Chisab, "A smart voltage and current monitoring system for three phase inverters using an android smartphone application," *Sensors*, vol. 17, no. 872, 2017, doi: 10.3390/s17040872.

[191] M. Ul Mehmood, A. Ulasyar, A. Khattak, K. Imran, H. S. Zad, and S. Nisar, "Cloud based IoT solution for fault detection and localization in power distribution systems," *Energies*, vol. 13, no. 2686, 2020, doi: 10.3390/en13112686.

[192] H. Shabani, N. Julai, M. M. Ahmed, S. Khan, S. A. Hameed, and M. H. Habaebi, "Wireless communication techniques, the right path to Smart Grid distribution Systems: A review," in *Proceedings of the 14th IEEE Student Conference on Research and Development: Advancing Technology for Humanity, (SCOReD)*, 2016, pp. 1–6. doi: 10.1109/SCORED.2016.7810047.

[193] A. Jain, T. C. Archana, and M. B. K. Sahoo, “A Methodology for Fault Detection and Classification Using PMU Measurements,” in *Proceedings of the 20th National Power Systems Conference (NPSC)*, 2018, pp. 1–6. doi: 10.1109/NPSC.2018.8771757.

[194] V. S. Bharath Kurukuru, A. Haque, R. Kumar, M. A. Khan, and A. K. Tripathy, “Machine learning based fault classification approach for power electronic converters,” in *9th IEEE International Conference on Power Electronics, Drives and Energy Systems, PEDES 2020*, 2020, vol. 9, no. 2, pp. 2002–2008. doi: 10.1201/9780429277450-6.

[195] U.S. Department of Energy, “Factors Affecting PMU Installation Costs,” Washington DC, USA, 2014.

[196] O. O. Babayomi and P. O. Oluseyi, “Intelligent Fault Diagnosis in a Power Distribution Network,” *Adv. Electr. Eng.*, vol. 2016, no. 8651630, pp. 1–10, 2016, doi: 10.1155/2016/8651630.

[197] A. M. Yousuf, E. M. Rochester, B. Ousat, and M. Ghaderi, “Throughput, Coverage and Scalability of LoRa LPWAN for Internet of Things,” in *Proceeding of the 2018 IEEE/ACM 26th International Symposium on Quality of Service (IWQoS)*, 2018, pp. 1–10. doi: 10.1109/IWQoS.2018.8624157.

[198] A. Muaz Abdul Rahman, F. Hafizhelmi Kamaru Zaman, and S. Afzal Che Abdullah, “Performance Analysis of LPWAN Using LoRa Technology for IoT Application,” *Int. J. Eng. Technol.*, vol. 7, no. 4.11, pp. 212–216, 2018, doi: 10.14419/ijet.v7i4.11.21387.

[199] S. Ahmed, “Realizing the Benefits of Energy Harvesting for IoT,” in *Role of IoT in Green Energy Systems*, Hershey, Pennsylvania: IGI Global, 2021, pp. 144–155. doi: 10.4018/978-1-7998-6709-8.ch006.

[200] S. Muzafar, “Energy Harvesting Models and Techniques for Green IoT,” in *Role of IoT in Green Energy Systems*, Hershey, Pennsylvania: IGI Global, 2021, pp. 117–143. doi: 10.4018/978-1-7998-6709-8.ch005.

[201] T. Sanislav, G. D. Mois, S. Zeadally, and S. C. Folea, “Energy Harvesting Techniques for Internet of Things (IoT),” *IEEE Access*, vol. 9, pp. 39530–39549,

2021, doi: 10.1109/ACCESS.2021.3064066.

[202] A. Mindang and P. Siripongwutikorn, “Solar Power Prediction in IoT Devices using Environmental and Location Factors,” in *Proceedings of the 2020 5th International Conference on Machine Learning Technologies (ICMLT)*, 2020, pp. 119–123. doi: 10.1145/3409073.3409086.

[203] M. Sinclair, “The Internet of things,” in *Ethical Ripples of Creativity and Innovation*, London, UK: Palgrave Macmillan, 2017. doi: 10.1057/9781137505545.

[204] J. A. Stankovic, “Research directions for the internet of things,” *IEEE Internet Things J.*, vol. 1, no. 1, pp. 3–9, 2014, doi: 10.1109/JIOT.2014.2312291.

[205] K. Oratile, I. Bassey, and M. A.-M. Adnan, “IoT Devices and Applications based on LoRa/LoRaWAN,” in *Proceedings of the 43rd Annual Conference of the IEEE Industrial Electronics Society (IECON)*, 2017, pp. 6107–6112. doi: 10.1109/IECON.2017.8217061.

[206] G. Gupta and R. Van Zyl, “Energy harvested end nodes and performance improvement of LoRa networks,” *Int. J. Smart Sens. Intell. Syst.*, vol. 14, no. 1, pp. 1–15, 2021, doi: 10.21307/IJSSIS-2021-002.

[207] F. Adelantado, X. Vilajosana, P. Tuset-Peiro, B. Martinez, and J. Melia, “Understanding the limits of LoRaWAN,” in *Proceedings of the 2016 International Conference on Embedded Wireless Systems and Networks*, 2016, no. September, pp. 8–12. doi: 10.1109/MCOM.2017.1600613.

[208] M. Iqbal, A. Y. M. Abdullah, and F. Shabnam, “An Application Based Comparative Study of LPWAN Technologies for IoT Environment,” in *Proceddings of the 2020 IEEE Region 10 Symposium, TENSYMP 2020*, 2020, pp. 1857–1860. doi: 10.1109/TENSYMP50017.2020.9230597.

[209] F. Turčinović, G. Šišul, and M. Bosiljevac, “LoRaWAN Base Station Improvement for Better Coverage and Capacity,” *J. Low Power Electron. Appl.*, vol. 12, no. 1, pp. 1–11, 2022, doi: 10.3390/jlpea12010001.

[210] U. Noreen, Ahcene bounceur, and L. Clavier, “A study of LoRa low power and wide area network technology,” in *Proceedings of the 2020 International Conference on Advanced Technologies for Signal and Image Processing (ATSIP)*, 2020, pp. 1–6.

doi: 10.1109/TENSYMP50017.2020.9230597.

[211] A. Augustin, J. Yi, T. Clausen, and W. M. Townsley, “A study of Lora: Long range & low power networks for the internet of things,” *Sensors*, vol. 16, no. 1466, 2016, doi: 10.3390/s16091466.

[212] E. Murdyantoro, A. W. W. Nugraha, A. W. Wardhana, A. Fadli, and M. I. Zulfa, “A review of LoRa technology and its potential use for rural development in Indonesia,” in *AIP Conference Proceedings*, 2019, vol. 2094, no. 020011, pp. 1–7. doi: 10.1063/1.5097480.

[213] E. Migabo, K. Djouani, A. Kurien, and T. Olwal, “A Comparative Survey Study on LPWA Networks: LoRa and NB–IoT,” in *Proceedings of the 2017 Future Technologies Conference (FTC)*, 2017, pp. 1045–1051. doi: 10.1016/j.procs.2019.08.090.

[214] L. P. Fraile, S. Tsampas, G. Mylonas, and D. Amaxilatis, “A Comparative Study of LoRa and IEEE 802.15.4-Based IoT Deployments Inside School Buildings,” *IEEE Access*, vol. 8, pp. 160957–160981, 2020, doi: 10.1109/ACCESS.2020.3020685.

[215] M. A. I. Mohd Ariff, Y. L. Then, and F. S. Tay, “Establish connection between remote areas and city to improve healthcare services,” in *Proceedings - 2019 7th International Conference on Green and Human Information Technology (ICGHIT)*, 2019, pp. 18–23. doi: 10.1109/ICGHIT.2019.00012.

[216] M. Centenaro, L. Vangelista, A. Zanella, and M. Zorzi, “Long-Range Communications in Unlicensed Bands: the Rising Stars in the IoT and Smart City Scenarios,” *IEEE Wirel. Commun.*, vol. 23, 2016, doi: 10.13140/RG.245.12409.90829.

[217] J. C. Gambiroza, T. Mastelic, P. Solic, and M. Cagalj, “Capacity in lorawan networks: Challenges and opportunities,” in *Proceedings of the 2019 4th International Conference on Smart and Sustainable Technologies (SpliTech)*, 2019, pp. 1–6. doi: 10.23919/SpliTech.2019.8783184.

[218] T. A. Salih and M. S. Noori, “Using LoRa Technology to Monitor and Control Sensors in the Greenhouse,” *IOP Conf. Ser. Mater. Sci. Eng.*, vol. 928, no. 032058, pp. 1–12, 2020, doi: 10.1088/1757-899X/928/3/032058.

[219] V. Eremin and A. Borisov, “A research of the propagation of LoRa signals at 433 and 868 MHz in difficult urban conditions,” *IOP Conf. Ser. Mater. Sci. Eng.*, vol. 363, no. 1, 2018, doi: 10.1088/1757-899X/363/1/012014.

[220] A. Raychowdhury and A. Pramanik, “Survey on LoRa Technology: Solution for Internet of Things,” *Adv. Intell. Syst. Comput.*, vol. 1148, pp. 259–271, 2020, doi: 10.1007/978-981-15-3914-5_20.

[221] T. Janssen, N. Bnilam, M. Aernouts, R. Berkvens, and M. Weyn, “Lora 2.4 ghz communication link and range,” *Sensors (Switzerland)*, vol. 20, no. 16, pp. 1–12, 2020, doi: 10.3390/s20164366.

[222] I. Cheikh, R. Aouami, E. Sabir, M. Sadik, and S. Roy, “Multi-Layered Energy Efficiency in LoRa-WAN Networks: A Tutorial,” *IEEE Access*, vol. 10, 2022, doi: 10.1109/ACCESS.2021.3140107.

[223] T. Attia *et al.*, “Experimental Characterization of LoRaWAN Link Quality,” in *Proceedings of the IEEE Global Communications Conference (GLOBECOM)*, 2019, pp. 1–7. doi: 10.1109/GLOBECOM38437.2019.9013371.

[224] R. Liang, L. Zhao, and P. Wang, “Performance evaluations of lora wireless communication in building environments,” *Sensors*, vol. 20, no. 3828, pp. 1–19, 2020, doi: 10.3390/s20143828.

[225] A. Kaur, Y. S. Brar, and G. Leena, “Fault detection in power transformers using random neural networks,” *Int. J. Electr. Comput. Eng.*, vol. 9, no. 1, pp. 78–84, 2019, doi: 10.11591/ijece.v9i1.pp78-84.

[226] I. Sahmi, A. Abdellaoui, T. Mazri, and N. Hmina, “MQTT-PRESENT: Approach to secure internet of things applications using MQTT protocol,” *Int. J. Electr. Comput. Eng.*, vol. 11, no. 5, pp. 4577–4586, 2021, doi: 10.11591/ijece.v11i5.pp4577-4586.

[227] S. Devalal and A. Karthikeyan, “LoRa Technology - An Overview,” in *Proceedings of the 2nd International Conference on Electronics, Communication and Aerospace Technology, (ICECA)*, 2018, pp. 284–290. doi: 10.1109/ICECA.2018.8474715.

[228] Atmel, “Arduino Mega 2560 Data Manual,” Chandler, Arizona, USA, 2015. [Online]. Available: https://www.microchip.com/

[229] Y. A. Badamasi, “The working principle of an Arduino,” in *Proceedings of the 11th*

International Conference on Electronics, Computer and Computation, ICECCO 2014, 2014, pp. 1–4. doi: 10.1109/ICECCO.2014.6997578.

[230] S. Chalasani and J. M. Conrad, "A survey of energy harvesting sources for embedded systems," *Conf. Proc. - IEEE SOUTHEASTCON*, pp. 442–447, 2008, doi: 10.1109/SECON.2008.4494336.

[231] X. Meng, X. Li, C. Y. Tsui, and W. H. Ki, "An indoor solar energy harvesting system using dual mode SIDO converter with fully digital time-based MPPT," in *2016 IEEE International Symposium on Circuits and Systems (ISCAS)*, 2016, pp. 2354–2357. doi: 10.1109/ISCAS.2016.7539057.

[232] G. Zhou, L. Huang, W. Li, and Z. Zhu, "Harvesting ambient environmental energy for wireless sensor networks: A survey," *J. Sensors*, vol. 2014, no. 815467, pp. 1–20, 2014, doi: 10.1155/2014/815467.

[233] P. Detterer, M. Nabi, H. Jiao, and T. Basten, "Receiver-Sensitivity Control for Energy-Efficient IoT Networks," *IEEE Commun. Lett.*, vol. 25, no. 4, pp. 1383–1386, 2021, doi: 10.1109/LCOMM.2020.3041935.

[234] B. Myagmardulam *et al.*, "Performance Evaluation of LoRa 920 MHz Frequency Band in a Hilly Forested Area," *Electronics*, vol. 10, no. 502, 2021, doi: 10.3390/electronics10040502.

[235] R. Bianchini *et al.*, "Toward ML-centric cloud platforms," *Commun. ACM*, vol. 63, no. 2, pp. 50–59, 2020, doi: 10.1145/3364684.

[236] Nur-A-Alam, M. Ahsan, M. A. Based, J. Haider, and E. M. G. Rodrigues, "Smart monitoring and controlling of appliances using Lora based IoT system," *Designs*, vol. 5, no. 1, 2021, doi: 10.3390/designs5010017.

[237] D. A. Barkas, S. D. Kaminaris, K. K. Kalkanis, G. C. Ioannidis, and C. S. Psomopoulos, "Condition Assessment of Power Transformers through DGA Measurements Evaluation Using Adaptive Algorithms and Deep Learning," *Energies (Switzerland)*, vol. 16, no. 54, 2023, doi: https://doi.org/10.3390/en16010054.

[238] E. B. Hansen and S. Bøgh, "Artificial Intelligence and Machine Learning," in *The Future of Smart Production for SMEs*, O. Madsen, U. Berger, C. Møller, A. H.

Lassen, and B. V. Waehrens, Eds. Cham: Springer International Publishing, 2023, pp. 323–326. doi: https://doi.org/10.1007/978-3-031-15428-7_27.

[239] M. Fernandes, J. M. Corchado, and G. Marreiros, "Machine learning techniques applied to mechanical fault diagnosis and fault prognosis in the context of real industrial manufacturing use-cases: a systematic literature review," *Appl. Intell.*, 2022, doi: 10.1007/s10489-022-03344-3.

[240] Ö. Gültekin', E. Cinar, K. Özkan, and A. Yazıcı, "Real-Time Fault Detection and Condition Monitoring for Industrial Autonomous Transfer Vehicles Utilizing Edge Artificial Intelligence," *Sensors (Switzerland)*, vol. 22, no. 3208, 2022, doi: https://doi.org/10.3390/s22093208.

[241] Y. H. Ali, "Artificial Intelligence Application in Machine Condition Monitoring and Fault Diagnosis," *Artif. Intell. - Emerg. Trends Appl.*, 2018, doi: 10.5772/intechopen.74932.

[242] G. Kimutai and A. Ngenzi, "Offloading an Energy Efficient IoT Solution to the Edge: A practical Solution for Developing Countries," in *IEEE Global Humanitarian Technology Conference (GHTC)*, 2021. doi: 10.1109/GHTC53159.2021.9612420.

[243] M. M. Ogore, K. Nkurikiyeyezu, and J. Nsenga, "Offline Prediction of Cholera in Rural Communal Tap Waters Using Edge AI inference," in *2021 IEEE Globecom Workshops (GC Wkshps)*, 2021, pp. 1–6. doi: 10.1109/gcwkshps52748.2021.9682128.

[244] S. O. Ooko, D. Mukanyiligira, J. P. Munyampundu, and J. Nsenga, "Edge AI-based Respiratory Disease Recognition from Exhaled Breath Signatures," in *2021 IEEE Jordan International Joint Conference on Electrical Engineering and Information Technology (JEEIT)*, 2021, pp. 89–94. doi: 10.1109/jeeit53412.2021.9634140.

APPENDIX 1: JOURNAL PUBLICATIONS

The publications that have been derived from this work are all listed below.

(1) George Odongo; Richard Musabe; Damien Hanyurwimfura. A Multinomial DGA Classifier for Incipient Fault Detection in Oil-Impregnated Power Transformers. Algorithms 2021, 14, 128. https://doi.org/10.3390/a14040128

(2) George Odongo; Richard Musabe; Damien Hanyurwimfura; Abubakar Bakari. An efficient LoRa-enabled smart fault detection and monitoring platform for the power distribution system using self-powered IoT devices, 2022 IEEE Access; IEEE https://doi.org/10.1109/ACCESS.2022.3189002

(3) George Odongo; Richard Musabe; Damien Hanyurwimfura; Abubakar Bakari. Condition Monitoring of Oil-immersed Transformers Using AI Edge Inference for Incipient Fault Prediction: A case study; IEEE; 2022 IEEE PES/IAS PowerAfrica Conference (PAC 2022). doi.org/10.1109/PowerAfrica53997.2022.9905325